



**Combined sea-level and climate controls on limestone formation, hiatuses and ammonite preservation in the Blue Lias Formation, South Britain (uppermost Triassic-Lower Jurassic)**

Journal:	<i>Geological Magazine</i>
Manuscript ID	GEO-16-1636.R1
Manuscript Type:	Article
Date Submitted by the Author:	n/a
Complete List of Authors:	Weedon, Graham; Met Office, Joint Centre for Hydro-Meteorological Research Jenkyns, Hugh; University of Oxford, Department of Earth Sciences; Page, Kevin; University of Plymouth, School of Geography, Earth and Environmental Sciences
Keywords:	Sedimentary cycles, Sea level, Climatic cycles, Blue Lias Formation, Diagenesis, Hiatuses

1  
2  
3  
4  
5  
6  
7  
8  
9  
10  
11  
12  
13  
14  
15  
16  
17  
18  
19  
20  
21  
22  
23  
24  
25  
26  
27  
28  
29  
30  
31  
32  
33  
34  
35  
36  
37  
38  
39  
40  
41  
42  
43  
44  
45  
46  
47  
48  
49  
50  
51  
52  
53  
54  
55  
56  
57  
58  
59  
60

1  
2  
3  
4  
5  
6  
7  
8  
9  
10  
11  
12  
13  
14  
15  
16  
17  
18  
19  
20  
21  
22  
23  
24  
25  
26  
27  
28  
29  
30  
31  
32  
33  
34  
35  
36  
37  
38  
39  
40  
41  
42  
43  
44  
45  
46  
47  
48  
49  
50  
51  
52  
53  
54  
55  
56  
57  
58  
59  
60

**Combined sea-level and climate controls on limestone formation, hiatuses and ammonite preservation in the Blue Lias Formation, South Britain (uppermost Triassic–Lower Jurassic)**

Short title/running head: **Sea level and climate controls of the Blue Lias**

Graham P. Weedon<sup>1\*</sup>, Hugh C. Jenkyns<sup>2</sup> and Kevin N. Page<sup>3</sup>

\* Corresponding author

**1** [graham.weedon@metoffice.gov.uk](mailto:graham.weedon@metoffice.gov.uk), Met Office, Maclean Building, Benson Lane, Crowmarsh Gifford, Wallingford, Oxfordshire, OX10 8BB, UK.

**2** Department of Earth Sciences, University of Oxford, South Parks Road, Oxford, OX1 3AN, UK.

**3** School of Geography, Earth and Environmental Sciences, Plymouth University, Drake Circus, Plymouth, PL4 8AA, UK.

**Revision for:** *Geological Magazine*

**December 2016**

**Abstract**

Lithostratigraphic and magnetic-susceptibility logs for four sections in the Blue Lias Formation are combined with a re-assessment of the ammonite biostratigraphy. A Shaw plot correlating the West Somerset coast with the Devon/Dorset coast at Lyme Regis, based on 63 common biohorizon picks and field evidence, demonstrates that intra-formational hiatuses are common. Compared to laminated shale deposition, the climate associated with light marl is interpreted as both drier and stormier. Storm-related non-deposition favoured initiation of limestone formation near the sediment-water interface. Areas and time intervals with reduced water depths had lower net accumulation rates and developed a greater proportion of limestone.

Many homogeneous limestone beds have no ammonites preserved, whereas others contain abundant fossils. Non-deposition encouraged shallow sub-seafloor cementation which, if occurring after aragonite dissolution, generated limestones lacking ammonites. Abundant ammonite preservation in limestones required both rapid burial by light marl during storms as well as later storm-related non-deposition and near-surface carbonate cementation that occurred prior to aragonite dissolution.

The limestones are dominated by a mixture of early framework-supporting cement that minimized compaction of fossils, plus a later micrograde cement infill. At Lyme Regis, the relatively low net accumulation rate ensured that final cementation of the limestones took place at relatively shallow burial depths. On the West Somerset coast, however, much higher accumulation rates led to deeper burial before final limestone cementation. Consequently, the oxygen-isotope ratios of the limestones on the West Somerset coast, recording precipitation of the later diagenetic calcite at higher temperatures, are lower than those at Lyme Regis.

**Keywords:**

1  
2  
3  
4  
5  
6  
7  
8  
9  
10  
11  
12  
13  
14  
15  
16  
17  
18  
19  
20  
21  
22  
23  
24  
25  
26  
27  
28  
29  
30  
31  
32  
33  
34  
35  
36  
37  
38  
39  
40  
41  
42  
43  
44  
45  
46  
47  
48  
49  
50  
51  
52  
53  
54  
55  
56  
57  
58  
59  
60

50 Sedimentary cycles; Sea level; Climatic cycles; Blue Lias Formation; Diagenesis; Hiatuses

51

52 **1. Introduction**

53 The origin and significance of the limestone beds and nodules in the uppermost  
54 Rhaetian (Triassic) to Sinemurian (Jurassic) Blue Lias Formation of Britain has long been a  
55 subject of interest (Day, 1865; Richardson, 1923; Kent, 1936). Hallam (1960; 1964) argued  
56 that the limestones owed their characteristics to both diagenetic and primary (i.e.  
57 depositional) factors. Shukri (1942) speculated on the possible role of climate but ruled out  
58 forcing by Milankovitch orbital-precession cycles because the limestone beds at Lyme Regis  
59 are more widely spaced in the lower Sinemurian compared to the Hettangian. Following the  
60 demonstration by Hays, Imbrie & Shackleton (1976) of orbital forcing of Pleistocene to  
61 Recent climate, House (1985; 1986) and Weedon (1985; 1986) revived the idea of orbital-  
62 climatic (Milankovitch cycle) forcing to explain the interbedded lithologies.

63 One of the reasons the Blue Lias Formation has attracted so much research interest is  
64 that it exhibits two styles of sedimentary cyclicity. Visually most obvious are the alternations  
65 of limestones and non-limestones, but also present are alternations of homogeneous, organic-  
66 carbon-poor strata (grey limestone plus light grey marl) with laminated organic-carbon-rich  
67 strata (black to very dark grey laminated shale plus laminated limestone). Dark grey marls  
68 represent intermediate compositions. The homogeneous limestone beds and layers of nodules  
69 are considered to have formed diagenetically within light marl beds while the much rarer  
70 laminated limestone beds and laminated limestone nodules formed within primary laminated  
71 shale beds (Hallam, 1964; Weedon, 1986; 1987a; Arzani, 2004).

72 Weedon (1986; 1987a) showed, using time-series analysis, that the alternation of the  
73 limestone with the non-limestones can encode a similar signal of regular cycles to that of the  
74 alternating homogeneous and laminated rock types. However, in thicker sections such as

those exposed on the West Somerset Coast, multiple limestone beds and/or nodule horizons occur within thick (tens of centimetre- to metre-scale) light marl beds. A recent analysis of orbital forcing in the relatively thick sections on the West Somerset Coast (Ruhl *et al.*, 2010) specifically avoided sampling the limestones that nonetheless represent a critical part of the sequence. This paper is designed to clarify the nature of the information conveyed by the limestones, both laminated and homogeneous.

----- Figure 1 near this position -----

New, high-resolution lithostratigraphic and magnetic-susceptibility logs for four sections (Fig. 1) are presented together with refinements of the ammonite biostratigraphy. The sections chosen within ‘typical offshore’ Blue Lias, span all the ammonite zones of the Hettangian Stage and represent a wide range of net accumulation rates. The aims are to explain why: a) limestone bed thicknesses are apparently independent of the net accumulation rate; b) the spacing of the limestone beds within ammonite zones can be related to Milankovitch orbital cycles although there are large variations in spacing from zone to zone and from place to place; c) laminated limestone beds and laminated limestone nodules are comparatively rare; and d) some limestone beds preserve abundant ammonite fossils, but others preserve none. We present new evidence for intra-formational hiatuses and a synthesis of limestone formation in terms of combined climatic and sea-level controls plus an improved understanding of the preservation of the ammonites.

## 2. Bio- and chronostratigraphy

### 2.a. Ammonite biochronology and correlation

The Jurassic System is divided into a sequence of 11 globally applicable stages that are subdivided, without gaps or overlap, into regional sequences of ammonite-correlated ‘zones’ (Ogg & Hinnov, 2012). Since ammonite zones completely fill each stage, and are

1  
2  
3  
4  
5  
6  
7  
8  
9  
10  
11  
12  
13  
14  
15  
16  
17  
18  
19  
20  
21  
22  
23  
24  
25  
26  
27  
28  
29  
30  
31  
32  
33  
34  
35  
36  
37  
38  
39  
40  
41  
42  
43  
44  
45  
46  
47  
48  
49  
50  
51  
52  
53  
54  
55  
56  
57  
58  
59  
60

100 now usually explicitly defined with a basal stratotype, they can also be considered to be  
101 chronostratigraphical units (Callomon, 1985; 1995; Page, 1995; 2003; **in press**). The great  
102 majority of zones do not conform in any way to a classical biozone since they do not  
103 correspond to the range of any ammonite species or assemblage.

104 In the present work, we refer neutrally to the ammonite-correlated stratigraphical units  
105 as ‘Standard’ Zones and Subzones (*sensu* Callomon, 1985), rather than using an epithet to  
106 describe their character (i.e. ‘chronozone’ and ‘subchronozone’ as in Page, 2010a; 2010b;  
107 2010c). However, as chronozones, these units can be explicitly correlated using proxies other  
108 than ammonites, such as local lithological changes, other faunal or floral elements and  
109 isotopic ‘events’ (Jenkyns *et al.*, 2002).

110 Throughout the Jurassic System, infra-subzonal units that are often referred to as  
111 biohorizons provide a very high-resolution biochronology. Biohorizons typically correspond  
112 to the stratigraphic range of a specific indicator species. Normally, the bases of ammonite  
113 Standard Zones are explicitly, or effectively, defined by the bases of specific biohorizons, and  
114 hence correlated, as potential timelines, by the stratigraphically lowest occurrences of the  
115 indicator species.

116 The initial biohorizonal framework for the Lower Sinemurian Stage in the UK of  
117 Page (1992) led to the schemes applied by Page (2002; 2010b) to the Devon and Dorset  
118 coastal sections. The scheme for the Hettangian Stage of the Devon/Dorset coast (Page,  
119 2010b; 2010c) was based largely on the version for West Somerset by Page (2005), but recent  
120 re-sampling of the latter area has revealed even greater biostratigraphical detail, which is used  
121 here. This new scheme provides a sequence of 55 biohorizons for the Hettangian, as opposed  
122 to the 27 used by Page (2010b; 2010c).

123 Zonal and subzonal boundaries throughout the Hettangian have been reviewed, based  
124 on new sampling by K. N. P. on coastal sections (Fig. 1a) in East Devon (Lyme Regis), West

Somerset (Doniford, St Audries Bay, East Quantocks Head to Kilve) and South Glamorgan, South Wales (St. Mary's Well Bay, Lavernock). The biohorizon boundaries, where constrained to within a few centimetres stratigraphically, are indicated in Table 1. Within the Lower Sinemurian of West Somerset, the placement of biohorizon boundaries are as previously published (e.g. Bloos & Page, 2000b; Page 2010b; 2010c).

-----Table 1 near this position-----

## 2.b. The base of the Jurassic

The Global Stratigraphic Section and Point (GSSP) for the base of the Jurassic has been defined in the Kuhjoch section in the Austrian Calcareous Alps (Hillebrandt, Krystyn & Kuerschner, 2007; Hillebrandt & Krystyn, 2009). Subsequently Page (2010b; 2010c) revised the zonal framework for the base of the Hettangian Stage in the UK by inserting the former authors' Tilmanni Zone below the Planorbis Zone (which was previously considered to be the lowest zone of the Jurassic System).

Page (2010b; 2010c) concluded that only the top of the Tilmanni Zone in the UK had yielded ammonites, specifically *Psiloceras erugatum* (Phillips) as illustrated by Bloos & Page (2000a). Nevertheless, in the UK the base of the Zone and hence the base of the Jurassic System can still be approximated using the most positive part of a positive  $\delta^{13}\text{C}_{\text{org}}$  interval, as demonstrated by Clémence *et al.* (2010). At St Audries Bay on the West Somerset coast (Fig. 1), the base of the Hettangian corresponds to a level less than 1.5 m above the base of the Blue Lias Formation (Clémence *et al.*, 2010). At St Mary's Well Bay near Lavernock, South Wales (Fig. 1), the  $\delta^{13}\text{C}_{\text{carb}}$  curve of Korte *et al.* (2009), based on measurements of *Liostrea* sp. samples, suggests that the base of the Jurassic System lies about 1.9 m above the top of the Langport Member (Penarth Group, Upper Triassic). The  $\delta^{13}\text{C}_{\text{carb}}$  curve produced

1  
2  
3  
4  
5  
6  
7  
8  
9  
10  
11  
12  
13  
14  
15  
16  
17  
18  
19  
20  
21  
22  
23  
24  
25  
26  
27  
28  
29  
30  
31  
32  
33  
34  
35  
36  
37  
38  
39  
40  
41  
42  
43  
44  
45  
46  
47  
48  
49  
50  
51  
52  
53  
54  
55  
56  
57  
58  
59  
60

from bulk sediment samples from the coast at Lyme Regis on the Devon/Dorset border by Korte *et al.* (2009) is, however, of limited use for correlation because it does not show the same signature as elsewhere. Nevertheless, it is likely that the base of the Jurassic System in the area also lies in the lowest part of the Blue Lias Formation.

154

155                   **2.c. The base of the Planorbis Zone**

156                   The base of the Planorbis Zone, as correlated by the first appearance of *Neophyllites* at the base of the Hn3 *imitans* Biohorizon (Page, 2010a), corresponds to the base of bed 9 of Whittaker & Green (1983) on the West Somerset Coast (Page & Bloos, 1995; Bloos & Page 2000a). In South Glamorgan, in St. Mary’s Well Bay, Lavernock, the base of the Planorbis Zone is about 12 cm below the base of bed 30 of Waters and Lawrence (1987): i.e. the level indicated by Hodges (1994) within his bed 38. At Lyme Regis, this level correlates with the base of bed H25 of Lang (1924); see Page (2002).

163

164                   **2.d. Southam Quarry near Long Itchington**

165                   At Southam Quarry, Long Itchington, Warwickshire, below bed 10 of Clements *et al.* (1975; 1977) ammonites are rare (Radley, 2008) and the lowest part of the Blue Lias Formation is inferred to belong to the Liasicus Zone (i.e. the Tilmanni and Planorbis zones are missing). This interpretation follows from the location of Long Itchington in relation to the reconstructed age of onlap of the Blue Lias Formation onto the London-Brabant Platform by Donovan, Horton & Ivimey-Cook (1979). Furthermore, it is consistent with the records of Old, Sumbler, & Ambrose (1984, p. 34), who cite *Laqueoceras* and *Waehneroceras* ‘close above the Langport Member’ at Southam Quarry. *Laqueoceras* certainly indicates the lower part of the Laqueus Subzone Hn18 Biohorizon of Page (2010b; 2010c). However, specimens of *Waehneroceras* from Southam Quarry include species from the upper part of the Portlocki



Subzone, including abundant examples of *W. portlocki* (Wright), in limestone nodules and rare *W. cf. shroederi* Lange in limestone beds. These observations suggest that at least biohorizons Hn16 and Hn17 of Page (2010b; 2010c) are also present.

178

### 179 **3. The sections studied and the lithostratigraphic and magnetic-susceptibility** 180 **logs**

181 Lithological logging, whilst measuring magnetic susceptibility (MS) in the field,  
182 utilized the five microfacies or rock-types of Weedon (1986; 1987a), as adopted by others  
183 (e.g. Bottrell & Raiswell 1989, Arzani 2004; 2006; Paul, Allison & Brett 2008) i.e.  
184 homogeneous grey limestone, laminated grey limestone, light grey marl, dark grey marl and  
185 millimetre-laminated black shale. Limestone nodules occur within light marl beds and locally  
186 pass laterally into continuous limestone beds (e.g. at Lyme Regis bed 37 or 'Rattle': Lang  
187 (1924) and Hesselbo & Jenkyns (1995) provide all the limestone bed names for the  
188 Devon/Dorset coast). Laminated limestone nodules occur within the laminated black shales.  
189 Large differences in net accumulation rates in the sections studied are suggested by the  
190 thicknesses of zones shown in Fig. 1b, and the average composition of the rock-types is  
191 indicated in Fig. 1c and discussed further in Section 4.

192

#### 193 **3.a. Measurements of magnetic susceptibility in the field**

194 Volume magnetic susceptibility (vol MS) logging of sections used a Bartington  
195 Instruments MS2 meter combined with an F-probe in direct contact with fresh faces of rock  
196 at right angles to the bedding. Instrument drift, related to temperature changes, was removed  
197 by taking measurements in the air more than 1 metre from the cliff face between each rock-  
198 surface measurement. At the levels of limestone nodules, MS was measured in the limestone  
199 rather than light marl in cases where limestone constituted more than half of that stratigraphic

1  
2  
3  
4  
5  
6  
7  
8  
9  
10  
11  
12  
13  
14  
15  
16  
17  
18  
19  
20  
21  
22  
23  
24  
25  
26  
27  
28  
29  
30  
31  
32  
33  
34  
35  
36  
37  
38  
39  
40  
41  
42  
43  
44  
45  
46  
47  
48  
49  
50  
51  
52  
53  
54  
55  
56  
57  
58  
59  
60

level (Weedon *et al.*, 1999). As far as possible, calcite ‘beef’ veins and lenses (Richardson, 1923; Marshall, 1982), most prevalent at the base of laminated shale beds at Lyme Regis, were avoided during MS measurement.

----- Figure 2 near this position -----

Measurements of weight-specific MS (wt MS) using a Bartington Instruments MS2B sensor for samples from Lyme Regis, and the West Somerset coast show the expected strong, linear correlation with vol MS (Pearson’s  $r = +0.967$ ,  $N = 74$ ,  $P < 0.001$ , Fig. 2a). This relationship and the similarity of both the vol MS and wt MS logs to %CaCO<sub>3</sub> in Fig. 2b confirm that the field measurements are neither significantly affected by changes in magnetic properties due to weathering, nor by incomplete rock sensing due to imperfect surface contact and/or undetected voids.

The lithological columns shown in Figs 3–6, with captions indicating the references used in bed numbering, illustrate large variations in the thickness of the marls and shales and highly variable spacing and overall proportions of limestone beds. In the logs, the laminated black shales are shown as the most recessed lithology on the profiles as a convention to aid their identification rather than as an indication of the lowest resistance to weathering. The fixed spacing of the MS measurements at each section was designed to resolve the smallest variations in bulk composition. The measurements were obtained at 2 cm spacing at Lyme Regis; 3 cm at Southam Quarry, Long Itchington and 4 cm spacing on both the West Somerset coast and at St. Mary’s Well Bay, Lavernock. In Southam Quarry, the faces were measured for magnetic susceptibility in 1994 when the section in the south west between the A423 and the A426 was fully accessible down to the disconformity with the Upper Triassic Langport Member. The vol MS log for Lyme Regis was reported previously (Weedon *et al.*, 1999) but Fig. 4, primarily of the Hettangian portion, shows revisions to the zonal and subzonal boundaries.

----- Figure 3 near this position -----

The log for the West Somerset coast (Fig. 5a and b; Palmer, 1972; Whittaker & Green, 1983) is composite. The section at St Audries Bay was measured from the base of the Blue Lias Formation to the top of bed 101 of Whittaker & Green (1983), overlapping the MS log at Quantock's Head by about 3.5 m. The Quantock's Head to Kilve section was measured for MS from bed 97 to bed 163. The splice level of the composite record in bed 96, at 56.90 m above the base of the Blue Lias Formation, represents the base of the Quantock's Head magnetic-susceptibility log. Note that in Table 1 the biohorizon levels of the Quantock's Head section are listed both relative to the base of the log (i.e. at the splice level) and relative to the base of the Formation according to the heights of the St Audries Bay section within the composite column.

----- Figure 4 near this position -----

### 3.b. Origin of the variations in vol MS

It was reported previously for the Blue Lias Formation that MS is inversely correlated with %CaCO<sub>3</sub> (Hounslow, 1985; Weedon *et al.*, 1999; Deconinck *et al.*, 2003; Ruhl *et al.*, 2010). This relationship is supported by current measurements of wt MS using a Bartington Instruments MS2B cavity sensor and vol MS (Fig. 2a). The right-hand linear regression line of Fig. 2a allows estimation of carbonate contents from the field measurement of vol MS (using: %CaCO<sub>3</sub> = 99.06 – (13.79 x vol MS),  $r = -0.892$ ,  $N = 74$ ,  $P < 0.001$ ). Calcium carbonate measurements have been shown as open circles on top of the MS logs in Figs 4 and 5 by scaling %CaCO<sub>3</sub> (bottom scale) relative to the vol MS (top scale) according to this regression. Despite the good agreement between the estimated and measured %CaCO<sub>3</sub> shown on the right of Fig 2b, the uncertainty (95% confidence interval) in individual estimates of %CaCO<sub>3</sub> from vol MS using the regression is about ±20.0% – ranging between ±19.6 and

1  
2  
3  
4  
5  
6  
7  
8  
9  
10  
11  
12  
13  
14  
15  
16  
17  
18  
19  
20  
21  
22  
23  
24  
25  
26  
27  
28  
29  
30  
31  
32  
33  
34  
35  
36  
37  
38  
39  
40  
41  
42  
43  
44  
45  
46  
47  
48  
49  
50  
51  
52  
53  
54  
55  
56  
57  
58  
59  
60

±20.4%, depending on the difference between the individual vol MS and the mean vol MS  
(Williams, 1984, p. 313).

----- Figure 5a near this position -----

----- Figure 5b near this position -----

The average MS values for these mudrocks are fairly low, thereby contrasting with  
younger British Jurassic cyclic mudrocks such as the Kimmeridge Clay Formation (Weedon  
*et al.*, 1999). It was shown for the Blue Lias Formation (Hounslow, 1985; Bixler, Elmore &  
Engel, 1998; Deconinck *et al.*, 2003; Hounslow, Posen & Warrington, 2004) that the  
stratigraphic variations in MS are consistent with variable dilution of paramagnetic clays by  
non-ferroan, and thus diamagnetic, calcite (wt MS = +0.84 x10<sup>-8</sup> SI, Bleil & Petersen, 1987).  
Note that despite the presence of locally rather large percentages of pyrite (maximum 12% in  
the laminated shales, Weedon, 1987a) in a pure, unweathered, state this mineral is also  
diamagnetic (wt MS = -0.48 x10<sup>-8</sup> SI, Collinson, 1983) and consequently contributes very  
little to the whole-rock MS signal. Hence, stratigraphic logs of MS in the Blue Lias  
Formation provide an accurate picture of the occurrence of the limestones (Figs 2a, 2b and 3).

The marls and shales of the Liasicus Zone at all four localities have consistently  
higher average MS than the underlying Tilmanni and Planorbis and overlying Angulata and  
Bucklandi zones (Figs 3–6, Weedon *et al.*, 1999; Deconinck *et al.*, 2003). This observation  
suggests that there were long-term (zonal-scale) variations in the composition of the  
paramagnetic (mainly clay mineral) components (Deconinck *et al.*, 2003). The relatively high  
average MS of the lower part of the section in Southam Quarry (Fig. 6) is consistent with the  
interpretation (Section 2.d) that the lowermost strata that lie disconformably on the Langport  
Member belong to the Liasicus Zone and not to the Planorbis Zone.

At about the 31 m level in the mid-Liasicus Zone (upper Portlocki Subzone) of the St  
Audries Bay section (Fig. 5a), the average vol MS is unusually high with values extending

outside the range of the %CaCO<sub>3</sub> versus vol MS regression of Fig. 2a. Lower stratigraphic resolution sampling by Deconinck *et al.* (2003) indicates that, at this level on the West Somerset coast, the clay minerals switch to higher kaolinite/illite ratios, but surprisingly, not to iron-rich clays. The unusually high MS might indicate an association of increased kaolinite with a source of different paramagnetic components and/or small amounts of ferromagnetic components such as magnetite-like minerals that, unusually for the Blue Lias Formation, survived dissolution by H<sub>2</sub>S during diagenesis (Deconinck *et al.*, 2003). A similar interval of unusually high values of vol MS, of around  $8.0 \times 10^{-8}$  SI, is found at about 8.2 m in Southam Quarry in the Liasicus Zone (Fig. 6). This interval of high average MS in the marls and shales is located at the top of the Portlocki subzone, Liasicus Zone at both St Audries and Lyme Regis and may provide a correlatable change in paramagnetic mineralogy (Figs 4 and 5a).

----- Figure 6 near this position -----

#### 4. Variations in whole-rock composition

The typical 'offshore' facies of the Hettangian Blue Lias Formation of interest here shows considerable lateral and stratigraphic variations in bulk composition as discussed in Sections 4.b and 4.c. To provide a context for these descriptions we start with consideration of the 'marginal facies'.

##### 4.a. Marginal facies and 'near-shore' Blue Lias

The Blue Lias was deposited at the same times as palaeo-coastline deposits that include the Sutton Stone and Southerndown Beds of South Glamorgan (Trueman, 1920; 1922; Hallam, 1960; Wobber, 1965; Fletcher, 1988; Sheppard, 2006) and the Brockley Down Stone of the Radstock Plateau near Bristol (D. L. Loughman, unpub. Ph.D. thesis, University of Birmingham, 1982; Donovan & Kellaway, 1984). These so-called marginal facies, formed

1  
2  
3  
4  
5  
6  
7  
8  
9  
10  
11  
12  
13  
14  
15  
16  
17  
18  
19  
20  
21  
22  
23  
24  
25  
26  
27  
28  
29  
30  
31  
32  
33  
34  
35  
36  
37  
38  
39  
40  
41  
42  
43  
44  
45  
46  
47  
48  
49  
50  
51  
52  
53  
54  
55  
56  
57  
58  
59  
60

at and close to palaeo-coastlines, lie unconformably on Carboniferous Limestone and comprise conglomeratic limestones with grainstone textures including Carboniferous Limestone and chert lithoclasts, derived bioclasts, ooids and bioclasts (Wobber, 1965; 1966; Fletcher, 1988).

On the coast near Southerndown, Glamorgan, 31 km west north west of the exposure at Lavernock (Fig. 1a), the unconformity surface is exposed and consists of multiple wave-cut platforms overlain by associated successive breccia and conglomeratic and grainstone limestones of the Sutton Stone (Fletcher, 1988; Sheppard, 2006). Both the unconformity surface and Carboniferous Limestone lithoclasts in the overlying Sutton Stone have *Trypanites* borings and are encrusted by oysters and colonial corals (Johnson & McKerrow, 1995; Simms, Little & Rosen, 2002; Sheppard, 2006). Some lithoclasts in the Sutton Stone are imbricated (Wobber, 1963) and elongate bioclasts have been used as palaeocurrent indicators that indicate long-shore drift and complex current movements influenced by the local islands of Carboniferous rocks (Wobber, 1966). The matrix-supported and rounded boulder- and cobble-sized lithoclasts in the Sutton Stone are succeeded stratigraphically by pebble-grade lithoclasts, micrites and thin shales of the Southerndown Beds, which grade laterally into the near-shore facies of Blue Lias (Trueman, 1922; Wobber, 1965; Wilson et al., 1990; Sheppard, 2006).

Although the platform erosion probably started in the latest Triassic, ammonites have been recovered in stratigraphic order from the Sutton Stone and Southerndown Beds from the Planorbis, Liasicus and Angulata Zones (Hodges, 1986; Sheppard, 2006). These observations are not consistent with nearly instantaneous deposition of the Sutton Stone by a single hurricane (Ager, 1986), but rather with the latest Triassic and Early Jurassic erosion of the wave-cut platforms and deposition of the marginal facies under storm influence over millions

324 of years during episodic rises in relative sea level (Trueman, 1922; Fletcher, 1988; Sheppard,  
325 2006).

326 Just six kilometres south of the palaeo-coastline of Southerndown at Nash Point, the  
327 Blue Lias of the Bucklandi Zone represents an atypical limestone-dominated facies often full  
328 of bioclast fragments in both the marls and limestones (Hallam, 1960; Weedon, 1987a;  
329 Trueman, 1930). These strata representing Units B and C of the Porthkerry Formation have  
330 much higher limestone proportions than found in more 'typical' Blue Lias (an average of 60  
331 to 85 % limestone by thickness in sections tens of metres thick, Waters & Lawrence, 1987;  
332 Wilson et al., 1990; Warrington & Ivimey-Cook, 1995). Units B and C consist of metre-scale  
333 bedding units formed of closely spaced nodular limestones and 'anastomosing mudstone  
334 beds' that probably result from pressure dissolution (Waters & Lawrence, 1987). Occasional  
335 decimetre-scale mudstone beds are present, permitting correlation of limestone-shale bed  
336 groups, but organic-carbon contents are low and neither laminated shales nor laminated  
337 limestones are present (Sheppard, Houghton & Swan, 2006). Although much of the bedding  
338 was formed purely during diagenesis, the presence of hummocky cross-stratification at Nash  
339 Point proves strong storm influences (Sheppard, Houghton & Swan, 2006).

340 Thirty kilometres from the palaeo-coastline of South Glamorgan, typical 'offshore'  
341 Blue Lias facies is present at Lavernock in the Tilmanni to Liasicus zones as logged here  
342 (Fig. 3). In the lower part of the Angulata Zone Unit A of the Porthkerry Formation consists  
343 of about 55 % by thickness of normal offshore Blue Lias with nodular limestones and marls.  
344 However, in the same area near Cardiff, the upper part of the Angulata Zone, 'Unit B' of the  
345 Porthkerry Formation of Waters and Lawrence (1987), is of a similar facies to the Bucklandi  
346 Zone at Nash Point. The Porthkerry Formation is overlain gradationally by uppermost  
347 Angulata Zone and Bucklandi Zone oolitic 'marginal facies' (Waters & Lawrence, 1987).  
348 Thus, Units B and C of the Porthkerry Formation near Cardiff and Nash Point represent a



1  
2  
3  
4  
5  
6  
7  
8  
9  
10  
11  
12  
13  
14  
15  
16  
17  
18  
19  
20  
21  
22  
23  
24  
25  
26  
27  
28  
29  
30  
31  
32  
33  
34  
35  
36  
37  
38  
39  
40  
41  
42  
43  
44  
45  
46  
47  
48  
49  
50  
51  
52  
53  
54  
55  
56  
57  
58  
59  
60

349 ‘near-shore’ facies of the Blue Lias, which has been envisaged as a storm-derived aragonitic  
350 lime mud deposited on a marine shelf (Sheppard, Houghton & Swan, 2006).

351

352 **4.b. Rock-type compositions**

353 The different rock-types of the ‘typical’ or ‘offshore’ Blue Lias consist mostly of  
354 various proportions of bioclasts, calcite microspar, clay minerals, organic matter, pyrite and  
355 minor quartz silt (Hallam, 1960; Weedon, 1986; 1987a). Whole rock compositions quoted  
356 here are based on the samples from both Lyme Regis and the Somerset Coast (Weedon,  
357 1987a). Numbers of samples by rock type and locality are indicated in the caption for Fig. 1c  
358 and sample locations are indicated in Figs 4 and 5. The limestones (total organic carbon,  
359 TOC, mean = 0.54% ± 0.09 (±95% confidence interval), range = 0.14 to 1.64%, *N* = 48;  
360 CaCO<sub>3</sub>, mean = 79.3% ± 2.2, range = 51.8 to 88.7%, *N* = 48) form beds with contacts ranging  
361 from planar to nodular. Limestone nodules are typically entirely enclosed by light marl but  
362 can be ‘welded’ onto limestone beds. On the Devon/Dorset and West Somerset coasts, when  
363 seen in plan on the foreshore, limestone nodules are often found to be linked laterally at some  
364 levels. The limestones generally have a homogeneous bioclastic wackestone to bioclastic  
365 carbonate mudstone fabric reflecting the thoroughly bioturbated nature of the precursor light  
366 marls. The light marls (TOC mean = 1.42% ± 0.26, range = 0.38 to 4.41%, *N* = 40; CaCO<sub>3</sub>,  
367 mean = 43.8% ± 2.7, range = 25.7 to 69.9%, *N* = 40) are friable and homogeneous with  
368 planar contacts against dark marls and laminated shale beds.

369 Normally the dark marls (TOC mean = 2.35% ± 0.41, range = 0.51 to 6.51%, *N* = 39;  
370 CaCO<sub>3</sub>, mean = 40.1% ± 3.7, range = 19.9 to 61.0%, *N* = 39) are homogeneous like the light  
371 marls and friable, but can become fissile on weathering. However, Fig. 7a shows a laminated  
372 dark marl fabric, not visible in the field, consisting of abundant microspar lenses in places  
373 forming nearly continuous laminae that alternate with other laminae comprising clay and



organic matter (Weedon, 1987a). The figure shows a *Chondrites* burrow with a homogeneous light marl filling that penetrates the dark marl fabric. Burrow mottles at the contacts of light and dark marl beds are common at Lyme Regis as both light marl burrow-fills within dark marl and *vice versa* (Hallam, 1964).

The laminated shales (TOC mean =  $5.46\% \pm 0.77$ , range = 1.53 to 12.80%,  $N = 51$ ;  $\text{CaCO}_3$ , mean =  $35.5\% \pm 3.4$ , range = 11.6 to 68.4%,  $N = 51$ ), usually with sharp basal bedding contacts against dark marl or light marl, produce a brown streak when scratched and weather into fissile, sometimes paper thin, laminae. Sub-microscopically they have scattered calcite microspar lenses dispersed within wavy sub-millimetre laminae of clay and organic matter (Weedon, 1987a). Laminated limestone (TOC mean =  $1.42\% \pm 0.67$ , range = 0.90 to 3.00%,  $N = 7$ ;  $\text{CaCO}_3$ , mean =  $77.2\% \pm 6.2$ , range = 62.4 to 87.2%,  $N = 9$ ) forms beds that have planar contacts with laminated shale beds or nodules that are enclosed entirely by laminated shale (Weedon, 1987a; Arzani, 2004).

----- Figure 7 near this position -----

Hallam (1987) and Arzani (2006) doubted the presence of rock-forming quantities of nannofossils as a possible precursor to the microspar. However, calcareous nannofossils, both as true coccoliths as well as *Schizosphaerella*, are well documented from throughout the Tilmanni to Bucklandi zone interval at Lyme Regis and on the West Somerset coast (Hamilton, 1982; Bown, 1987; Bown & Cooper, 1998; Van de Schootbrugge *et al.*, 2007; Clémence *et al.*, 2010). Indeed, Weedon (1986; 1987a; 1987b) argued that the microspar lenses in the dark marls and laminated shales represent neomorphosed zooplankton faecal pellets containing calcareous nannofossils. Very similar fabrics to Fig. 7a are known in the Kimmeridge Clay Formation of Dorset (Kimmeridgian to Tithonian, Fig. 2d, f and g of Pearson, Marshall & Kemp, 2004), which has abundant nannofossils (e.g. Young & Bown, 1991; Lees, Bown & Young, 2006). Aggregates of nannofossils surrounded by clay minerals

1  
2  
3  
4  
5  
6  
7  
8  
9  
10  
11  
12  
13  
14  
15  
16  
17  
18  
19  
20  
21  
22  
23  
24  
25  
26  
27  
28  
29  
30  
31  
32  
33  
34  
35  
36  
37  
38  
39  
40  
41  
42  
43  
44  
45  
46  
47  
48  
49  
50  
51  
52  
53  
54  
55  
56  
57  
58  
59  
60

and organic matter in the Blue Lias Formation (Figs 8b, 8c and 8d; figure 3 of Weedon, 1986; figures 6B and 6C of Arzani, 2006) have similar dimensions to the microspar lenses, supporting their interpretation as neomorphosed zooplankton faecal pellets (Pearson, Marshall & Kemp, 2004).

Weedon (1986; 1987a) argued that nannofossil preservation was best in the more organic carbon-rich laminated shales and dark marls, as confirmed recently by Clémence *et al.* (2010). The high organic-carbon contents may have helped the preservation of primary organic coatings on the coccoliths, which in turn prevented calcite dissolution by acidic pore waters during diagenesis (Bukri, Dent Glasser & Smith, 1982). In the less organic-carbon-rich sediments, partial or total microspar aggradation of nannofossils (e.g. Fig. 8b) was inferred to be the normal situation in the Blue Lias (Weedon, 1986; 1987a; 1987b). The homogeneity of the light marls and most of the dark marls was explained as resulting from burrowers mixing the organic-matter- and clay-rich laminae with faecal pellets. In the limestones and light marls, however, very rare isolated elliptical structures, representing partially corroded or overgrown coccoliths provide the only *in situ* evidence for calcareous nannofossil precursors to the microspar (Fig. 8e; Fig. 2.4B of Weedon, 1987a).

If most carbonate mud in the ‘offshore’ Blue Lias Formation was derived from very shallow coastal waters rather than from nannofossil material, different localities would be expected to have different rock-type compositions. However, the average %CaCO<sub>3</sub> and %TOC of the limestone, light marl, dark marl and laminated shales are statistically indistinguishable between the Devon/Dorset coast and the West Somerset coast sections (i.e. overlapping 95% confidence intervals in Fig. 1c). Therefore, considering the large difference in zonal and average bed thicknesses between these locations, the lithological composition of the offshore Blue Lias facies was not influenced by either the local net accumulation rates or by local differences in water depth. The consistency of facies between localities and across

the range of accumulation rates represented is consistent with a primarily hemipelagic, rather than shoreline-influenced origin for the carbonate mud (Weedon, 1986).

The majority of the laminated limestone beds were formed by the coalescence of laminated limestone nodules (Weedon, 1987a; Arzani, 2004). However, at Lyme Regis, bed H30 categorized as laminated limestone does not have internal lamination but is homogeneous and without macrofossils. As for laminated limestone beds H32 and H36, it is underlain and overlain by laminated shale, has sharp planar top and bottom contacts, and has exceptionally low, slightly negative magnetic susceptibility values. The lowest measured vol MS of  $-0.13 \times 10^{-8}$  SI implies, by extrapolating the regression of Fig. 2a (Section 3.b), 97.3 %CaCO<sub>3</sub> and hence these limestones represent cementation of a primary sediment almost devoid of organic matter and clay. Partly due to the sharp, planar base Hesselbo & Jenkyns (1995) inferred a dilute turbidity-current origin for bed H30 (which they named 'Intruder'). However, in the absence of direct evidence for basal erosion, grading or cross-lamination alternative explanations for the deposition of almost pure carbonate mud should be considered.

439

#### 440 **4.c. Lateral and stratigraphic variations in limestone proportions**

Unlike the marls and laminated shale beds, average limestone bed thicknesses are consistently close to 10-15 cm at all the logged localities and in every zone of the Hettangian (Fig. 1b). Hallam (1964; 1986) regarded the consistency in limestone bed thickness of the Blue Lias, independent of locality and zonal thickness, as indicative of a diagenetic rather than a primary control on limestone formation. Although average limestone bed thicknesses remain nearly constant, the proportion of limestone beds by thickness per ammonite zone varies substantially from place to place and stratigraphically (Fig. 1b). Areas with thinner biozones (lower net accumulation rate or 'condensed sections') have higher average

1  
2  
3  
4  
5  
6  
7  
8  
9  
10  
11  
12  
13  
14  
15  
16  
17  
18  
19  
20  
21  
22  
23  
24  
25  
26  
27  
28  
29  
30  
31  
32  
33  
34  
35  
36  
37  
38  
39  
40  
41  
42  
43  
44  
45  
46  
47  
48  
49  
50  
51  
52  
53  
54  
55  
56  
57  
58  
59  
60

449 proportions of limestone (Fig. 1b, figure 2 of Page, 1995). For example, all four ammonite  
450 zones of the Hettangian of Lyme Regis have a far higher proportion of limestone than those  
451 on the West Somerset coast (Fig. 1b).

452         At Lyme Regis, representing an area of low net accumulation rate, all the zones of the  
453 Hettangian are of similar thickness and the average bed thicknesses for all rock types are also  
454 similar in the different zones (Fig. 1b). By contrast, on the West Somerset coast the oldest  
455 zones (Tilmannti and Planorbis) are much thinner than the succeeding (Liasicus and Angulata)  
456 zones; significantly, the large change in zonal thickness there is mirrored by changes in  
457 average bed thickness of the light and dark marls and the laminated shales (Fig. 1b).

458         The association of changes in average non-limestone bed thickness with changing  
459 zonal thickness is interpreted here as indicating a large change in net accumulation rates at  
460 the end of the Planorbis Zone times or start of the Liasicus Zone for sections on the West  
461 Somerset coast. In this study, only the base of the Liasicus Zone was logged at Lavernock  
462 (Fig. 3). However, the much greater thickness of the Liasicus Zone interval at Lavernock  
463 compared to the Tilmannti and Planorbis zones (Waters & Lawrence, 1987; Warrington &  
464 Ivimey-Cook, 1995) indicates a similar change in net accumulation rate to that of the West  
465 Somerset coast.

466         The Liasicus Zone is consistently associated with lower proportions of limestone than  
467 preceding and succeeding Hettangian zones in different localities (Fig. 1b, Hallam, 1960;  
468 Palmer, 1972). This difference in character has led to member-scale subdivisions of the Blue  
469 Lias Formation with locally applied names i.e. the Lavernock Shales (Richardson, 1905;  
470 Waters & Lawrence, 1987); the St Audries Shales (Palmer, 1972) and the Saltford Shales  
471 (Donovan, 1956; Ambrose, 2001).

472         In the lower Liasicus Zone, higher velocities on downhole sonic logs related to  
473 relatively higher clay content, and higher gamma-ray counts related both to thorium and

1  
2  
3 474 potassium in the marls and shales and to uranium within organic matter, allow ready  
4  
5 475 correlation of this portion of the Blue Lias across Britain (Whittaker, Holliday & Penn,  
6  
7 476 1985). The base of this mudrock-dominated interval is diachronous because, in the English  
8  
9 477 Midlands, there is biostratigraphical evidence that it occurs within the Planorbis Zone (Old,  
10  
11 478 Sumbler & Ambrose 1987; Ambrose 2001), whereas in West Somerset and Lavernock the  
12  
13 479 base is close to the base of the Liasicus Zone (Figs 3 and 5).  
14  
15

16 480 Mapping of the oldest strata of the Blue Lias Formation on the London-Brabant  
17  
18 481 Platform and the Radstock Plateau near Bristol shows that the Liasicus Zone in the  
19  
20 482 Hettangian and Semicostatum Zone of the Sinemurian were times of accelerated onlap  
21  
22 483 (Donovan, Horton & Ivimey-Cook, 1979; Donovan & Kellaway, 1984). An inferred sea-level  
23  
24 484 rise during these zones was suggested by Hallam (1981) and broadly supported by Hesselbo  
25  
26 485 & Jenkyns (1998) and Hesselbo (2008).  
27  
28

29 486 At Lyme Regis, in the Liasicus Zone, the zonal thickness and the average thicknesses  
30  
31 487 of the various rock-types are similar in the overlying and underlying zones, but there is  
32  
33 488 nevertheless a lower proportion of limestone (Fig. 1b). Therefore, rising sea levels were  
34  
35 489 apparently associated with reduced probability of limestone formation. The near-constancy of  
36  
37 490 net accumulation rate at Lyme Regis, as indicated by the near-uniform average bed  
38  
39 491 thicknesses of the marl and laminated shale, presumably resulted from an underlying tectonic  
40  
41 492 block maintaining a relatively level sea floor within turbulent-water depths (due to storm  
42  
43 493 winnowing) despite sea-level rise (Sellwood & Jenkyns, 1975). Apparently, rising sea levels  
44  
45 494 during the Liasicus Zone times at Lyme Regis led to slight increases in water depth and less  
46  
47 495 probability of limestone formation, but the increase in accommodation space was too small to  
48  
49 496 allow substantially increased net sedimentation rates.  
50  
51  
52  
53

54 497 On the West Somerset coast and at Lavernock, increased accommodation space and  
55  
56 498 higher sedimentation rates during the Liasicus Zone account for locally greater thicknesses of  
57  
58  
59  
60

1  
2  
3  
4  
5  
6  
7  
8  
9  
10  
11  
12  
13  
14  
15  
16  
17  
18  
19  
20  
21  
22  
23  
24  
25  
26  
27  
28  
29  
30  
31  
32  
33  
34  
35  
36  
37  
38  
39  
40  
41  
42  
43  
44  
45  
46  
47  
48  
49  
50  
51  
52  
53  
54  
55  
56  
57  
58  
59  
60

499 mudrocks (i.e. greater zonal thicknesses and greater average thickness of marl and laminated  
500 shale beds) compared to the Tilmanni and Planorbis zones (Figs 1b, 3, 5a). In these localities,  
501 the rapid increase in net accumulation rates apparently resulted from faster, probably fault-  
502 related, subsidence that was coincident with the sea-level rise (i.e. the increased subsidence  
503 rates exaggerated the effect of sea-level rise on local water depths). Fault-related activity is  
504 documented for the Hettangian in the Wessex Basin (Jenkyns & Senior, 1991) and South  
505 Glamorgan in South Wales (Wilson et al., 1990) and fault movement occurred at some point  
506 during the Jurassic associated with the Bristol Channel area (Waters & Lawrence, 1987;  
507 Bixler, Elmore & Engel, 1998). Furthermore, fossil methane seeps dating from the Bucklandi  
508 Zone in the Sinemurian might be related to fault movement on the West Somerset coast  
509 (Allison, Hesselbo & Brett, 2008; Price, Vowles-Sheridan & Anderson, 2008).

510         At Southam Quarry near Long Itchington, the majority of the Liasicus Zone strata  
511 consist of laminated shale (Figs 1b and 6). This observation might be thought to indicate that  
512 greater water depth due to sea-level rise in the Liasicus Zone was associated with the  
513 conditions required for the preservation of lamination (especially bottom-water dysoxia and  
514 anoxia, cf. Hallam & Bradshaw, 1979). However, in both West Somerset and Lyme Regis,  
515 although there is a reduction in the proportions of limestone in the Liasicus Zone, unlike  
516 Long Itchington the proportions of laminated shale are lower than in the succeeding Angulata  
517 Zone (Figs 1b, 4 and 5a and b; Weedon, 1987a). Hence, it is the formation of a lower  
518 proportion of limestones, not the development of laminated shales, which can be consistently  
519 related to rising sea level/greater water depth.

520

521         **5. Intra-formational hiatuses**

522         Weedon (1986; 1987a; 1987b) reasoned that differences between localities in the  
523 numbers of regular sedimentary cycles, thought to result from Milankovitch orbital forcing of

climate, could be explained by the presence of intra-formational hiatuses. Although Hallam (1960; 1987) disagreed, there are numerous lines of evidence, summarized in the sub-sections below, for both intermittent sea-floor erosion and for missing stratigraphic intervals within the offshore Blue Lias Formation of southern Britain.

----- Figure 8 near this position -----

### 5.a. Shaw plot

In Table 1 there are 63 levels in the Hettangian and Lower Sinemurian, out of 130 available, where the same biohorizon level (i.e. biohorizon top or biohorizon base) has been located to within a few centimetres both at Lyme Regis and on the West Somerset coast. This stratigraphic refinement allowed construction of the Shaw plot in Fig. 8 that illustrates the correlation of these two sites. At Lyme Regis, the base of the Angulata Zone lies somewhere between the lowest level with recorded *Schlotheimia* at 11.06 m (base of bed H84) and the highest recorded level with *Waehneroceras* at 9.66 m (within bed H71), as indicated by short horizontal lines in Fig. 8. Using the line of correlation between St Audries and Lyme Regis, its location has been inferred to be close to 10.54 m (within bed H77 Fig. 4, Table 1) as indicated using the long grey horizontal arrow in Fig. 8. Alternatively, the line of correlation from Quantock's Head rather than St Audries Bay, with fewer biohorizon constraints, would imply that the base of the Angulata Zone lies close to 10.13 m at Lyme Regis (within bed H73).

Subzones on the West Somerset coast sections are thicker than those in the corresponding section at Lyme Regis, as indicated in figures at the bottom of Fig. 8. Treating the biohorizon picks as time lines, the amount of strata within each interval results from the combination of the sedimentation rates and the effects of intra-formational hiatuses: i.e. the



1  
2  
3  
4  
5  
6  
7  
8  
9  
10  
11  
12  
13  
14  
15  
16  
17  
18  
19  
20  
21  
22  
23  
24  
25  
26  
27  
28  
29  
30  
31  
32  
33  
34  
35  
36  
37  
38  
39  
40  
41  
42  
43  
44  
45  
46  
47  
48  
49  
50  
51  
52  
53  
54  
55  
56  
57  
58  
59  
60

548 net accumulation rate. Shallower slopes on the line of correlation indicate higher net  
549 accumulation rates on the West Somerset Coast relative to the Devon/Dorset coast.

550 In contrast to the Lyme Regis section, on the West Somerset Coast the much thicker  
551 Liasicus and Angulata zones compared to the Tilmanni and Planorbis zones are mirrored by  
552 the increased average thicknesses of the corresponding marl and shale beds (Fig. 1b, Section  
553 4.c). Hence the major decrease in the average slope of the line of correlation in Fig. 8 at the  
554 base of the Liasicus Zone is interpreted as due to substantially increased net accumulation  
555 rates in West Somerset. In detail, the breaks in slope (nearly horizontal or nearly vertical  
556 segments) of the line of correlation are interpreted as due to hiatuses or intervals of  
557 exceptionally low accumulation rate, and have been labelled with the corresponding bed  
558 numbers. These breaks in slope of the line of correlation are discussed in Section 5.c. The  
559 breaks in slope are defined by multiple points, significantly reducing the likelihood that they  
560 simply result from mis-placing the tie-levels due to collection failure for key ammonites.

561  
562 **5.b. Minor erosion**

563 Several lines of field evidence for minor sea-floor erosion were used by Weedon  
564 (1986) to argue for storm-induced bottom-water turbulence. Protrusive *Diplocraterion*  
565 burrow mottles, which are found only within the limestones and light marls, have been  
566 described at all four localities studied here as well as at Saltford, Avon (Fig. 9c, Sellwood,  
567 1970; Donovan & Kellaway, 1984; Weedon, 1987a; Mogadam & Paul, 2000; Barras &  
568 Twitchett, 2007). Tiering analysis at Lyme Regis (Mogadam & Paul, 2000) showed that  
569 *Diplocraterion* cross-cuts all other trace fossils except *Chondrites* which is well known to  
570 have been produced by late-stage deposit feeders within anoxic sediments (Bromley &  
571 Ekdale, 1984). The observations of Mogadam & Paul (2000) suggest re-excavation of the



1  
2  
3 572 vertical U-shaped burrow following rapid centimetre-scale sediment removal (Seilacher,  
4  
5 573 2007).

6  
7 574 At Lyme Regis, dark marl beds that are only a few centimetres thick are locally  
8  
9 575 missing for several metres laterally (Weedon, 1986). Within limestone bed 23 ('Mongrel')  
10  
11 576 locally a thin dark marl bed is replaced laterally by centimetre-scale, metre-wide scours filled  
12  
13 577 with bioclastic packstone. The former presence of a thin bed of dark marl is in some places  
14  
15 578 recorded by a layer of isolated dark marl burrow mottles within what otherwise appears to be  
16  
17 579 a single limestone bed (e.g. in bed 19, Fig. 9d). In West Somerset, this phenomenon is  
18  
19 580 occasionally observed in thick light marl beds but more typically an opposite arrangement  
20  
21 581 occurs with isolated bands of light burrow-fills within dark marls representing relics of thin  
22  
23 582 light marl beds. Paul, Allison & Brett (2008) also noted that occasional 'exotic' sediment fills  
24  
25 583 within uncrushed ammonites at Lyme Regis could indicate material subsequently removed by  
26  
27 584 erosion.  
28  
29  
30

31  
32 585 Radley (2008) argued that at Southam Quarry, Long Itchington, erosion within  
33  
34 586 laminated shale was linked to distal storm influences below normal storm wave-base. He  
35  
36 587 described siltstone scour-fills within Liasicus Zone laminated shales as well as highly  
37  
38 588 elongated limestone nodules containing imbricated ammonites, which were interpreted as  
39  
40 589 gutter casts. The scour fills are associated with a trace fossil indicative of a crustacean escape  
41  
42 590 structure and therefore very rapid deposition (Radley, 2008; O'Brien, Braddy & Radley,  
43  
44 591 2009). Similar presumed scour fills, full of ammonites and shell fragments, within light marl  
45  
46 592 beds are also known in West Somerset, albeit mainly in the Planorbis Subzone (e.g. bed 24).  
47  
48

49  
50 593 A scour fill at Lyme Regis in the top of a limestone bed, probably from the Rotiforme  
51  
52 594 Subzone, Bucklandi Zone, consists of a shallow depression around 50 cm across filled with  
53  
54 595 coarse shelly debris and abundant small articulated echinoids (*Diademopsis*) and common  
55  
56 596 articulated ophiuroids (Page collection, Bristol City Museum and Art Gallery). These  
57  
58  
59  
60

1  
2  
3  
4  
5  
6  
7  
8  
9  
10  
11  
12  
13  
14  
15  
16  
17  
18  
19  
20  
21  
22  
23  
24  
25  
26  
27  
28  
29  
30  
31  
32  
33  
34  
35  
36  
37  
38  
39  
40  
41  
42  
43  
44  
45  
46  
47  
48  
49  
50  
51  
52  
53  
54  
55  
56  
57  
58  
59  
60

echinoderms retained their articulation due to rapid burial, presumably as waning storm-currents deposited previously suspended sediment. A second level with common, but more scattered *Diademopsis* in laminated mudstone bed 17 (Planorbis Zone and Subzone) near Watchet, West Somerset, may indicate a similar event, although there is no equivalent concentration of shelly debris (K. N. P. pers. obs. 2015).

Found commonly throughout the sections on the Devon/Dorset and West Somerset coast are centimetre-scale horizons with: a) concentrated bivalve fragments; b) lenses of echinoid debris; c) abundant large ammonites on the surface or base of limestone beds, and/or d) scattered large ammonites and nautiloids with encrusting oysters and/or crinoid debris on the tops of limestone beds. Some of these features have been previously recorded by Paul, Allison & Brett (2008) and they indicate either periods of increased sea-floor turbulence that led to winnowing of fines, fragmentation of shells and the concentration of bioclasts or periods of very slow, or halted deposition. In the latter case, epifauna such as oysters and crinoids had time to attach to the ‘benthic islands’ created by large shells. Such observations can coincide with additional evidence for significant intervals of missing strata.

**5.c. Major hiatuses**

The following sub-sections summarize the Shaw plot and field evidence for significant hiatuses at many levels within the Hettangian and Lower Sinemurian offshore facies of the Blue Lias of southern Britain. Note that in some cases these major hiatuses can be potentially linked to sea-level rises and in others to sea-level falls.

**5.c.1. Tilmanni and Planorbis zones, Hettangian**

A widespread, diachronous erosion surface across southern Britain at the base of the Blue Lias Formation has been explained in terms of latest Triassic sea-level fall followed by

a rise in the earliest Jurassic (Tilmanian Zone, Donovan, Horton & Ivimey-Cook, 1979; Hallam, 1981; 1997; Wignall, 2001; Hesselbo, Robinson & Surlyk, 2004). In the Bristol area at several localities (Filton railway cutting, Chipping Sodbury, Henleaze, Wick and Doynton), Donovan & Kellaway (1984) recorded Johnstoni Subzone (i.e. upper Planorbis Zone) strata directly on top of the 'Pre-planorbis Beds' (i.e. the Tilmanian Zone). Widespread condensation by winnowing of mud-grade sediment during the Tilmanian and Planorbis zones apparently led to numerous centimetre-scale horizons of small bivalve fragments and closely spaced limestone beds at Lyme Regis, West Somerset Coast, and Lavernock (Kent, 1937; Hallam, 1960; Hesselbo & Jenkyns, 1995; 1998). Furthermore, Kent (1937) noted limestone intraclasts encrusted by serpulids as well as borings, indicative of sea-floor erosion and non-deposition, within the Tilmanian and/or Planorbis zones of Nottinghamshire (the precise stratigraphic levels not being reported).

The apparent thinness of the *Neophyllites*-bearing levels at the base of the Planorbis Subzone (biohorizons Hn3 and Hn4, bed 9 of Whittaker & Green, 1983), suggests that there is condensation at this level in West Somerset (Page, 1995; Bloos & Page, 2000a). This supposition is confirmed by a corresponding break in slope in Fig. 8. A similar break in slope, implying a gap in the West Somerset coast section, occurs at the base of the Johnstoni Subzone (bed 25). A break in slope associated with bed 25 is also found on a Shaw plot of the West Somerset coast versus Lavernock (Table 1 data, not illustrated). Currently there is no independent biostratigraphical evidence for a gap at this level on the West Somerset coast but, as noted in Section 5.b, presumed scour fills are present in bed 24.

643

#### 644 **5.c.2. Liasicus Zone, Hettangian**

Liasicus Zone strata have not provided much field evidence for stratigraphic gaps. Radley (2008) noted in Southam Quarry, near Long Itchington, the presence of limestone

1  
2  
3  
4  
5  
6  
7  
8  
9  
10  
11  
12  
13  
14  
15  
16  
17  
18  
19  
20  
21  
22  
23  
24  
25  
26  
27  
28  
29  
30  
31  
32  
33  
34  
35  
36  
37  
38  
39  
40  
41  
42  
43  
44  
45  
46  
47  
48  
49  
50  
51  
52  
53  
54  
55  
56  
57  
58  
59  
60

647 nodules encrusted by serpulids and oysters (*Liostrea*) with scratches and grooves attributed to  
648 crustaceans. This evidence certainly indicates sea-floor exhumation of the nodules and a  
649 period of non-deposition (though this might have been short-lived). He inferred an Angulata  
650 Zone age, assuming causal factors such as lowered sea level rather than sediment starvation.  
651 However, comparison of the stratigraphic level shown (figure 5 of Radley, 2008) for the  
652 encrusted nodules with Fig. 3, combined with the biostratigraphy of Clements *et al.* (1975;  
653 1977), indicates that this erosion and non-deposition occurred during the Liasicus Zone.

654       Breaks in slope in Fig. 8 indicate possible hiatuses within the Liasicus Zone at Lyme  
655 Regis associated with unnamed limestone beds H58 and H68. Consistent with increased  
656 bottom-water turbulence, if not direct evidence for non-deposition, is the presence of  
657 abundant macroconch *Waehneroceras* commonly with encrusting *Liostrea* on the top surface  
658 of bed H58, as well as lenses of echinoid debris, especially spines in a few centimetres of the  
659 overlying marl. Figure 8 also indicates a stratigraphic gap at the base of bed 67 at the base of  
660 the Laqueus Subzone on the West Somerset Coast. Two metres below bed 67, the top of bed  
661 65 (Fig. 5a) also yields common macroconch *Waehneroceras*.

662       Hence, there was apparently increased bottom-water turbulence at the end of the  
663 Portlocki Subzone and beginning of the Laqueus Subzone in both relatively slowly and  
664 relatively quickly subsiding areas. Since bed H68 at Lyme Regis and beds 65 to 67 on the  
665 West Somerset coast occur at the levels of increased MS (Section 3.b), the mid-Liasicus  
666 increase in bottom-water turbulence was apparently associated with a change in sediment  
667 composition. Sequence stratigraphic analysis of the marginal facies in Glamorgan (Section  
668 4.a) led Sheppard (2006) to infer a major flooding surface in the mid Liasicus Zone –  
669 consistent with the analysis by Hesselbo & Jenkyns (1998) of coeval marine strata from  
670 across Britain.

671

### 5.c.3. Angulata Zone, Hettangian

Correlation of a downhole log from the borehole at Burton Row in north Somerset, 20 km north east of Quantock's Head (Fig. 1a), with the lithological log of Weedon (1987a) from the Devon coast suggested to Smith (1989) that a gap exists in the Angulata Zone at Lyme Regis. Deconinck *et al.* (2003) inferred, using kaolinite/illite ratios from the West Somerset coast, that a stratigraphic gap occurs at Lyme Regis at the top of the Angulata Zone. Hesselbo & Jenkyns (1995; 1998) also argued for condensation and thus reduced accumulation rates in the middle Angulata Zone at Lyme Regis, as indicated by the unusually close spacing of limestone beds and nodule-bearing horizons (e.g. bed 1 or 'Brick Ledge').

Figure 8 confirms the presence of stratigraphic gaps in the Angulata Zone at Lyme Regis with at least at one level in the Complanata Subzone (bed 1c within 'Brick Ledge') and at two levels within the Depressa Subzone (bed 7c or 'Lower Skulls', and bed 17 or 'Upper White'). The Shaw plot also indicates a gap at bed 134 in the Depressa Subzone on the West Somerset coast (Fig. 8), a level characterized by abundant large macroconch ammonites (*Schlotheimia*), again suggesting low net accumulation rates.

----- Figure 9 near this position -----

### 5.c.4. Bucklandi Zone, Sinemurian

Direct evidence for erosion at Lyme Regis during the Conybeari Subzone, Bucklandi Zone, is provided by a limestone intraclast with the size and shape reminiscent of a small limestone nodule, but found *in situ* within limestone bed 25 ('Top Copper', Fig. 9a, Weedon, 1987a). The intraclast surface has the characteristics of a hardground as it is bored both by bivalves (possible *Lithophaga* crypts, Fig. 2.5e of Weedon, 1987a) and by *Talpina ramosa* Von Hagenow (150–250 µm diameter, possibly made by phoronids). The intraclast surface is encrusted by at least two generations of *Liostrea*, which also have *Talpina ramosa* borings

1  
2  
3  
4  
5  
6  
7  
8  
9  
10  
11  
12  
13  
14  
15  
16  
17  
18  
19  
20  
21  
22  
23  
24  
25  
26  
27  
28  
29  
30  
31  
32  
33  
34  
35  
36  
37  
38  
39  
40  
41  
42  
43  
44  
45  
46  
47  
48  
49  
50  
51  
52  
53  
54  
55  
56  
57  
58  
59  
60

(Figs 9ai and aii). The intraclast surface is directly overlain by an unusual packstone of small gastropods, benthic foraminifera and larger bivalve fragments and succeeded by normally bioturbated wackestone. Thus, it appears that a period of increased turbulence led to exhumation of a limestone nodule, exposure for sufficient time for repeated colonization and boring (over at least two years based on the two or three generations of bivalves), followed by burial whilst the turbulence was sufficient to lead to generation of the packstone (i.e. grain-supported fabric) before a return to typical carbonate mudstone and wackestone deposition.

There is no biostratigraphic evidence for missing strata at the level of bed 25 at Lyme Regis containing the limestone intraclast (Fig. 9a). However, large ammonites are common in the limestone bed 153 on the West Somerset coast, which correlates biostratigraphically with bed 24 at Lyme Regis (i.e. Biohorizon Sn3b with *Metophioceras* ex *grp rouvillei* (Reynès), etc). In Fig. 8, the kink in the line of correlation at the level of bed 153 (at about 81.5 m) indicates condensation of the West Somerset section relative to Lyme Regis. Hence, erosion/non-deposition was apparently simultaneous at Lyme Regis and on the West Somerset coast during the middle part of the Conybeari Subzone. The break in slope of the line of correlation was determined more by sediment condensation at the level of bed 153 in West Somerset than by erosion associated with beds 24 and 25 at Lyme Regis.

In bed 29 at Lyme Regis ('Top Tape', Fig. 4), also within the Conybeari Subzone, Hallam (pp8–9, 1960) noted the presence of glauconite, both as discrete 'granules' and in microfossil infills, this mineral being an indicator of reduced accumulation rate (Odin & Matter, 1981). At beach level on either side of Seven Rock Point, west of Lyme Regis, bed 29 forms a prominent ammonite 'pavement' covered with large specimens of *Metophioceras* ex *grp. conybeari* (J. Sowerby) (Sn5b *conybeari* Biohorizon: Page 2002, 2010b; 2010c), and this is matched by its correlative bed 161 in West Somerset, which has the same group of

species in abundance on its base. The equivalent level is also recognizable palaeontologically near Pilton in north Somerset (pers. obs. by K.N.P., 1992) and correlates with the Calcaria Bed in the Bristol-Bath area where the widespread evidence for truncation, condensation and phosphatization of fossils has been specifically attributed to shallowing (Kellaway & Donovan, 1984). Figure 2 of Page (1995) clearly illustrates, for the Hettangian/Sinemurian boundary interval of the West Somerset Coast, Lyme Regis area and Saltford Cutting near Bristol, the way that lateral loss and condensation of biohorizons is associated with an increased proportion of limestone compared to marl and shale.

A widespread late Angulata–early Bucklandi erosive phase is also indicated by the non-sequences and condensation at this level described in eastern France, southern Germany and Austria, contrasting with the relative completeness of the Sinemurian GSSP section on the West Somerset coast (Page *et al.*, 2000; Bloos & Page, 2002). An indication for shallowing at this time is also provided in South Wales near Cardiff where typical offshore Blue Lias of Unit A of the Porthkerry Formation in the Angulata Zone is overlain by the near-shore Unit B facies (i.e. limestone dominated and lacking laminated shales and laminated limestones, Section 4.a). Unit B and C facies are, in turn, overlain by uppermost Angulata Zone and Bucklandi Zone oolitic marginal facies suggesting further shallowing (Waters & Lawrence, 1987; Wilson *et al.*, 1990).

In the Cardiff area the Porthkerry Formation with Bucklandi and Semicostatum Zone ammonites is found on top of a bored surface on the oolitic marginal facies (Waters & Lawrence, 1987). Similarly, near Southerndown Porthkerry Formation Unit D of the same zones (normal offshore Blue Lias with about 60 % nodular limestones and marls) occurs on top of marginal facies (Wilson *et al.*, 1990). The nature of these successions is consistent with a rise in relative sea level at the end of the Bucklandi Zone.



1  
2  
3  
4  
5  
6  
7  
8  
9  
10  
11  
12  
13  
14  
15  
16  
17  
18  
19  
20  
21  
22  
23  
24  
25  
26  
27  
28  
29  
30  
31  
32  
33  
34  
35  
36  
37  
38  
39  
40  
41  
42  
43  
44  
45  
46  
47  
48  
49  
50  
51  
52  
53  
54  
55  
56  
57  
58  
59  
60

747                                   **5.c.5. Early Semicostatum Zone, Sinemurian**

748                   As reviewed by Donovan & Kellaway (1984, e.g. their figures 5 and 6), a non-  
749 conformity in the Bristol area is overlain by phosphatised sediments and fossils with  
750 truncation of the Bucklandi Zone and successive overstepping of all the Hettangian biozones  
751 and the Rhaetian onto the Radstock Plateau to the south (i.e. approaching the Carboniferous  
752 Limestone massif of the Mendip Hills).

753                   As evidence for coeval erosion and condensation at Lyme Regis, Hallam (1960)  
754 illustrated the truncation of a *Diplocraterion* burrow, and noted glauconite and phosphate  
755 associated with bed 49 ('Grey Ledge'). This level is now known to be associated with up to  
756 four missing biohorizons from the top of the Bucklandi Subzone to the base of the  
757 Scipionianum Subzone, within the lower part of the Semicostatum Zone (Page, 2003, 2010b;  
758 2010c). Additionally, on the Devon/Dorset coast, Gallois & Paul (2009) showed that there are  
759 lateral variations in the amount of strata removed at this level from the uppermost Blue Lias  
760 Formation and that locally there is a bored surface on bed 49 and, throughout the area, deep  
761 *Diplocraterion* burrows are present, commonly at more than one level in beds 47–49. It  
762 should be noted, however, that the ammonite faunas recorded through this interval indicate  
763 that these levels may be of slightly different ages in different places and hence what are  
764 termed beds 47, 48 or 49 in different places may not be exactly the same lithostratigraphical  
765 entities. Hallam (1981) linked the change in facies above bed 49 to both the accelerated onlap  
766 on the London Platform described by Donovan, Horton & Ivimey-Cook (1979) and to sea-  
767 level rise.

768                   There is no evidence for a break in sedimentation in the late Bucklandi to basal  
769 Semicostatum zones on the West Somerset coast where the biohorizon succession appears to  
770 be complete. Interestingly, however, there is a concentration of ammonites at the level of bed  
771 247 of Whittaker & Green (1983) in the Lyra Subzone (Page 1992; 2009, biohorizon Sn 15b



of Page, 2010b), which may indicate at least one phase of reduced accumulation rates in the early Semicostatum Zone. There are several levels in the 5–6 m of shale-marl/limestone alternations, below which are concentrations of shelly debris, with common large ammonites, and one prominent level of *Diplocraterion* burrows in bed 242 (K. N. P. pers. obs. 2013–2015). Notably, the ammonite fauna of bed 247 (e.g. *Paracoronicerias ex grp charlesi* Donovan) is very close in terms of biohorizontal assignment to that recorded from the top c. 6–10 cm of bed 49 at the ‘Slabs’, between Axmouth and Lyme Regis (Page, 2002), immediately below the non-sequence and with Scipionianum Subzone strata immediately above. The lower part of bed 49, however, still appears to belong the Bucklandi Subzone (and Zone) because large *Arietites* are common.

## 6. Preservation of ammonites

It has long been believed that since the macrofossils, especially ammonites and nautiloids, are largely uncrushed, and horizontal sections of burrow mottles are nearly circular in limestone beds of the Blue Lias Formation, cementation must have started prior to significant compaction, and hence was both early and at shallow depth (Kent, 1936; Hallam, 1964; Weedon 1987a; Arzani, 2006; Paul, Allison & Brett, 2008). Since the uncrushed ammonite and gastropod shells in the limestones would have originally been aragonite, the cementation must also have pre-dated dissolution or inversion to calcite.

At Lyme Regis, ammonites completely enclosed within limestone beds typically have their originally aragonitic shells replaced by sparry calcite and the inner and outer whorls are uncrushed. By contrast, ammonites diagenetically ‘welded’ onto the surfaces of such beds usually present an uncrushed internal mould of the outer whorls with the shell entirely absent. Importantly, their inner, septate whorls are represented predominantly by an external mould on the surface of the limestone bed.

1  
2  
3  
4  
5  
6  
7  
8  
9  
10  
11  
12  
13  
14  
15  
16  
17  
18  
19  
20  
21  
22  
23  
24  
25  
26  
27  
28  
29  
30  
31  
32  
33  
34  
35  
36  
37  
38  
39  
40  
41  
42  
43  
44  
45  
46  
47  
48  
49  
50  
51  
52  
53  
54  
55  
56  
57  
58  
59  
60

797           This differential preservation according to the location of the ammonite specimens  
798 can be explained by the carbonate cementation generating a framework-supporting fabric that  
799 formed first at the centres of (i.e. mid-way through) what became the limestone beds. When  
800 and where the cementation and framework support occurred before aragonite dissolution, the  
801 full three-dimensional shape of the aragonitic ammonite shell was preserved, allowing for a  
802 later sparry calcite replacement and infill. However, on the outer margins of limestone beds,  
803 cementation and framework support appears to have been later than aragonite dissolution,  
804 albeit before significant compaction. Consequently, although this later cementation could  
805 preserve the three-dimensional shape of the shell where already filled with marl (in the body  
806 chamber and, in some cases, perforated sections of the phragmocone), it could not preserve  
807 the thickness of the shell or support inner whorls that lacked internal sediment. Arzani's  
808 (2006) study of the limestone micro-fabrics also showed that, despite the typically uncrushed  
809 nature of the macrofossils, cementation of the edges of the limestones did occur during  
810 compaction.

811           Although a cursory examination of the Devon–Dorset and West Somerset sections  
812 may give an impression that ammonites do not occur in every limestone bed, they have been  
813 recorded at far more levels than noted by Paul, Allison & Brett (2008) at Lyme Regis (Page,  
814 2002). Ammonites are common only in certain beds but prolonged examination over many  
815 years by K.N.P. has led to the recovery of very rare isolated specimens from many levels  
816 throughout the Devon–Dorset and West Somerset coastal successions. The simplest  
817 explanation for the apparent lack of ammonites within some limestone beds at Lyme Regis is  
818 preservation failure caused by cementation following a combination of aragonite dissolution,  
819 burrowing and compaction that destroyed all trace of the shells. Which leads to the critical  
820 question: why do some limestones record cementation before aragonite dissolution and others  
821 do not? This issue is re-visited in Section 8.

Paul, Allison & Brett (2008) suggested that the apparent lack of dissolution and encrustation of uncrushed ammonite and nautiloid shells within limestone beds, given the average bed thickness, implies much more rapid sedimentation of these lithologies than the net rate for the formation as a whole. As evidence for rapid sedimentation, they cited the presence of ammonite shells preserved in a near-vertical orientation within limestone beds, as well as cases of ammonite imbrication. However, their observations were primarily based on bed 41 ('Best Bed', Bucklandi Zone), which has abundant small ammonites (including *Vermiceras scylla* (Reynès)) that would have been readily re-oriented by large burrowers. Just two additional beds in the Johnstoni Subzone in the Planorbis Zone have common small ammonites. Otherwise the limestone beds typically have a large-bodied ammonite fauna.

In addition, although encrustation on ammonites appears to be mainly observed on the surfaces of limestone beds, its reported absence from specimens *within* limestone beds (Paul, Allison & Brett 2008) is not necessarily evidence for rapid sedimentation because biologically relevant factors may have been influential. In fact, the benthic macrofauna of the limestone beds is commonly characterized by low diversity and locally high density, indicative of either a 'high-stress' environment or opportunistic colonization during brief periods of 'improved' conditions. For example, rhynchonellid brachiopods dominate bed 11 and the tops of beds 19 and 23 at Lyme Regis, beds 147 and 151 on the Somerset Coast and bed 21c at Long Itchington, whereas *Gryphaea* dominates at the tops of bed 13 and beds 14 to 17 and 31 at Lyme Regis and at the tops of beds 136 and 138 on the Somerset Coast. It is likely that these controls on benthic colonization were due to intermittent bottom-water dysoxia which would have also inhibited encrustation of ammonites. There are some exceptions to these general observations, however, as there is evidence that some of the rhynchonellid brachiopods may have inhabited *Thalassinoides* burrows preferentially. Additionally, occasional winnowing may have concentrated some of the shelly material, for

1  
2  
3  
4  
5  
6  
7  
8  
9  
10  
11  
12  
13  
14  
15  
16  
17  
18  
19  
20  
21  
22  
23  
24  
25  
26  
27  
28  
29  
30  
31  
32  
33  
34  
35  
36  
37  
38  
39  
40  
41  
42  
43  
44  
45  
46  
47  
48  
49  
50  
51  
52  
53  
54  
55  
56  
57  
58  
59  
60

instance in bed 31 at Lyme Regis. At this latter level, *Gryphaea* apparently show current sorting as they are dominated by the larger, heavier lower valve in random orientations throughout the bed – possibly indicative of rapid deposition after a storm (C. R. C. Paul, pers. comm. 2016).

In the light and dark marls and the black laminated shales, without the early cementation of the limestones, the aragonitic fossils were much less likely to be preserved and subject to compaction and early diagenetic dissolution. At Lyme Regis in particular, ammonites are absent from most of the light and dark marls, but in some of the laminated shales very poorly preserved shell-less impressions can sometimes be found. Scattered oyster xenomorphs in the marls, however, prove that ammonites were once present (Paul, Allison & Brett 2008). Dissolution of aragonite and bioturbation and hence destruction of any remaining trace of shell can be assumed to have removed most of the ammonites from such levels, especially when no traces of other aragonitic shells, such as bivalves, are observed (Wright, Cherns & Hodges, 2003).

In West Somerset, however, the situation is more complex. White aragonitic shells persist in laminated shales through much of the succession, although they are only well preserved and iridescent at certain levels in the Planorbis and middle Liasicus zones. By analogy with calcareous nannofossil preservation (Section 4.b), the preservation of iridescent aragonite is likely to be connected to the high organic-carbon contents of the laminated shales, as has proven to be the case in other Jurassic shale sequences from the British Isles (e.g. Hall & Kennedy, 1967; Hudson & Martill, 1991).

Commonly, on the West Somerset coast in the laminated shales and especially in the marls, only an impression of the shell remains, picked out by a residual brown organic film: the remains of the organic content of the shell, in particular the periostracum. This pattern of preservation indicates that the aragonite dissolution post-dated the end of bioturbation in the

marls. In the upper Bucklandi and Lyra subzones, levels with white aragonite preservation can pass laterally into areas with brown calcitic shell preservation as major faults are approached. In such cases, the inversion of aragonite to calcite in the marls and shales is clearly associated with the circulation of fluids along such faults, for instance during the tectonic inversion of the basin, as described by Bixler, Elmore & Engel (1998). At some levels, both brown calcitic and white aragonitic shells may also contain pyrite, commonly associated with specific layers in the shell.

In the Burton Row borehole in North Somerset, pristine iridescent aragonite is characteristic of the laminated shales of most of the Hettangian and Sinemurian succession. On the coast, inversion to brown calcite (e.g. in parts of the Liasicus and Semicostatum zones) was due to the effects of fluids and/or raised temperatures generated during tectonic inversion (Water & Lawrence, 1983; Bixler, Elmore & Engel, 1998), whereas conversion of iridescent aragonite in the laminated shales to white and powdery aragonite was probably due to near-surface weathering and/or the effects of ground-water penetration.

----- Figure 10 near this position -----

## **7. Oxygen and carbon isotopes and timing of limestone formation**

### **7.a. Lyme Regis**

Figures 2b and 10a show that, at Lyme Regis, oxygen isotopes in the centres of the limestone beds are as high as -1.5 ‰ VPDB with carbon-isotope values close to 0.0 ‰ VPDB. These values are not much lighter than the isotopes of unaltered benthic bivalve (*Gryphaea*) calcite (Weedon, 1987a). Hence, carbon and oxygen isotopes of the Blue Lias, combined with the near-absence of evidence for compaction of macrofossils, have long been considered consistent with early cementation (Campos & Hallam, 1979; Gluyas, 1984; Weedon, 1987a; Arzani, 2006; Paul, Allison & Brett, 2008). The decreases of oxygen-isotope

1  
2  
3  
4  
5  
6  
7  
8  
9  
10  
11  
12  
13  
14  
15  
16  
17  
18  
19  
20  
21  
22  
23  
24  
25  
26  
27  
28  
29  
30  
31  
32  
33  
34  
35  
36  
37  
38  
39  
40  
41  
42  
43  
44  
45  
46  
47  
48  
49  
50  
51  
52  
53  
54  
55  
56  
57  
58  
59  
60

values towards the edges of limestone beds, where calcium carbonate contents are lower, are consistent with cementation occurring progressively during the early stages of compaction (Gluyas, 1984; Weedon, 1987a; Arzani, 2006; Paul, Allison & Brett, 2008). Disseminated framboidal and euhedral pyrite found throughout the limestones and the non-ferroan nature of the calcite microspar indicate at least some carbonate generation during sulphate reduction (Gluyas, 1984).

Raiswell (1988) postulated that cementation of the Blue Lias limestone beds and nodules was associated with anaerobic methane oxidation by sulphate within the sulphate reduction zone. Both normal sulphate reduction and anaerobic methane oxidation generate carbonate that neutralizes the acidity produced during the precipitation of iron monosulphide and pyrite oxidation (Raiswell, 1988; Bottrell & Raiswell, 1989). Since there is a restricted depth interval involved, anaerobic methane oxidation was used by Raiswell (1988) to explain Hallam's (1964) observations of the limited range of limestone bed thickness. In particular, Raiswell's model requires that shallow cementation (<1 m burial) occurred during a pause in sedimentation.

Bottrell & Raiswell (1989) further demonstrated that pyrite formation occurred over a longer period in the limestones than in the light marl and dark marls. To explain the sulphur-isotope composition of the pyrite in the limestones they invoked incorporation of sulphur derived from the bioturbational oxidation of previously formed pyrite. Such a process implies limestone cementation close to the zone of burrowing and hence not greatly below the sediment-water interface.  $\delta^{13}\text{C}$  of carbonate from sulphate reduction or aerobic methane oxidation is typically less than -10.0 ‰ VPDB. Bottrell & Raiswell (1989) explained the relatively heavy carbon-isotope values of around 0.0 ‰ VPDB in the limestones as indicating that the bulk of the carbonate was derived from dissolution of aragonite and high-Mg bioclasts. Later authors concurred with this suggested source of carbonate (Wright, Cherns &

1  
2  
3 922 Hodges, 2003; Arzani, 2004; 2006; Paul, Allison & Brett, 2008). Some limestone beds at  
4  
5 923 Lyme Regis contain centimetre-scale cracks partly filled with bioclastic sediment, indicating  
6  
7 924 that cementation and fissuring occurred close enough to the sediment-water interface to allow  
8  
9  
10 925 access to unconsolidated material, presumably following a phase of sea-floor erosion  
11  
12 926 (Hesselbo and Jenkyns, 1995).

13  
14 927 Plots of isotope ratios in the Blue Lias Formation show measurements lying near a  
15  
16 928 trend-line that slopes from near the origin down towards more negative oxygen- and carbon-  
17  
18 929 isotope ratios. Trends in isotope composition from heavier oxygen isotopes at the centres of  
19  
20 930 nodules to lighter oxygen isotopes at the edges (Fig. 10, Weedon, 1987a, Arzani, 2006)  
21  
22 931 apparently confirm the supposition that oxygen isotopes became lighter through time, most  
23  
24 932 likely due to increasing pore-water temperatures. However, the carbon isotopes in limestone  
25  
26 933 nodules can increase rather than decrease towards the outside of nodules and consequently do  
27  
28 934 not lie along the main trend of measurements at Lyme Regis (Fig 10a) and West Somerset  
29  
30 935 (Fig. 10c).

31  
32  
33  
34 936 Assuming that oxygen-isotope values only decreased during the diagenesis of the  
35  
36 937 Blue Lias Formation, an explanation is needed for why the limestone beds can have average  
37  
38 938 carbonate with  $\delta^{18}\text{O} = -4.5$  and  $\delta^{13}\text{C} = -1.5$  ‰ VPDB while limestone nodules can have  
39  
40 939 average carbonate with the same  $\delta^{18}\text{O}$ , but  $\delta^{13}\text{C} = -3.0$  ‰ VPDB (Fig. 10a). The key to this  
41  
42 940 problem is to regard the main trend in the isotopes in the limestone beds as indicating a  
43  
44 941 mixing line between the composition of early and late carbonate rather than as a time series.

45  
46  
47 942 It is now recognized that early meniscus calcite cement associated with carbonate  
48  
49 943 nodule formation could have provided a supporting framework that allowed the bulk of  
50  
51 944 cementation to occur much later during compaction (Curtis *et al.*, 2000; Raiswell & Fisher,  
52  
53 945 2000). This model helps explain why it is so rare to find shallow limestone nodules forming  
54  
55 946 in modern organic-rich marine sediments. In the Blue Lias Formation, the very early cement  
56  
57  
58  
59  
60



1  
2  
3  
4  
5  
6  
7  
8  
9  
10  
11  
12  
13  
14  
15  
16  
17  
18  
19  
20  
21  
22  
23  
24  
25  
26  
27  
28  
29  
30  
31  
32  
33  
34  
35  
36  
37  
38  
39  
40  
41  
42  
43  
44  
45  
46  
47  
48  
49  
50  
51  
52  
53  
54  
55  
56  
57  
58  
59  
60

947 in the limestones with oxygen and carbon isotopes relatively close to 0.0 ‰ VPDB was  
948 apparently sufficient to prevent the compaction of large macrofossils. At a later phase of  
949 diagenesis, once compaction had started in earnest, the remaining pore spaces within the  
950 limestone beds could then be partly filled with carbonate that had much lighter oxygen and,  
951 typically also lighter carbon isotopes. This model means that, if cemented relatively quickly,  
952 limestone nodules can show progressive changes in isotopes that, unlike the limestone beds,  
953 record a snapshot of the history of changing pore-water isotopic composition in concentric  
954 zones (including pore-water carbon isotopes becoming heavier while oxygen isotopes became  
955 lighter). Although Arzani (2006) demonstrated that microspar growth was displacive, the  
956 cementation cannot have continued much beyond the end of occlusion of the pore spaces  
957 because the limestone beds and nodules have oxygen isotopes not lighter than about -6.0 ‰.

958 At Lyme Regis, the oxygen isotopes of the calcite microspar in the light and dark  
959 marls and the black laminated shale (-3.5 to -6.0 ‰ VPDB) are much lighter on average than  
960 the limestone beds (Fig. 10a). Hence, the marls and shales appear to have been cemented later  
961 than the limestone beds. However, one sample of light marl from mid-way through bed 15c  
962 (BL307, Table 3B of Weedon, 1987a, Figs 2b and 10a) with %CaCO<sub>3</sub> = 38.2 and %TOC =  
963 0.61 has an oxygen-isotope value that is far heavier ( $\delta^{18}\text{O} = -1.99$  ‰ VPDB) than the other  
964 marl and shale samples. This sample is interpreted to represent light marl that was cemented  
965 by early meniscus cement, as though destined to become the centre of a limestone bed or  
966 nodule, but the amount of cement was apparently insufficient to provide enough framework  
967 support to prevent compaction during burial.

968 Ferroan and non-ferroan calcite beef occurring near the bases of some laminated  
969 shales at Lyme Regis with  $\delta^{18}\text{O}$  less than -6 ‰ (Campos & Hallam, 1979), not shown in Fig.  
970 10a, probably formed as a result of over-pressuring during deep burial (Marshall, 1982).

971



### 7.b. West Somerset Coast

Unaltered carbonate of *Liostrea* from the Tilmanni Zone of the West Somerset Coast have generally much heavier carbon isotopes (+1.6 to +3.9 ‰, Fig. 10c, van de Schootbrugge *et al.*, 2007) than those found in *Gryphaea* from the Angulata and Bucklandi Zones at Lyme Regis (+0.5 to +2.5 ‰ VPDB, Figs 2b and 10b, Weedon, 1987a). Korte *et al.* (2009) measured  $\delta^{13}\text{C}$  of between +1.5 and +5.0 ‰ VPDB for *Liostrea* in the Tilmanni Zone of Lavernock (not shown) with progressively lighter average values in the upper part of the Tilmanni, Planorbis and lower Liasicus zones. The different ranges of values in the Tilmanni and the Angulata–Bucklandi zones have been related to secular trends in carbon isotopes within the Hettangian rather than diagenetic factors (Korte *et al.*, 2009). However, all three groups of measurements of unaltered benthic bivalve calcite indicate  $\delta^{18}\text{O}$  between about 0.0 and -2.0 ‰ VPDB.

The limestones on the West Somerset Coast with  $\delta^{18}\text{O} = -4.0$  to  $-12.5$  ‰ VPDB have far lighter oxygen isotopes than those at Lyme Regis (compare Fig. 10a with Figs 10b and 10c). The isotopically lightest values from a limestone bed (Fig. 10b) are derived from beds associated with mud volcanoes developed in the Bucklandi Zone strata near Kilve (Cornford, 2003; Allison, Hesselbo & Brett, 2008; Price, Vowles-Sheridan & Anderson, 2008). Isotope values from material described as comprising the mud volcano mounds themselves (i.e. breccia, ‘tufa’, crust etc) have been excluded from Fig. 10b.

Oxygen isotopes from limestone beds from the Tilmanni and Planorbis Zones on the West Somerset Coast are not only lighter than the limestone beds at Lyme Regis, but also generally lighter, rather than heavier, than their associated marls and black laminated shales (Fig. 10c, Arzani, 2004). The much lighter oxygen isotopes suggest that the limestones were cemented later than the marls and shales. Nevertheless, large macrofossils within the limestone beds of the West Somerset Coast are preserved uncrushed in the same manner as

1  
2  
3  
4  
5  
6  
7  
8  
9  
10  
11  
12  
13  
14  
15  
16  
17  
18  
19  
20  
21  
22  
23  
24  
25  
26  
27  
28  
29  
30  
31  
32  
33  
34  
35  
36  
37  
38  
39  
40  
41  
42  
43  
44  
45  
46  
47  
48  
49  
50  
51  
52  
53  
54  
55  
56  
57  
58  
59  
60

997 observed at Lyme Regis. Accordingly, cementation started prior to compaction. These  
998 apparently conflicting interpretations can be reconciled if it is hypothesised that the West  
999 Somerset Coast limestone beds had an early framework cement with oxygen isotopes close to  
1000 0.0 ‰ VPDB that was joined by carbonate formed much later that had much lighter oxygen-  
1001 isotope values. Thus, the marls and laminated shales became fully compacted and fully  
1002 cemented at a time when there remained framework-supported pores within the limestone  
1003 beds still available for later cementation by calcite with very light oxygen-isotope values.

1004 Campos & Hallam (1979) explained their observations of much heavier average  
1005 oxygen isotopes in the limestones of the Lower Jurassic of Devon/Dorset compared to the  
1006 Lower Jurassic of the Yorkshire Coast in terms of net sedimentation rate. Their explanation is  
1007 followed here with respect to the comparison of the West Somerset with the Devon/Dorset  
1008 coast, assuming that the total time for cementation was approximately the same in both cases.  
1009 In both areas cementation appears to have started very early, but the limestones at Lyme  
1010 Regis were buried more slowly and so their final carbonate was probably precipitated at  
1011 relatively low temperatures (overall oxygen isotopes heavier than the marls and shales). The  
1012 more rapidly buried limestone beds on the West Somerset Coast apparently ceased full  
1013 cementation at much greater depths and thus were formed from pore waters with higher  
1014 temperatures (overall oxygen isotopes lighter than the marls and shales).

1015 A prolonged cementation history on the West Somerset Coast is indicated by very  
1016 negative  $\delta^{18}\text{O}$  in vein calcite (-9 to -12 ‰ VPDB - not shown in Fig. 10), probably associated  
1017 with Late Jurassic to Early Cretaceous extensional and Cenozoic compressional faulting  
1018 (Bixler, Elmore & Engel, 1998).

1019

1020 **8. Synthesis**

1  
2  
3 1021 In the offshore facies, at the scale of ammonite zones, lateral and stratigraphic  
4  
5 1022 variations in the characteristics of the Blue Lias Formation are not due to variations in the  
6  
7 1023 composition of specific rock types. Neither the water depth nor the net accumulation rate  
8  
9 1024 influenced the average composition of the rock type (Fig. 1c), a conclusion that follows from  
10  
11 1025 the hemipelagic origin of the sediment (Section 4.b). The key variables determining the  
12  
13 1026 characteristics of the Formation are: a) the average thicknesses of beds of light marl, dark  
14  
15 1027 marl and black laminated shale; and b) the proportion of limestone.

16  
17  
18 1028 Variations in the average thickness of the marls and shales are associated with  
19  
20 1029 variations in zonal thickness and were determined by the net accumulation rate (Section 4.c).  
21  
22 1030 The uniformly and relatively thin zones of the Hettangian at Lyme Regis are associated with  
23  
24 1031 thin beds of marls and shales. On the West Somerset Coast, the younger stratigraphically  
25  
26 1032 thicker zones are associated with thicker beds of marls and shales whose deposition post-  
27  
28 1033 dated a major increase in accumulation rate at the start of the Liasicus Zone (Figs 1b and 8,  
29  
30 1034 Section 4.c).

31  
32  
33 1035 On the scale of ammonite zones, the proportion of limestones was linked to the net  
34  
35 1036 accumulation rate as determined by rates of subsidence and sea-level variations. The  
36  
37 1037 abundant evidence for intra-formational hiatuses and evidence for storm-related scours and  
38  
39 1038 winnowing episodes (Section 5) are consistent with the overall deposition of fines limited by  
40  
41 1039 the storm wave base. Raiswell's (1988) model for the formation of limestone nodules and  
42  
43 1040 beds within a restricted interval of anaerobic methane oxidation by sulphate during pauses in  
44  
45 1041 sedimentation accords with the field and geochemical evidence for cementation close to the  
46  
47 1042 sediment-water interface (Sections 6 and 7). However, although initiation of limestone  
48  
49 1043 formation started early, final cementation appears to have occurred well below the sediment-  
50  
51 1044 water interface (Section 7). Such a history explains the overall rarity of limestone intraclasts  
52  
53  
54  
55 1045 despite the prevalence of sea-floor erosion and re-deposition of sediments in storm events.  
56  
57  
58  
59  
60

1  
2  
3  
4  
5  
6  
7  
8  
9  
10  
11  
12  
13  
14  
15  
16  
17  
18  
19  
20  
21  
22  
23  
24  
25  
26  
27  
28  
29  
30  
31  
32  
33  
34  
35  
36  
37  
38  
39  
40  
41  
42  
43  
44  
45  
46  
47  
48  
49  
50  
51  
52  
53  
54  
55  
56  
57  
58  
59  
60

1046           The restriction of protrusive *Diplocraterion* traces to light marls and limestone beds  
1047 supports the idea that deposition of light marl, rather than dark marl or black laminated-shale,  
1048 was often associated with significant bottom-water turbulence. At Lyme Regis, increased  
1049 proportions of angular- compared to rounded-wood particles, interpreted as indicating  
1050 relatively high bottom-water turbulence, occur near the tops of many limestone beds and light  
1051 marls (Waterhouse, 1999a). This observation has apparently not been tested for the West  
1052 Somerset Coast (e.g. Bonis, Ruhl & Kürschner, 2010) probably because woody material is  
1053 much rarer.

1054           The explanation of orbital-climatic (Milankovitch) control of the alternations of  
1055 homogenized organic-carbon poor sediments with laminated organic carbon-rich sediments  
1056 in the offshore facies of the Blue Lias and correlatives remains popular (House, 1985; 1986;  
1057 Weedon, 1986; 1987a; 1987b, Waterhouse 1999a; 1999b; Weedon *et al.*, 1999; Hanzo *et al.*,  
1058 2000; Bonis, Ruhl & Kürschner, 2010; Ruhl *et al.*, 2010). Intervals of increased fluvial  
1059 drainage during wetter climates are likely to have led to salinity stratification, enhanced  
1060 stability of the water column and increased fluxes of clay minerals from land. These factors  
1061 were probably significant in promoting both higher productivity and preservation of marine  
1062 organic matter in the darker laminated and more clay-rich sediments (Weedon, 1986; Fleet et  
1063 al., 1987).

1064           The precursors to the limestone beds, the light marls, were probably not only  
1065 associated with a relatively dry climate compared to the dark marl and black laminated shale  
1066 deposition (Weedon, 1986), but also stormier conditions (Waterhouse, 1999b). The increased  
1067 storminess causing erosion and/or winnowing during the deposition of light marl would have  
1068 frequently led to pauses in sedimentation (non-deposition and/or hiatuses) so that limestone  
1069 beds could be formed. However, increases in water depth and accommodation space, such as

1  
2  
3 1070 during the Liasicus Zone, would have reduced the probability that storms would promote the  
4  
5 1071 formation of limestones during deposition of light marl.  
6

7 1072 The palaeo-latitude of southern Britain was about 35° N in the Early Jurassic (Smith,  
8  
9  
10 1073 Smith & Funnell, 1994). The ‘stormier’ climate associated with deposition of light marl is  
11  
12 1074 envisaged as resulting from rare intense tropical cyclones, rather from than frequent mid-  
13  
14 1075 latitude depressions. Increased storm influence during deposition of light marl (more frequent  
15  
16 1076 turbulent bottom water) is consistent with a drier climate overall (less rainfall and lower flux  
17  
18 1077 of clay). Such storm events led to episodic increases in bottom-water turbulence well below  
19  
20 1078 the normal storm wave-base. Individual storm events could have led to sea-floor erosion, but  
21  
22 1079 multiple storms would have been necessary for the prolonged phases of non-deposition  
23  
24 1080 required for the initiation of limestone formation by carbonate cementation of light marls  
25  
26 1081 near the sediment-water interface.  
27  
28

29 1082 In the Blue Lias Formation as a whole, beds of dark grey to black laminated limestone  
30  
31 1083 and layers of laminated limestone nodules are much rarer than the homogeneous limestones.  
32  
33 1084 This was apparently because at the associated water depths and in the wetter climatic regime  
34  
35 1085 associated with the laminated shales (with high clay fluxes), storms were usually too rare  
36  
37 1086 and/or too weak to cause pauses in sedimentation. In the field, laminated limestone nodules at  
38  
39 1087 Lavernock and Southam Quarry show thicker laminae in the centres of nodules that pinch  
40  
41 1088 laterally into much thinner laminae within the enclosing laminated shales (Weedon, 1987a).  
42  
43 1089 Hence, laminated limestones apparently formed prior to significant compaction just like the  
44  
45 1090 homogeneous grey limestone beds (Weedon, 1986; 1987a; Arzani, 2004). However,  
46  
47 1091 exceptionally ‘clean’ laminated limestone beds such as bed H30 (Intruder) at Lyme Regis  
48  
49 1092 may represent deposition from low-density turbidity currents (Hesselbo & Jenkyns, 1995).  
50  
51  
52  
53

54 1093 The observations of gutter casts and crustacean escape structures in Southam Quarry  
55  
56 1094 at Long Itchington prove that storms manifestly caused sea-floor erosion and re-deposition  
57  
58  
59  
60

1  
2  
3  
4  
5  
6  
7  
8  
9  
10  
11  
12  
13  
14  
15  
16  
17  
18  
19  
20  
21  
22  
23  
24  
25  
26  
27  
28  
29  
30  
31  
32  
33  
34  
35  
36  
37  
38  
39  
40  
41  
42  
43  
44  
45  
46  
47  
48  
49  
50  
51  
52  
53  
54  
55  
56  
57  
58  
59  
60

1095 during times of laminated-shale deposition (Radley, 2008; O’Brien, Braddy & Radley, 2009).  
1096 In general, laminated limestones are most abundant within the Tilmanni and Planorbis zones.  
1097 Hence during the early Hettangian, water depths were apparently shallow enough for even  
1098 rare/weak storms to cause the pauses in sedimentation required to generate laminated  
1099 limestone beds and laminated limestone nodule layers.

1100 According to the Raiswell (1988) model of anaerobic methane oxidation by sulphate,  
1101 limestone formation started a metre so below the sediment-water interface. The range of  
1102 preservation of ammonites (Section 6) indicates that for different limestone beds the  
1103 cementation formed a framework-supporting fabric: a) before aragonite dissolution and  
1104 before compaction (ammonites fully preserved), b) after aragonite dissolution, but before  
1105 significant compaction (only external moulds of sediment-free inner whorls preserved,  
1106 especially on the edges of limestone beds) and c) after aragonite dissolution and after  
1107 compaction started (no ammonites shells preserved, although calcitic oyster xenomorphs may  
1108 be present).

1109 Paul, Allison & Brett (2008) argued that the ammonites within the limestones at Lyme  
1110 Regis were preserved due to rapid deposition, which seems plausible, given the evidence for  
1111 storm-related deposition (Section 5, Weedon, 1986; 1987a; Waterhouse, 1999b; Radley,  
1112 2008). However, not mentioned by Paul, Allison & Brett (2008), was that additionally an  
1113 interval of non-deposition after the rapid burial by light marl seems also to have been  
1114 necessary to initiate limestone formation. Given the homogenization of the light marl by  
1115 burrowers prior to limestone formation, the non-deposition and cementation apparently did  
1116 not immediately follow rapid sedimentation. However, unless non-deposition occurred before  
1117 aragonite dissolution (i.e. within a few thousand years), cementation would not have been  
1118 early enough to preserve the ammonites.

1  
2  
3 1119 The Blue Lias Formation is well known for fully articulated ichthyosaur and  
4  
5 1120 plesiosaur fossils (e.g. Milner & Walsh, 2010). Skeletons enclosed by laminated shale were  
6  
7 1121 probably protected from scavengers by bottom-water anoxia. However, given that many fully  
8  
9 1122 articulated skeletons that somehow avoided disarticulation by scavengers are found also in  
10  
11 1123 the marls and homogeneous limestones, rapid burial of carcasses during storms could also  
12  
13 1124 explain their preservation.

14  
15  
16 1125 Normally, the aragonite of ammonites buried within accumulating light marl would  
17  
18 1126 have dissolved and left no trace unless pyritized (very rare in the Blue Lias Formation) or  
19  
20 1127 preserved as external moulds in oyster xenomorphs. Limestone beds that do not preserve  
21  
22 1128 ammonites were apparently formed during phases of non-deposition that did not quickly  
23  
24 1129 follow an episode of rapid light marl deposition.

25  
26  
27 1130

## 28 29 1131 **9. Conclusions**

30  
31  
32 1132 In the offshore hemipelagic facies of the Blue Lias Formation, the spacing of  
33  
34 1133 individual limestones within zones and the varying limestone proportions of limestones from  
35  
36 1134 zone-to-zone and from site-to-site, can all be related to the bottom-water turbulence. The  
37  
38 1135 model adopted represents a synthesis of several key papers accompanied by the new  
39  
40 1136 biostratigraphic and sedimentological data presented here.

41  
42  
43 1137 There is abundant evidence for winnowing, non-deposition and sea-floor erosion  
44  
45 1138 within the formation, as indicated by the Shaw plot (Fig. 8) and the field evidence (Section  
46  
47 1139 5). Initiation of limestone formation is explained by periods of non-deposition causing  
48  
49 1140 cementation of the zone of anaerobic methane oxidation by sulphate close to the sediment-  
50  
51 1141 water interface (Raiswell, 1988, Bottrell & Raiswell, 1989). This mechanism explains the  
52  
53 1142 decoupling of limestone bed thickness from lateral and stratigraphic variations in net  
54  
55 1143 accumulation rate (Hallam, 1964; Raiswell, 1988). The periods of increased sea-floor erosion



1  
2  
3  
4  
5  
6  
7  
8  
9  
10  
11  
12  
13  
14  
15  
16  
17  
18  
19  
20  
21  
22  
23  
24  
25  
26  
27  
28  
29  
30  
31  
32  
33  
34  
35  
36  
37  
38  
39  
40  
41  
42  
43  
44  
45  
46  
47  
48  
49  
50  
51  
52  
53  
54  
55  
56  
57  
58  
59  
60

1144 or non-deposition that initiated the formation of individual limestone beds and horizons of  
1145 limestone nodules can be attributed to storms (Weedon, 1986; 1987a; Waterhouse 1999b;  
1146 Radley, 2008).

1147 Deposition of light marl was associated with a drier climate characterized by much  
1148 stronger and/or more frequent, though possibly still rare, major storms whereas more tranquil  
1149 conditions were typical for the deposition of dark marl and laminated shale (Waterhouse,  
1150 1999b). Thus, limestone beds and nodule horizons were much more likely to form within  
1151 light marl beds. However, occasionally during deposition of laminated shale, storms did lead  
1152 to non-deposition and formation of laminated limestone beds and laminated limestone nodule  
1153 horizons (Radley, 2008). Relatively shallow water depths during the Tilmanni and Planorbis  
1154 Zones, and thus greater influence of storms on bottom-water turbulence during laminated-  
1155 shale deposition, explains the concentration of laminated limestones within this interval.  
1156 Conversely, relatively greater water depths, for example during the Liasicus Zone, meant that  
1157 storm-related bottom-water turbulence was reduced and thus less likely to cause non-  
1158 deposition and the formation of homogeneous limestone beds and nodule horizons within the  
1159 light marls.

1160 A strong storm influence on deposition in the offshore Blue Lias Formation is not  
1161 surprising, given the well-known storm-related deposition of the ‘marginal facies’ (Johnson  
1162 & McKerrow, 1995; Simms, 2004; Sheppard, 2006) and of the near-shore facies of the Blue  
1163 Lias in South Wales (Section 4.a, Sheppard, Houghton & Swan, 2006). Storm influences  
1164 have also been documented from Hettangian and Lower Sinemurian strata, of Blue Lias  
1165 character, in the Paris Basin (Hanzo *et al.*, 2000).

1166 In the Lower Pliensbachian of Yorkshire, Van Buchem, McCave & Weedon (1994)  
1167 showed that the orbitally forced cycles of grain size were related to varying storm intensity.  
1168 The coeval Belemnite Marls of Dorset (or Stonebarrow Marl Member of the Charmouth



1  
2  
3 1169 Mudstone Formation of Page, 2010b) exhibit orbitally controlled alternations of light and  
4  
5 1170 dark marls (Weedon & Jenkyns, 1999). Similar orbitally controlled cyclicity has been  
6  
7 1171 documented in the Pliensbachian strata of the Mochras borehole at Llanbedr, Wales (Ruhl et  
8  
9 1172 al., 2016). Sellwood (1970) believed the rhythms of the Belemnite Marls indicated cycles in  
10  
11 1173 bottom-water turbulence but invoked short-term changes in sea level as a primary forcing  
12  
13 1174 mechanism. However, similarly to the Blue Lias, the changes in sediment composition in the  
14  
15 1175 Belemnite Marls can be linked to orbital climatic cycles (Weedon & Jenkyns, 1999), with  
16  
17 1176 indications of varying bottom-water turbulence (variations in characteristics of and types of  
18  
19 1177 burrow traces, Sellwood, 1970) linked to cycles in storminess. Deeper water conditions  
20  
21 1178 compared to the depositional environment of the Blue Lias may explain the lack of non-  
22  
23 1179 sequences and consequent lack of limestones except at the base and top of the Belemnite  
24  
25 1180 Marls (Hesselbo & Jenkyns, 1995; Weedon & Jenkyns, 1999).

26  
27  
28  
29 1181 Normally, ammonites in the Blue Lias are not preserved in the light marls unless  
30  
31 1182 represented by crushed specimens, commonly with associated organic films; or their former  
32  
33 1183 presence may be indicated by oyster xenomorphs. Ammonites preserved within limestone  
34  
35 1184 beds required rapid burial under light marl (Paul, Allison & Brett, 2008), most likely caused  
36  
37 1185 by storm-related re-deposition (Section 5, Radley, 2008). However, preservation would only  
38  
39 1186 normally occur when rapid burial was followed fairly quickly by a period of non-deposition  
40  
41 1187 that initiated limestone formation. Non-deposition was probably also linked to storm activity  
42  
43 1188 and occurred after homogenization of the sediment by burrowers, but before aragonite  
44  
45 1189 dissolution. If non-deposition or hiatus formation did not quickly follow rapid deposition,  
46  
47 1190 formation of limestone beds devoid of ammonites took place, as a combination of aragonite  
48  
49 1191 dissolution, bioturbation and early compaction removed all trace of the shells. Ammonites  
50  
51 1192 within the laminated shales on the west coast of Somerset are preserved as: a) shell-less  
52  
53 1193 impressions, b) impressions with residual brown films, c) as white aragonite or d) as pristine  
54  
55  
56  
57  
58  
59  
60

1  
2  
3 1194 (i.e. iridescent) aragonite that is likely to have owed its survival to the protective effects of  
4  
5 1195 organic matter.  
6  
7 1196 To account for the stable-isotope signatures of the limestone beds, it is suggested that  
8  
9  
10 1197 initially early carbonate cementation produced framework-supporting fabrics that were  
11  
12 1198 usually strong enough to resist compaction of large macrofossils such as ammonites (if not  
13  
14 1199 previously dissolved). However, the final oxygen- and carbon-isotope signatures within the  
15  
16 1200 limestones represent a mixture of the early plus much later cement that filled the micrograde  
17  
18 1201 framework pores. At Lyme Regis, due to the low net accumulation rate and the relatively  
19  
20  
21 1202 shallow depths at which cementation finished, the oxygen isotopes in the limestone beds are  
22  
23 1203 heavier than those of marls and shales. By contrast, on the West Somerset coast, the much  
24  
25 1204 higher net accumulation rates ensured that final cementation of the limestone beds occurred  
26  
27 1205 much deeper in the sediment pile so that the overall oxygen-isotope values are generally  
28  
29 1206 lighter than the associated marls and shales and also lighter than the limestones at Lyme  
30  
31 1207 Regis.

32  
33  
34 1208  
35  
36 1209 **Acknowledgements**

37  
38 1210 The Royal Society provided a grant to G.P.W. in the early 1990s for the purchase of a  
39  
40 1211 Bartington MS meter. Stuart Robinson kindly supplied 38 ‘SAB’ samples (Hesselbo,  
41  
42 1212 Robinson & Surlyk, 2004) from the Tilmanni and Planorbis biozones from St Audries Bay  
43  
44 1213 for MS analysis to supplement the collection obtained by Weedon (1987a). Simon Robinson  
45  
46 1214 provided helpful advice on interpretations of MS. Our thanks go to Chris Paul for his  
47  
48 1215 constructive review.

49  
50  
51 1216 K.N.P. thanks the Orchard-Wyndham estate, including the late Dr Catherine  
52  
53 1217 Wyndham, and the East Quantoxhead Estate, including the late Colonel Sir Walter Luttrell,  
54  
55 1218 for ongoing permission to sample on the Estate’s foreshore areas in West Somerset. Bob  
56  
57  
58  
59  
60

1219 Cornes and Tom Sunderland of Natural England provided help and advice regarding  
 1220 permission for sampling in West Somerset and within the Axmouth-Lyme Regis National  
 1221 Nature Reserve, west of Lyme Regis, respectively. Raymond Roberts of Natural Resources  
 1222 Wales (formerly Countryside Council for Wales) advised on the St. Mary's Well Bay section  
 1223 at Lavernock. K.N.P. would also like to thank María-José Bello-Villalba and Joseph Bello-  
 1224 Page for assistance in the field.

1225

# 1226 **References**

- 1227 Ager, D. 1986. A reinterpretation of the basal 'Littoral Lias' of the Vale of Glamorgan.  
 1228 *Proceedings of the Geologists' Association* **97**, 29–35.
- 1229 Allison, P. A., Hesselbo, S. P., & Brett, C. A. 2008. Methane seeps on an Early Jurassic  
 1230 seafloor. *Palaeogeography, Palaeoclimatology, Palaeoecology* **270**, 230–238.
- 1231 Ambrose, K. 2001. The lithostratigraphy of the Blue Lias Formation (Late Rhaetian-Early  
 1232 Sinemurian) in the southern part of the English Midlands. *Proceedings of the*  
 1233 *Geologists' Association* **112**, 97–110.
- 1234 Arzani, N. 2004. Diagenetic evolution of mudstones: black shales to laminated limestones, an  
 1235 example from the Lower Jurassic of SW Britain. *Journal of Sciences Islamic Republic*  
 1236 *of Iran* **15**, 257–267.
- 1237 Arzani, N. 2006. Primary versus diagenetic bedding in the limestone-marl/shale alternations  
 1238 of the epeiric seas, an example from the Lower Lias (Early Jurassic) of SW Britain.  
 1239 *Carbonates and Evaporites* **21**, 94–109.
- 1240 Barras, C. G. & Twitchett, R. J., 2007. Response of the marine infauna to Triassic-Jurassic  
 1241 environmental change: ichnological data from southern England. *Palaeogeography,*  
 1242 *Palaeoclimatology, Palaeoecology* **244**, 223–241.

1  
2  
3  
4  
5  
6  
7  
8  
9  
10  
11  
12  
13  
14  
15  
16  
17  
18  
19  
20  
21  
22  
23  
24  
25  
26  
27  
28  
29  
30  
31  
32  
33  
34  
35  
36  
37  
38  
39  
40  
41  
42  
43  
44  
45  
46  
47  
48  
49  
50  
51  
52  
53  
54  
55  
56  
57  
58  
59  
60

1243 Bixler, W. G., Elmore, R. D., & Engel, M. H. 1998. The origin of magnetization and  
1244 geochemical alteration in a fault zone, Kilve, England. *Geological Journal* **33**, 89–  
1245 105.

1246 Bleil, S. & Petersen, N. 1987. Magnetic properties of natural minerals. In *Physical properties*  
1247 *of rocks Volume 1 subvolume B* (ed G. Angenheister) pp. 308–365. Springer.

1248 Bloos, G. & Page, K. N. 2000a. The basal Jurassic ammonite succession in the North-West  
1249 European Province - Review and new results. In: *Advances in Jurassic Research*  
1250 *2000. Proceedings of the Fifth International Symposium on the Jurassic System* (eds  
1251 R. L. Hall & P. Smith), pp. 27–40. GeoResearch Forum **6**, Trans Tech Publications.

1252 Bloos, G. & Page, K. N. 2000b. The proposed GSSP for the base of the Sinemurian Stage  
1253 near East Quantoxhead/West Somerset (SW England) - The ammonite sequence. In:  
1254 *Advances in Jurassic Research 2000. Proceedings of the Fifth International*  
1255 *Symposium on the Jurassic System* (eds R. L. Hall & P. L. Smith) pp. 13–26.  
1256 GeoResearch Forum **6**, Trans Tech Publications.

1257 Bloos, G. & Page, K. N. 2002. The Global Stratotype Section and Point for base of the  
1258 Sinemurian Stage (lower Jurassic). *Episodes* **25**, 22–28.

1259 Bonis, N. A., Ruhl, M. & Kürschner, W.M. 2010. Milankovitch-scale palynological turnover  
1260 across the Triassic–Jurassic transition at St. Audrie’s Bay, SW UK. *Journal of the*  
1261 *Geological Society, London* **167**, 877–888.

1262 Bottrell, S. & Raiswell, R. 1989. Primary versus diagenetic origin of Blue Lias rhythms  
1263 (Dorset, UK): evidence from sulphur geochemistry. *Terra Nova* **1**, 457–456.

1264 Bown, P.R. 1987. Taxonomy, evolution, and biostratigraphy of late Triassic-early Jurassic  
1265 calcareous nannofossils. *Special Papers in Palaeontology* **38**, Palaeontological  
1266 Association, 118 pp.

- 1267 Bown, P. R. & Cooper, M. K. E. 1998. Jurassic. In *Calcareous Nannofossil Biostratigraphy*,  
 1268 (ed. P. R. Bown), pp. 34–85. British Micropalaeontological Society Publications  
 1269 Series, Chapman and Hall.
- 1270 Bromley, R. G. & Ekdale, A. A. 1984. *Chondrites*: a trace fossil indicator of anoxia in  
 1271 sediments. *Science* **224**, 872–874.
- 1272 Bukri, P. M., Dent Glasser, L. S. & Smith, D. N. 1982. Surface coatings on ancient  
 1273 coccoliths. *Nature* **297**, 145–147.
- 1274 Callomon, J. 1985. Biostratigraphy, chronostratigraphy and all that - again! In: *International*  
 1275 *Symposium on Jurassic Stratigraphy, Erlangen 1984* (eds O. Michelsen, O. & A. A.  
 1276 Zeiss), pp. 611-624. Geological Survey of Denmark, Copenhagen 3.
- 1277 Callomon, J. 1995. Time from fossils: S.S. Buckman and Jurassic high-resolution  
 1278 geochronology. *Milestones in Geology* (ed. M. L. Le Bas), pp. 127–150. Geological  
 1279 Society Memoir 16.
- 1280 Campos, J. G. & Hallam, A. 1979. Diagenesis of English Lower Jurassic limestones as  
 1281 inferred from oxygen and carbon isotope analysis. *Earth and Planetary Science*  
 1282 *Letters* **45**, 23–31.
- 1283 Clémence, M-E., Bartolini, A., Gardin, S., Paris, G., Beaumont, V. & Page, K. N. 2010. Early  
 1284 Hettangian benthic-planktonic coupling at Doniford (SW England).  
 1285 Palaeoenvironmental implications from the aftermath of the end-Triassic crisis.  
 1286 *Palaeogeography, Palaeoclimatology, Paleoecology* **295**, 102–115.
- 1287 Clements, R. G. & members of the field studies in local geology class 1975. *The geology of*  
 1288 *the Long Itchington Quarry (Rugby Portland Cement Co. Ltd., Southam Works)*.  
 1289 Percival Guildhall, Rugby and Dept. of Geology, University of Leicester, 30 pp.
- 1290 Clements, R. G. & members of the field studies in local geology class, Percival Guildhouse,  
 1291 Rugby 1977. *The Geology of the Parkfield Quarry, Rugby (Rugby Portland Cement*

- 1292 *Co. Ltd., Rugby Works, Rugby, Warwickshire*). Dept. of Geology, University of  
 1293 Leicester, 54 pp.
- 1294 Collinson, D. W., 1983. *Methods in rock magnetism and palaeomagnetism: Techniques and*  
 1295 *Instrumentation*. Chapman and Hall, London, 503 pp.
- 1296 Cornford, C. 2003. Triassic palaeopressure and Liassic mud volcanoes near Kilve, west  
 1297 Somerset. *Geoscience in South-West England* **10**, 430–434.
- 1298 Curtis, C. D., Cope, J. C. W., Plant, D. & Macquaker, J. H. S. 2000. ‘Instantaneous’  
 1299 sedimentation, early microbial sediment strengthening and a lengthy record of  
 1300 chemical diagenesis preserved in Lower Jurassic ammonitiferous concretions from  
 1301 Dorset. *Journal of the Geological Society, London* **157**, 165–177.
- 1302 Day, E. C. H. 1865. On the Lower Lias of Lyme Regis. *Geological Magazine* **2**, 518–519.
- 1303 Deconinck, J-F., Hesselbo, S. P., Debuissier, N., Averbuch, O., Baudin, F. and Bessa, J. 2003.  
 1304 Environmental controls on clay mineralogy of an Early Jurassic mudrock (Blue Lias  
 1305 Formation, southern England). *International Journal of Earth Sciences* **92**, 255–266.
- 1306 Donovan, D. T. 1956. The zonal stratigraphy of the Blue Lias around Keynsham, Somerset.  
 1307 *Proceedings of the Geologists’ Association* **66**, 182–212.
- 1308 Donovan, D. T., Horton, A., & Ivimey-Cook, H. C. 1979. The transgression of the Lower  
 1309 Lias over the northern flank of the London Platform. *Journal of the Geological*  
 1310 *Society, London* **136**, 165–173.
- 1311 Donovan, D. T. & Kellaway, G. A. 1984. *Geology of the Bristol District; the Lower Jurassic*  
 1312 *rocks*. Memoir of the British Geological Survey Special Sheet. HMSO, 69 pp.
- 1313 Fleet, A. J., Clayton, C. J., Jenkyns, H. C. & Parkinson, D. N. (1987). Liassic source rock  
 1314 deposition in western Europe (eds J. Brooks & K. Glennie) pp 59–70. In *Petroleum*  
 1315 *Geology of north-west Europe, 1*, Graham & Trotman, London.

- 1  
2  
3 1316 Fletcher, C. J. N. 1988. Tidal erosion, solution cavities and exhalative mineralization  
4  
5 1317 associated with the Jurassic unconformity at Ogmore, South Glamorgan. *Proceedings*  
6  
7 1318 *of the Geologists' Association* **99**, 1–14.  
8  
9  
10 1319 Gallois, R. W. & Paul, C. R. C. 2009. Lateral variations in the topmost part of the Blue Lias  
11  
12 1320 and basal Charmouth Mudstone Formations (Lower Jurassic) on the Devon and  
13  
14 1321 Dorset Coast. *Geoscience in South-West England* **12**, 125–133.  
15  
16 1322 Gluyas, J. G. 1984. Early carbonate diagenesis within Phanerozoic shales and sandstones of  
17  
18 1323 the NW European shelf. *Clay Minerals* **19**, 309–321.  
19  
20  
21 1324 Hall, A. & Kennedy, W. J. 1967. Aragonite in fossils. *Philosophical Transactions of the*  
22  
23 1325 *Royal Society, London* **B168**, 377–412.  
24  
25 1326 Hallam, A. 1960. A sedimentary and faunal study of the Blue Lias of Dorset and Glamorgan.  
26  
27 1327 *Philosophical Transactions of the Royal Society, London* **B243**, 1–44.  
28  
29 1328 Hallam, A. 1964. Origin of limestone-shale rhythms in the Blue Lias of England: a composite  
30  
31 1329 theory. *Journal of Geology* **72**, 157–169.  
32  
33 1330 Hallam, A. 1981. A revised sea-level curve for the early Jurassic. *Journal of the Geological*  
34  
35 1331 *Society, London* **138**, 735–743.  
36  
37 1332 Hallam, A., 1986. Origin of minor limestone-shale cycles: climatically induced or diagenetic?  
38  
39 1333 *Geology* **14**, 609–612.  
40  
41 1334 Hallam, A., 1987. Reply to Weedon, 1987 Comment on: 'Origin of limestone-shale cycles:  
42  
43 1335 climatically induced or diagenetic?' *Geology* **15**, 93–94.  
44  
45 1336 Hallam, A. 1997. Estimates of the amount and rate of sea-level change across the Rhaetian–  
46  
47 1337 Hettangian and Pliensbachian–Toarcian boundaries (latest Triassic to early Jurassic).  
48  
49 1338 *Journal of the Geological Society, London* **154**, 773–779.  
50  
51  
52  
53  
54  
55  
56  
57  
58  
59  
60



- 1339 Hallam, A. & Bradshaw, M. J. 1979. Bituminous shales and oolitic ironstones as indicators of  
1340 transgression and regression. *Journal of the Geological Society, London* **136**, 157–  
1341 164.
- 1342 Hamilton, G. B. 1982. Triassic and Jurassic calcareous nannofossils. In *A stratigraphical*  
1343 *index of calcareous nannofossils* (ed. A. R. Lord), pp. 17–39. British  
1344 Micropalaeontological Society Series, Ellis Horwood, Chichester.
- 1345 Hanzo, M., Lathuilière, B., Alméras, Y., Dagallier, G., Guérin-Franiatte, S., Guillocheau, F.,  
1346 Huault, V., Nori, L. & Rauscher, R. 2000. Paléoenvironnements dans le Calcaire à  
1347 gryphées du Lias de Lorraine, de la carrière de Xeuilley au Bassin parisien. *Eclogae*  
1348 *Geologicae Helvetiae* **93**, 183–206.
- 1349 Hays, J. D., Imbrie, J. & Shackleton, N. J. 1976. Variations in the Earth's orbit: pacemaker of  
1350 the ice ages. *Science* **194**, 1121–1132.
- 1351 Hesselbo, S. P. 2008. Sequence stratigraphy and inferred relative sea-level change from the  
1352 onshore British Jurassic. *Proceedings of the Geologists' Association* **119**, 19–34.
- 1353 Hesselbo, S. P. & Jenkyns, H. C. 1995. A comparison of the Hettangian to Bajocian  
1354 successions of Dorset and Yorkshire. In *Field Geology of the British Jurassic* (ed P.  
1355 D. Taylor) pp. 105–150. Geological Society, London.
- 1356 Hesselbo, S. P. & Jenkyns, H. C. 1998. British Lower Jurassic sequence stratigraphy. In  
1357 *Mesozoic and Cenozoic Sequence Stratigraphy of European Basins* (eds J. Hardenbol,  
1358 J. Thierry, M. B. Farley, T. Jacquin, P-C. de Graciansky & P. Vail) pp. 562–581.  
1359 SEPM Special Publication 60.
- 1360 Hesselbo, S. P., Robinson, S. A. & Surlyk, F. 2004. Sea-level change and facies development  
1361 across potential Triassic-Jurassic boundary horizons, SW Britain. *Journal of the*  
1362 *Geological Society, London* **161**, 365–379.

- 1363 Hillebrandt, A. V., Krystyn, L., & Kuerschner, W. M. 2007. A candidate GSSP for the base  
 1364 of the Jurassic in the Northern Calcareous Alps (Kuhjoch section, Karwendel  
 1365 Mountains, Tyrol, Austria). *International Sub-commission on Jurassic Stratigraphy*  
 1366 *Newsletter* **34**, 2–20.
- 1367 Hillebrandt, A. V. & Krystyn, L. 2009. On the oldest Jurassic ammonites of Europe  
 1368 (Northern Calcareous Alps, Austria) and their global significance. *Neues Jahrbuch für*  
 1369 *Geologie und Paläontologie, Abhandlungen* **253**, 163–195.
- 1370 Hodges, P. 1986. The Lower Lias (Lower Jurassic) of the Bridgend area, South Wales.  
 1371 *Proceedings of the Geologists' Association* **97**, 237–242.
- 1372 Hodges, P. 1994. The base of the Jurassic System: new data on the first appearance of  
 1373 *Psiloceras planorbis* in southwest Britain. *Geological Magazine* **131**, 841–844.
- 1374 Hounslow, M. W. 1985. Magnetic fabric arising from paramagnetic phyllosilicate minerals in  
 1375 mudrocks. *Journal of the Geological Society, London* **142**, 995–1106.
- 1376 Hounslow, M. W., Posen, P. E. & Warrington, G. 2004. Magnetostratigraphy and  
 1377 biostratigraphy of the Upper Triassic and lowermost Jurassic succession, St. Audrie's  
 1378 Bay, UK. *Palaeogeography, Palaeoclimatology, Palaeoecology* **213**, 331–358.
- 1379 House M. R. 1985. A new approach to an absolute time scale from measurements of orbital  
 1380 cycles and sedimentary microrhythms. *Nature* **313**, 17–22.
- 1381 House, M. R. 1986. Are Jurassic microrhythms due to orbital forcing? *Proceedings of the*  
 1382 *Ussher Society* **6**, 299–311.
- 1383 Hudson, J. D. & Martill, D. M. 1991. The Lower Oxford Clay: production and preservation  
 1384 of organic matter in the Callovian (Jurassic) of central England. In *Modern and*  
 1385 *ancient continental Shelf Anoxia* (eds R. V. Tyson & T. H. Pearson), pp. 363–379.  
 1386 Geological Society, London Special Publication 58.

- 1387 Jenkyns, H. C., Jones, C. E., Gröcke, D. R., Hesselbo, S. P. & Parkinson, D. N. 2002.  
1388 Chemostratigraphy of the Jurassic System: applications, limitations and implications  
1389 for palaeoceanography. *Journal of the Geological Society, London* **159**, 351–378.
- 1390 Jenkyns, H. C. & Senior, J. R. 1991. Geological evidence for intra-Jurassic faulting in the  
1391 Wessex Basin and its margins. *Journal of the Geological Society, London* **148**, 245–  
1392 260.
- 1393 Johnson, M. E. & McKerrow, W. S. 1995. The Sutton Stone: an early Jurassic rocky  
1394 shoreline deposit in South Wales. *Palaeontology* **38**, 529–541.
- 1395 Kent, P. E. 1936. The formation of hydraulic limestones of the Lower Lias. *Geological*  
1396 *Magazine* **73**, 476–478.
- 1397 Kent, P. E. 1937. The Lower Lias of South Nottinghamshire. *Proceedings of the Geologist's*  
1398 *Association* **48**, 163–174.
- 1399 Korte, C., Hesselbo, S. P., Jenkyns, H. C., Rickaby, R. E., & Spotl, C. 2009.  
1400 Palaeoenvironmental significance of carbon- and oxygen-isotope stratigraphy of  
1401 marine Triassic–Jurassic boundary sections in SW Britain. *Journal of the Geological*  
1402 *Society, London* **166**, 432–445.
- 1403 Lang, W. D. 1924. The Blue Lias of the Devon and Dorset Coasts. *Proceedings of the*  
1404 *Geologists' Association* **35**, 169–184.
- 1405 Lees, J. A., Bown, P. R. & Young, J. R. 2006. Photic zone palaeoenvironments of the  
1406 Kimmeridge Clay Formation (Upper Jurassic, UK) suggested by calcareous  
1407 nannoplankton palaeoecology. *Palaeogeography, Palaeoclimatology, Palaeoecology*  
1408 **235**, 110–134.
- 1409 Loughman, D. L. 1982. *A facies analysis of the Triassic/Jurassic boundary beds of the world:*  
1410 *with special reference to North-West Europe and the Americas*. Ph.D. Thesis  
1411 University of Birmingham (unpublished).

- 1412 Marshall, J. D. 1982. Isotopic composition of displacive fibrous calcite veins: reversals in  
 1413 pore-water composition trends during burial diagenesis. *Journal of Sedimentary*  
 1414 *Petrology* **52**, 615–630.
- 1415 Milner, A.C. and Walsh, S., 2010. Reptiles. In *Fossils from the Lower Lias of the Dorset*  
 1416 *Coast*, (eds A. R. Lord & P. G. Davis), pp. 372–394. Palaeontological Association,  
 1417 London.
- 1418 Moghadam, H. V. & Paul., C. R. C. 2000. Trace fossils of the Jurassic, Blue Lias, Lyme  
 1419 Regis, Southern England. *Ichnos* **7**, 283–306.
- 1420 O'Brien, L. J., Braddy, S. J., & Radley, J. D. 2009. A new arthropod resting trace and  
 1421 associated suite of trace fossils from the Lower Jurassic of Warwickshire, England.  
 1422 *Palaeontology* **52**, 1099–1112.
- 1423 Odin, G. S. & Matter, A. 1981. De glauconiarum origine. *Sedimentology* **28**, 611–641.
- 1424 Ogg, J. G. & Hinnov, L. A. 2012. Jurassic. In *The Geologic Time Scale 2012* (eds F. M.  
 1425 Gradstein, J. G. Ogg, M. Schmitz & G. Ogg), pp. 731–791. Elsevier.
- 1426 Old, R. A., Sumblar, M. G., & Ambrose. K. 1987. *Geology of the Country around Warwick*.  
 1427 Memoir of the British Geological Survey Sheet 84 (England and Wales).
- 1428 Page, K. N. 1992. The sequence of ammonite-correlated horizons in the British Sinemurian  
 1429 (Lower Jurassic). *Newsletters on Stratigraphy* **27**, 129–156.
- 1430 Page, K. N. 1995. East Quantoxhead, Somerset, England: a potential Global Stratigraphic  
 1431 Section and Point (GSSP) for the base of the Sinemurian Stage (Lower Jurassic).  
 1432 *Proceedings of the Ussher Society* **9**, 446–450.
- 1433 Page, K. N. 2002. A review of the ammonite faunas and standard zonation of the Hettangian  
 1434 and Lower Sinemurian succession (Lower Jurassic) of the East Devon Coast (South  
 1435 west England). *Geoscience in South-West England* **10**, 293–303.

- 1436 Page, K. N. 2003. The Lower Jurassic of Europe - its subdivision and correlation. In *The*  
1437 *Jurassic of Denmark and adjacent areas* (eds J. Ineson, & F. Surlyk), pp. 23–59.  
1438 Geological Survey of Denmark and Greenland, Bulletin 1.
- 1439 Page, K. N. 2005. The Hettangian ammonite faunas of the west Somerset Coast (South West  
1440 England) and their significance for the correlation of the candidate GSSP (Global  
1441 Stratotype and Point) for the base of the Jurassic System at St. Audries Bay. *Colloque*  
1442 *l'Hettangien a Hettange de la science au patrimoine*, Université Henri Poincaré, pp.  
1443 15–19.
- 1444 Page, K. N. 2010a. High resolution ammonite stratigraphy of the Charmouth Mudstone  
1445 Formation (Lower Jurassic: Sinemurian-Lower Pliensbachian) in south-west England,  
1446 UK. *Volumina Jurassica* 7, 19–29.
- 1447 Page, K. N. 2010b. Stratigraphical framework. In *Fossils from the Lower Lias of the Dorset*  
1448 *Coast* (eds A. R. Lord & P. G. Davis), pp. 33–53. Palaeontological Association Field  
1449 Guides to Fossils 13.
- 1450 Page, K. N. 2010c. Ammonites. In *Fossils from the Lower Lias of the Dorset Coast* (eds A.  
1451 R. Lord & P. G. Davis), pp. 169–261. Palaeontological Association Field Guides to  
1452 Fossils 13.
- 1453 Page, K. N. in press. From Oppel to Callomon (and beyond!): building a high resolution  
1454 ammonite-based biochronology for the Jurassic System. *Lethaia*.
- 1455 Page, K. N. & Bloos, G. 1995. The base of the Jurassic System in West Somerset, South-  
1456 West England – new observations on the succession of ammonite faunas of the  
1457 lowermost Hettangian Stage. *Geoscience in South-West England* 9, 231–235.
- 1458 Page, K. N., Bloos, G., Bessa, J. L., Fitzpatrick, M., Hart, M. B., Hesselbo, S., Hylyon, M.,  
1459 Morris, A. & Randall, D. E. 2000. East Quantoxhead, Somerset: A candidate Global  
1460 Stratotype Section and Point for the base of the Sinemurian Stage (Lower Jurassic).

- 1  
2  
3 1461 In *Advances in Jurassic Research 2000* (eds R. L. Hall & P. L. Smith), pp. 163–72.  
4  
5 1462 Proc. Fifth International Symposium on the Jurassic System, GeoResearch Forum 6,  
6  
7 1463 Trans Tech Publications.  
8  
9  
10 1464 Palmer, C. P. 1972. The Lower Lias (Lower Jurassic) between Watchet and Lillstock in North  
11  
12 1465 Somerset (United Kingdom). *Newsletters on Stratigraphy* **2**, 1–30.  
13  
14 1466 Paul, C. R. C., Allison, P.A. & Brett, C. E. 2008. The occurrence and preservation of  
15  
16 1467 ammonites in the Blue Lias Formation (lower Jurassic) of Devon and Dorset, England  
17  
18 1468 and their palaeoecological, sedimentological and diagenetic significance.  
19  
20 1469 *Palaeogeography, Palaeoclimatology, Palaeoecology* **270**, 258–272.  
21  
22  
23 1470 Paris, G., Beaumont, V., Bartolini, A., Clémence, M-E. & Gardin, S. 2010. Nitrogen isotope  
24  
25 1471 record of a perturbed paleoecosystem in the aftermath of the end-Triassic crisis,  
26  
27 1472 Doniford section, SW England. *Geochemistry, Geophysics, Geosystems* **11**, Q08021,  
28  
29 1473 doi:10.1029/2010GC003161.  
30  
31  
32 1474 Pearson, S. J., Marshall, J. E. A. & Kemp, A. E. S. 2004. The White Stone Band of the  
33  
34 1475 Kimmeridge Clay Formation, an integrated high-resolution approach to understanding  
35  
36 1476 environmental change. *Journal of the Geological Society, London* **161**, 675–683.  
37  
38 1477 Price, G. D., Vowles-Sheridan, N. & Anderson, M. W. 2008. Lower Jurassic mud volcanoes  
39  
40 1478 and methane, Kilve, Somerset, UK. *Proceedings of the Geologists' Association* **119**,  
41  
42 1479 193–201.  
43  
44  
45 1480 Radley, J. D. 2008. Seafloor erosion and sea-level: Early Jurassic Blue Lias Formation of  
46  
47 1481 central England. *Palaeogeography, Palaeoclimatology, Palaeoecology* **270**, 287–294.  
48  
49 1482 Raiswell, R. 1988. Chemical model for the origin of minor limestone-shale cycles by  
50  
51 1483 anaerobic methane oxidation. *Geology* **16**, 641–644.  
52  
53  
54  
55  
56  
57  
58  
59  
60

1  
2  
3 1484 Raiswell, R. & Fisher, Q. J. 2000. Mudrock-hosted carbonate concretions: a review of growth  
4  
5 1485 mechanisms and their influence on chemical and isotopic composition. *Journal of the*  
6  
7 1486 *Geological Society, London* **157**, 239–251.  
8  
9  
10 1487 Richardson, L. 1905. The Rhaetic and contiguous deposits of Glamorganshire. *Quarterly*  
11  
12 1488 *Journal of the Geological Society, London* **61**, 385–424.  
13  
14 1489 Richardson, W. A. 1923. Petrology of the Shales-with-‘Beef’. *Quarterly Journal of the*  
15  
16 1490 *Geological Society, London* **79**, 88–98.  
17  
18 1491 Ruhl, M., Deenen, M. H. L., Abels, H. A., Bonis, N. R., Krijgsman, W. & Kürschner, W. M.  
19  
20 1492 2010. Astronomical constraints on the duration of the early Jurassic Hettangian stage  
21  
22 1493 and recovery rates following the end-Triassic mass extinction (St. Audrie’s Bay/East  
23  
24 1494 Quantoxhead, UK). *Earth and Planetary Science Letters* **296**, 262–276.  
25  
26 1495 Ruhl, M., Hesselbo, S. P., Hinnov, L., Jenkyns, H. C., Xu, W., Riding, J. B., Storm, M.,  
27  
28 1496 Minisini, D., Ullmann, C. V. & Leng, M. J. 2016. Astronomical constraints on the  
29  
30 1497 duration of the Early Jurassic Pliensbachian Stage and global climatic fluctuations.  
31  
32 1498 *Earth and Planetary Science Letters* **455**, 149–165.  
33  
34 1499 Seilacher, A. 2007. *Trace Fossil Analysis*. Springer, 226 pp.  
35  
36 1500 Sellwood, B. W. 1970. The relation of trace fossils to small-scale sedimentary cycles in the  
37  
38 1501 British Lias. In *Trace Fossils* (eds T. R. Crimes & J. C. Harper), pp. 489–504.  
39  
40 1502 Geological Journal Special Issue 3.  
41  
42 1503 Sellwood, B. W. & Jenkyns, H. C. 1975. Basins and swells and the evolution of an epeiric sea  
43  
44 1504 (Pliensbachian–Bajocian of Great Britain). *Journal of the Geological Society, London*  
45  
46 1505 **131**, 373–388.  
47  
48 1506 Sheppard, H. T. 2006. Sequence architecture of ancient rocky shorelines and their response to  
49  
50 1507 sea-level change: an Early Jurassic example from South Wales, UK. *Journal of the*  
51  
52 1508 *Geological Society, London* **163**, 595–606.  
53  
54  
55  
56  
57  
58  
59  
60



- 1509 Sheppard, H. T., Houghton, R. D. & Swan, A. R. H. 2006. Bedding and pseudo-bedding in  
 1510 the Early Jurassic of Glamorgan: deposition and diagenesis of the Blue Lias in South  
 1511 Wales. *Proceedings of the Geologists' Association* 117, 249–264.
- 1512 Shukri, N. M. 1942. Rhythmic bedding in the Lower Lias of England. *Faculty of Science*  
 1513 *Fouad I University Cairo Bulletin* 24, 66–73.
- 1514 Simms, M. J. 2004. British Lower Jurassic Stratigraphy: an Introduction. In *British Lower*  
 1515 *Jurassic Stratigraphy* (eds M. J. Simms, N. Chidlaw, N. Morton, & Page, K. N.) pp.  
 1516 3–51. Geological Conservation Review Series 30.
- 1517 Simms, M. J., Little, C. T. S. & Rosen, B. R. 2002. Corals not serpulids: mineralized colonial  
 1518 fossils in the Lower Jurassic marginal facies of South Wales. *Proceedings of the*  
 1519 *Geologists' Association* 113, 31–36.
- 1520 Smith, A. G. Smith, D. G. & Funnell, B. M. 1994. *Atlas of Mesozoic and Cenozoic*  
 1521 *Coastlines*. Cambridge University Press, 99 pp.
- 1522 Smith, D. G. 1989. Stratigraphic correlation of presumed Milankovitch cycles in the Blue  
 1523 Lias (Hettangian to earliest Sinemurian), England. *Terra Nova* 1, 457–460.
- 1524 Trueman, A. E., 1920. The Liassic rocks of the Cardiff District. *Proceedings of the*  
 1525 *Geologists' Association* 31, 93–107.
- 1526 Trueman, A. E. 1922. The Liassic rocks of Glamorgan. *Proceedings of the Geologists'*  
 1527 *Association* 33, 245–284.
- 1528 Trueman, A. E. 1930. The Lower Lias (Bucklandi Zone) of Nash Point, Glamorgan.  
 1529 *Proceedings of the Geologists' Association* 61, 149–159.
- 1530 Van Buchem, F. S. P., McCave, I. N. & Weedon, G. P. 1994. Orbitally induced small-scale  
 1531 cyclicity in a siliciclastic epicontinental setting (Lower Lias, Yorkshire, UK). In  
 1532 *Orbital Forcing and Cyclic Sequences* (eds P.L. de Boer & D.G. Smith), pp. 345–366.  
 1533 International Association of Sedimentologists Special Publication 19.

- 1534 van de Schootbrugge, B., Tremolada, F., Rosenthal, Y., Bailey, T. R., Feist-Burkhardt, S.,  
1535 Brinkhuis, H., Pross, J., Kent, D. V. & Falkowski, P.G. 2007. End-Triassic  
1536 calcification crisis and blooms of organic-walled 'disaster species'. *Palaeogeography*,  
1537 *Palaeoclimatology, Palaeoecology* **244**, 126–141.
- 1538 Warrington, G. & Ivimey-Cook, H. C. 1995. The Late Triassic and Early Jurassic of coastal  
1539 sections in west Somerset and South and Mid-Glamorgan. In *Field Geology of the*  
1540 *British Jurassic* (ed P. D. Taylor) pp. 9–30. Geological Society, London.
- 1541 Waterhouse, H. K. 1999a. Orbital forcing of palynofacies in the Jurassic of France and the  
1542 United Kingdom. *Geology* **27**, 511–514.
- 1543 Waterhouse, H. K. 1999b. Regular terrestrially derived palynofacies cycles in irregular  
1544 marine sedimentary cycles, Lower Lias, Dorset, UK. *Journal of the Geological*  
1545 *Society, London* **156**, 1113–1124.
- 1546 Waters, R. A. & Lawrence, D. J. D. 1987. *Geology of the South Wales Coalfield, Part III, the*  
1547 *country around Cardiff*. Memoir 1:50,000 Geological sheet 263 (England and Wales),  
1548 HMSO.
- 1549 Weedon, G. P. 1985. Palaeoclimatic information from ancient pelagic and hemipelagic cyclic  
1550 sediments. *Terra Cognita* **5**, 110.
- 1551 Weedon, G. P. 1986. Hemipelagic shelf sedimentation and climatic cycles: the basal Jurassic  
1552 (Blue Lias) of South Britain. *Earth and Planetary Science Letters* **76**, 321–335.
- 1553 Weedon, G. P. 1987a. *Palaeoclimatic significance of open-marine cyclic sequences*. D. Phil.  
1554 Thesis University of Oxford, 2 volumes available at:  
1555 <http://ora.ox.ac.uk/objects/uuid:aa009e6b-d429-4340-b3c5-30f5227f0148>.
- 1556 Weedon, G. P. 1987b. Comment on: 'Origin of limestone-shale cycles: climatically induced  
1557 or diagenetic?' by Hallam, A., 1986. *Geology* **15**, 92–94.

- 1  
2  
3 1558 Weedon, G. P., & Jenkyns, H. C. 1999. Cyclostratigraphy and the Early Jurassic time scale:  
4  
5 1559 data from the Belemnite Marls, Dorset, southern England. *Geological Society of*  
6  
7 1560 *America Bulletin* **111**, 1823–1840.  
8  
9  
10 1561 Weedon, G. P., Jenkyns, H. C., Coe, A. L. & Hesselbo, S. P. 1999. Astronomical calibration  
11  
12 1562 of the Jurassic time-scale from cyclostratigraphy in British mudrock formations.  
13  
14 1563 *Philosophical Transactions of the Royal Society, London* **357**, 1787–1813.  
15  
16 1564 Whittaker, A. & Green, G. W. 1983. Geology of the country around Weston-super-Mare.  
17  
18 1565 Memoire 1:50,000 Geological sheet 279, New series with parts of sheets 263 and 295,  
19  
20 1566 HMSO.  
21  
22  
23 1567 Whittaker, A., Holliday, D. W. & Penn, I. E. 1985. *Geophysical logs in British Stratigraphy*.  
24  
25 1568 Geological Society Special Report 18, Geological Society, London, 74 pp.  
26  
27 1569 Wignall, P. B. 2001. Sedimentology of the Triassic-Jurassic boundary beds in Pinhay Bay  
28  
29 1570 (Devon, SW England). *Proceedings of the Geologists' Association* **112**, 349–360.  
30  
31 1571 Williams, R. B. G. 1984. *Introduction to Statistics for Geographers and Earth Scientists*.  
32  
33 1572 MacMillan, 349 pp.  
34  
35  
36 1573 Wilson, D., Davies, J. R., Fletcher, C. J. N. & Smith, M. 1990. *Geology of the South Wales*  
37  
38 1574 *Coalfield, Part VI, the country around Bridgend*. Memoir 1:50,000 Geological sheets  
39  
40 1575 261 and 262 (England and Wales), HMSO.  
41  
42  
43 1576 Wobber, F. J. 1963. A directional structure from the Lower Jurassic of Great Britain. *Journal*  
44  
45 1577 *of Sedimentary Petrology* **34**, 692–693.  
46  
47 1578 Wobber, F. J. 1965. Sedimentology of the Lias (Lower Jurassic) of South Wales. *Journal of*  
48  
49 1579 *Sedimentary Petrology* **35**, 683–703.  
50  
51  
52 1580 Wobber, F. J. 1966. A study of the depositional area of the Glamorgan Lias. *Proceedings of*  
53  
54 1581 *the Geologists' Association* **77**, 127–137.  
55  
56  
57  
58  
59  
60

1  
2  
3 1582 Wright, V. P., Cherns, L. & Hodges, P. 2003. Missing molluscs: field testing taphonomic loss  
4  
5 1583 in the Mesozoic through large-scale aragonite dissolution. *Geology* **31**, 211–214.  
6  
7 1584 Young, J. R. & Bown, P. R. 1991. An ontogenetic sequence of coccoliths from the Late  
8  
9 1585 Jurassic Kimmeridge Clay of England. *Palaeontology* **4**, 843–850.  
10  
11 1586

12  
13  
14 1587 **Figure captions**

15 1588 Figure 1.  
16  
17 1589 (a) Location of the sections illustrated in Figs 3–6.  
18  
19 1590 (b) Formation characteristics according to Hettangian ammonite zone and location. Data from  
20  
21 1591 logs shown in Fig 3–6. The symbols in Fig. 1a indicate the localities. The percentage of  
22  
23 1592 limestone refers to the thickness of limestone logged as limestone or laminated limestone  
24  
25 1593 beds, or if more than 50% of a particular level, limestone or laminated limestone nodules.  
26  
27 1594 Ave. = average, L/D = Light/Dark, Lam. = laminated.  
28  
29 1595 (c) Average rock-type composition at Lyme Regis and on the West Somerset coast (St  
30  
31 1596 Audries Bay and Quantock’s Head sections) in terms of weight per cent calcium carbonate  
32  
33 1597 (%CaCO<sub>3</sub>), total organic carbon (TOC) and TOC re-expressed on a carbonate-free basis  
34  
35 1598 (TOCcf). Horizontal bars denote 95% confidence intervals around the mean. Data and  
36  
37 1599 analytical methods from Weedon (1987a): 90 samples from the Angulata and Bucklandi  
38  
39 1600 zones at Lyme Regis and 57 samples from the Tilmanni to Bucklandi zones on the West  
40  
41 1601 Somerset coast. These data are supplemented using a further 38 SAB samples (Hesselbo *et*  
42  
43 1602 *al.*, 2008) from the Tilmanni and Planorbis zones at St Audries Bay. Numbers of samples  
44  
45 1603 analyzed by rock-type for Lyme Regis vs West Somerset coast respectively are: limestone  
46  
47 1604 and limestone nodules 31 vs 17; light marl 23 vs 17; dark marl 20 vs 19; laminated shale 16  
48  
49 1605 vs 35; laminated limestone samples from west Somerset coast alone, 7. The average %TOCcf  
50  
51 1606 values and their uncertainties in the different rock types are consistent with the limestones  
52  
53  
54  
55  
56  
57  
58  
59  
60

1607 formed by carbonate cementation of light marls and with the laminated limestones formed by  
 1608 carbonate cementation of laminated shales.

1609

1610 Figure 2.

1611 (a) Scatter plots of field measurements of vol MS, and laboratory measurements of wt MS  
 1612 and %CaCO<sub>3</sub>.  $N$  = number of samples,  $r$  = Pearson's  $r$  (degree of correlation).  $\circ$  = sample  
 1613 from Lyme Regis,  $+$  = sample from West Somerset coast. The stratigraphic locations of the  
 1614 samples are indicated in Figs 4 and 5.

1615 (b) Profiles of vol MS and %CaCO<sub>3</sub> measurements at Lyme Regis in beds 13 to 23 (bed  
 1616 numbers from Lang, 1924).  $+$  = measurement of vol MS, wt MS or %CaCO<sub>3</sub>,  $\circ$  = estimated  
 1617 %CaCO<sub>3</sub> based on regression between vol MS and %CaCO<sub>3</sub> (Fig. 2a) – see text Section 3.b.

1618 (c) Profiles of measurements of  $\delta^{18}\text{O}$  and  $\delta^{13}\text{C}$  and %TOC at Lyme Regis in beds 13 to 23.  $+$   
 1619 = bulk sample  $\delta^{18}\text{O}$  and  $\delta^{13}\text{C}$  from Weedon (1987a),  $\square$  = bulk sample  $\delta^{18}\text{O}$  and  $\delta^{13}\text{C}$  from  
 1620 Paul, Allison, & Brett (2008),  $\circ$  = *Gryphaea* sp. sample  $\delta^{18}\text{O}$  and  $\delta^{13}\text{C}$  from Weedon (1987a).

1621 Key to rock-types in Fig. 3.

1622

1623 Figure 3. Lithostratigraphic log, vol MS measurements and ammonite biostratigraphy at St.  
 1624 Mary's Well Bay, Lavernock, Wales. Homogeneous limestone nodules are indicated by black  
 1625 ellipses. Laminated limestone nodules are indicated by white ellipses. At the levels where vol  
 1626 MS was measured within limestone nodules rather than light marl, the nodules are indicated  
 1627 on the right of the lithostratigraphic log. Bed numbers from Waters & Lawrence (1987).

1628

1629 Figure 4. Lithostratigraphic log, vol MS and %CaCO<sub>3</sub> measurements and ammonite  
 1630 biostratigraphy to the west of Lyme Regis, Devon. The location of the base of the Angulata  
 1631 Zone is discussed in Section 5.a. For key to lithologies see Fig. 3. The concentration of

1632 samples at the level of bed 37 relates to the profile shown in Figs 2b and 2c. ○ = sample  
 1633 measured for %CaCO<sub>3</sub> plotted with reference to lower horizontal axis, B = level with  
 1634 abundant calcite beef, Lport Mbr = Langport Member, Angul. = Angulata, Buc. = Bucklandi,  
 1635 Extra. = Extranodosa, Ext. = Extranodosa. Bed numbers from Lang (1924). Lang (1924) and  
 1636 Hesselbo & Jenkyns (1995) provide the names of limestone beds on the Devon/Dorset coast.

1637

1638 Figure 5. (a) Lithostratigraphic log, vol MS and %CaCO<sub>3</sub> measurements and ammonite  
 1639 biostratigraphy at St Audries Bay, Somerset. For key to lithologies see Fig. 3. Black circles  
 1640 indicate samples measured for %CaCO<sub>3</sub> plotted with reference to lower horizontal axis. ○ =  
 1641 sample measured for %CaCO<sub>3</sub> plotted with reference to lower horizontal axis, B = level with  
 1642 abundant calcite beef. Bed numbering from Whittaker and Green (1983). (b) As for 5a but a  
 1643 composite section from St Audries Bay and Quantock's Head. The join (splice) of the St  
 1644 Audries Bay section (St A.) with the Quantocks Head section (Q. H.) is indicated within bed  
 1645 96 (Section 3.a). GSSP = Global Stratigraphic Section and Point.

1646

1647 Figure 6. Lithostratigraphic log, vol MS measurements and ammonite biostratigraphy at  
 1648 Southam Quarry, near Southam and Long Itchington, Warwickshire. For key to lithologies  
 1649 see Fig. 3. L. M. = Langport Member. Bed numbers from Clements *et al.* (1975).

1650

1651 Figure 7.

1652 (a) Photomicrograph of dark marl thin-section (plane polarized light, width of view 3 mm).  
 1653 Sample BL120 and Fig. 2.2M of Weedon, (1987a) bed 32a, Rotiforme Subzone, Bucklandi  
 1654 Zone, Lyme Regis.

1655 (b) SEM photograph showing coccoliths *in situ* partly engulfed by euhedral microspar  
 1656 overgrowth (width of view 14  $\mu\text{m}$ ). Dark marl sample BL120 and Fig. 2.4G of Weedon  
 1657 (1987a), bed 32a, Bucklandi Zone, Lyme Regis.

1658 (c) SEM photograph showing an aggregate of coccoliths surrounded by a matrix of organic  
 1659 matter and clay (width of view 56  $\mu\text{m}$ ). Dark marl sample BL120 and Fig. 2.4F of Weedon  
 1660 (1987a), bed 32a, Bucklandi Zone, Lyme Regis.

1661 (d) SEM photograph showing an aggregate of coccoliths next to *Schizosphaerella punctulata*  
 1662 (centre) both surrounded by a matrix of organic matter, clay and calcite microspar (width of  
 1663 view 53  $\mu\text{m}$ ). Laminated shale sample BL117, and Fig. 2.4H of Weedon (1987a), topmost  
 1664 laminated shale of bed 32, Bucklandi Zone, Lyme Regis.

1665 (e) SEM photograph showing a corroded coccolith in limestone (width of view  $\sim 8 \mu\text{m}$ ).  
 1666 Limestone sample BL103 and Fig. 2.4A of Weedon (1987a), bed 29, Conybeari Subzone,  
 1667 Bucklandi Zone, Lyme Regis.

1668

1669 Figure 8. Shaw plot constructed using the joint locations of biohorizon bases and biohorizon  
 1670 tops at Lyme Regis and the West Somerset Coast (St Audries Bay and Quantock's Head  
 1671 sections) as listed in Table 1. The location of the base of the Angulata Zone at Lyme Regis  
 1672 has been estimated using the West Somerset data via the line of correlation data (long grey  
 1673 arrows, Section 5.a). The ratios of the thicknesses of subzones in the West Somerset  
 1674 composite section to subzones in the Lyme Regis section are indicated at the bottom of the  
 1675 plot. Vertical or horizontal arrows with bed numbers indicate the levels at which breaks in  
 1676 slope of the line of correlation imply relative condensation or intra-formational hiatuses. + =  
 1677 Lyme Regis section versus St Audries Bay section versus Lyme Regis section,  $\times$  Quantock's  
 1678 Head section versus Lyme Regis section. Tilm. = Tilmanni, Planorb. = Planorbis, Pl. =



1  
2  
3 1679 Planorbis, Jo. = Johnsoni, Laq. = Laqueus, Extran. = Extranodosa, Depr. = Depressa, Conyb.  
4  
5 1680 = Conybeari, Roti. = Rotiforme.  
6  
7 1681  
8  
9  
10 1682 Figure 9.  
11  
12 1683 (a) Photograph of polished limestone section showing bored and encrusted limestone  
13  
14 1684 intraclast with a hardground-like surface (diagrammatic description below) collected *in situ*  
15  
16 1685 from within bed 25 (Top Copper) below Devonshire Head, Lyme Regis. *i*) Photographic  
17  
18 1686 negative image of acetate peel showing *Liostrea* encrusting the intraclast surface and overlain  
19  
20 1687 by bioclastic packstone. Two *Liostrea* individuals (left and right) encrust a third individual –  
21  
22 1688 demonstrating at least two generations of encrustation. Short arrows indicate the *Talpina*  
23  
24 1689 *ramosa* Von Hagenow borings into the intraclast surface and within the encrusting *Liostrea*.  
25  
26 1690 *ii*) As for *i*) but a different section of the intraclast surface (see diagram for location).  
27  
28  
29 1691 (b) Limestone intraclasts on the surface of a fallen block of limestone, Monmouth Beach,  
30  
31 1692 Lyme Regis. The lens cap is 5 cm in diameter.  
32  
33  
34 1693 (c) Protrusive *Diplocraterion* forming dark marl burrow-fill within limestone bed 19  
35  
36 1694 (Specketty), Seven Rock Point, Lyme Regis.  
37  
38 1695 (d) Horizon of isolated dark marl burrow fills indicating the former presence of a bed of dark  
39  
40 1696 marl that has been removed locally by seafloor erosion, bed 19, Seven Rock Point, Lyme  
41  
42 1697 Regis.  
43  
44  
45 1698  
46  
47 1699 Figure 10.  
48  
49 1700 (a) Compilation of oxygen- and carbon-isotope measurements for Lyme Regis from the  
50  
51 1701 Angulata and Bucklandi Zones. Note several data points from limestone beds (black squares)  
52  
53 1702 near  $\delta^{18}\text{O} = -4.5$  and  $\delta^{13}\text{C} = -1.5$  ‰ VPDB are obscured by the data for marl or laminated  
54  
55 1703 shale (unfilled triangles). Sources of measurements for whole-rock: Campos and Hallam  
56  
57  
58  
59  
60

1  
2  
3 1704 (1979); Gluyas (1984); Weedon (1987a); Arzani (2004; 2006); Paul, Allison & Brett (2008),  
4  
5 1705 for *Gryphaea* sp.: Weedon (1987a).  
6  
7 1706 (b) Compilation of oxygen- and carbon-isotope measurements for West Somerset Coast  
8  
9 1707 (Kilve) for the Bucklandi Zone. Sources of measurements for whole rock: Allison, Hesselbo  
10  
11 1708 & Brett (2008); Price, Vowles-Sheridan & Anderson (2008). Measurements plotted exclude  
12  
13 1709 atypical rock-types associated with the Bucklandi Zone mud mounds.  
14  
15 1710 (c) Compilation of oxygen- and carbon-isotope measurements for West Somerset Coast (St  
16  
17 1711 Audries and Doniford) for the Tilmanni and Planorbis Zones. Sources of measurements for  
18  
19 1712 whole rock: Arzani (2004; 2006); Clémence *et al.* (2010 as listed in Supplementary  
20  
21 1713 information of Paris *et al.*, 2010); for *Liostrea* sp.: van Schootbrugge *et al.*, (2007, their  
22  
23 1714 ‘unaltered’ samples only).  
24  
25  
26  
27  
28  
29  
30  
31  
32  
33  
34  
35  
36  
37  
38  
39  
40  
41  
42  
43  
44  
45  
46  
47  
48  
49  
50  
51  
52  
53  
54  
55  
56  
57  
58  
59  
60

1  
2  
3  
4  
5  
6  
7  
8  
9  
10  
11  
12  
13  
14  
15  
16  
17  
18  
19  
20  
21  
22  
23  
24  
25  
26  
27  
28  
29  
30  
31  
32  
33  
34  
35  
36  
37  
38  
39  
40  
41  
42  
43  
44  
45  
46  
47  
48  
49  
50  
51  
52  
53  
54  
55  
56  
57  
58  
59  
60

1715 Table 1. Ammonite biohorizon limits on the West Somerset (St Audries Bay and Quantock's  
1716 Head), Devon/Dorset (Lyme Regis) and South Wales (Lavernock) coast sections.

1717

1718	Zone	Subzone	Biohorizon	Pos.	St A.	Qu. H.	CWS	Lav.	L.R.
	Bucklandi	Rotiforme	Sn7 <i>rotiforme</i>	Base	-	92.69	92.69	-	18.06
	Bucklandi	Rotiforme	Sn6 cf. <i>defneri</i>	Top	-	90.66	90.66	-	17.94
	Bucklandi	Rotiforme	Sn6 cf. <i>defneri</i>	Base	-	90.38	90.38	-	17.90
	Bucklandi	Rotiforme	Sn5c <i>silvestri</i>	Top	-	87.76	87.76	-	17.76
	Bucklandi	Rotiforme	Sn5c <i>silvestri</i>	Base	-	87.70	87.70	-	17.70
	Bucklandi	Conybeari	Sn5b <i>conybeari</i>	Top	-	86.72	86.72	-	17.56
	Bucklandi	Conybeari	Sn5b <i>conybeari</i>	Base	-	86.52	86.52	-	17.43
	Bucklandi	Conybeari	Sn5a <i>elegans</i>	Top	-	86.48	86.48	-	-
	Bucklandi	Conybeari	Sn5a <i>elegans</i>	Base	-	86.16	86.16	-	-
	Bucklandi	Conybeari	Sn4 <i>rotator</i>	Top	-	82.40	82.40	-	16.78
	Bucklandi	Conybeari	Sn4 <i>rotator</i>	Base	-	82.32	82.32	-	16.76
	Bucklandi	Conybeari	Sn3b <i>rouvillei</i>	Top	-	81.64	81.64	-	16.64
	Bucklandi	Conybeari	Sn3b <i>rouvillei</i>	Base	-	81.46	81.46	-	16.40
	Bucklandi	Conybeari	Sn3a <i>rotarius</i>	Top	-	81.28	81.28	-	16.14
	Bucklandi	Conybeari	Sn3a <i>rotarius</i>	Base	-	81.18	81.18	-	16.12
	Bucklandi	Conybeari	Sn2b <i>conybearoides</i>	Top	-	79.98	79.98	-	-
	Bucklandi	Conybeari	Sn2b <i>conybearoides</i>	Base	-	79.78	79.78	-	-
	Bucklandi	Conybeari	Sn2a <i>Metophioceras</i> sp. A	Top	-	79.34	79.34	-	-
	Bucklandi	Conybeari	Sn2a <i>Metophioceras</i> sp. A	Base	-	78.64	78.64	-	15.22
	Bucklandi	Conybeari	Sn1 <i>quantoxense</i>	Top	-	78.14	78.14	-	15.21
	Bucklandi	Conybeari	Sn1 <i>quantoxense</i>	Base	-	78.06	78.06	-	15.16
	Angulata	Depressa	Hn27b <i>quadrata</i> 2	Top	-	77.50	77.50	-	14.96
	Angulata	Depressa	Hn27b <i>quadrata</i> 2	Base	-	77.42	77.42	-	14.94
	Angulata	Depressa	Hn27a <i>quadrata</i> 1	Top	-	73.42	73.42	-	-
	Angulata	Depressa	Hn27a <i>quadrata</i> 1	Base	-	73.38	73.38	-	14.56
	Angulata	Depressa	Hn26b <i>princeps</i>	Top	-	72.14	72.14	-	13.66
	Angulata	Depressa	Hn26b <i>princeps</i>	Base	-	72.04	72.04	-	13.50
	Angulata	Depressa	Hn26a <i>depressa</i> 1	Top	-	69.94	69.94	-	-
	Angulata	Depressa	Hn26a <i>depressa</i> 1	Base	-	69.52	69.52	-	13.36
	Angulata	Complanata	Hn25 <i>striatissima</i>	Top	-	67.10	67.10	-	-
	Angulata	Complanata	Hn25 <i>striatissima</i>	Base	-	66.90	66.90	-	-
	Angulata	Complanata	Hn24d grp. <i>vaihingensis</i>	Top	-	65.68	65.68	-	-
	Angulata	Complanata	Hn24d grp. <i>vaihingensis</i>	Base	-	65.26	65.26	-	-
	Angulata	Complanata	Hn24c aff. <i>complanata</i>	Top	-	63.78	63.78	-	12.58
	Angulata	Complanata	Hn24c aff. <i>complanata</i>	Base	-	63.60	63.60	-	12.46
	Angulata	Complanata	Hn24b <i>phoebetica</i>	Top	-	63.14	63.14	-	-
	Angulata	Complanata	Hn24b <i>phoebetica</i>	Base	-	63.04	63.04	-	-
	Angulata	Complanata	Hn24a <i>complanata</i>	Top	-	57.40	57.40	-	12.22
	Angulata	Complanata	Hn24a <i>complanata</i>	Base	-	57.26	57.26	-	12.12
	Angulata	Complanata	Hn23c cf. <i>polyeides</i>	Top	54.74	-	54.74	-	-
	Angulata	Complanata	Hn23c cf. <i>polyeides</i>	Base	54.60	-	54.60	-	-
	Angulata	Complanata	Hn23b <i>similis</i>	Top	52.66	52.09	52.66	-	12.10
	Angulata	Complanata	Hn23b <i>similis</i>	Base	52.58	51.95	52.58	-	12.06
	Angulata	Complanata	Hn23a grp. <i>stenorhyncha</i>	Top	49.48	-	49.48	-	12.00
	Angulata	Complanata	Hn23a grp. <i>stenorhyncha</i>	Base	49.26	-	49.26	-	11.90
	Angulata	Extranodosa	Hn22 cf. <i>germanica</i>	Top	47.42	51.24	47.42	-	-
	Angulata	Extranodosa	Hn22 cf. <i>germanica</i>	Base	47.22	51.02	47.22	-	-
	Angulata	Extranodosa	Hn21c <i>amblygonia</i> 3	Top	45.40	-	45.40	-	11.36
	Angulata	Extranodosa	Hn21c <i>amblygonia</i> 3	Base	45.00	-	45.00	-	11.28
	Angulata	Extranodosa	Hn21b cf. <i>pyncnotycha</i>	Top	43.26	-	43.26	-	-
	Angulata	Extranodosa	Hn21b cf. <i>pyncnotycha</i>	Base	43.12	-	43.12	-	-
	Angulata	Extranodosa	Hn21a <i>atrox</i>	Top	42.24	-	42.24	-	-

1									
2									
3	Angulata	Extranodosa	Hn21a <i>atrox</i>	Base	42.14	-	42.14	-	-
4	Angulata	Extranodosa	Hn20c <i>hadrotychus</i>	Top	40.86	-	40.86	-	-
5	Angulata	Extranodosa	Hn20c <i>hadrotychus</i>	Base	40.76	-	40.76	-	-
6	Angulata	Extranodosa	Hn20b <i>Schlotheimia</i> sp. 1b	Top	40.64	-	40.64	-	-
7	Angulata	Extranodosa	Hn20b <i>Schlotheimia</i> sp. 1b	Base	40.58	-	40.58	-	-
8	Angulata	Extranodosa	Hn20a <i>Schlotheimia</i> sp. 1a	Top	40.08	-	40.08	-	-
9	Angulata	Extranodosa	Hn20a <i>Schlotheimia</i> sp. 1a	Base	39.96	40.10	39.96	-	10.54
10	Liasicus	Laqueus	Hn19d aff. <i>bloomfieldense</i>	Top	39.72	-	39.72	-	-
11	Liasicus	Laqueus	Hn19d aff. <i>bloomfieldense</i>	Base	39.60	-	39.60	-	-
12	Liasicus	Laqueus	Hn19c <i>bloomfieldense</i>	Top	38.80	-	38.80	-	-
13	Liasicus	Laqueus	Hn19c <i>bloomfieldense</i>	Base	38.66	-	38.66	-	-
14	Liasicus	Laqueus	Hn19b cf. <i>subliassicus</i>	Top	37.22	-	37.22	-	-
15	Liasicus	Laqueus	Hn19b cf. <i>subliassicus</i>	Base	36.98	-	36.98	-	-
16	Liasicus	Laqueus	Hn19a cf. <i>laqueolus</i>	Top	36.80	-	36.80	-	-
17	Liasicus	Laqueus	Hn19a cf. <i>laqueolus</i>	Base	36.32	-	36.32	-	-
18	Liasicus	Laqueus	Hn18d cf. <i>polyspeirum</i>	Top	35.80	-	35.80	-	-
19	Liasicus	Laqueus	Hn18d cf. <i>polyspeirum</i>	Base	35.68	-	35.68	-	-
20	Liasicus	Laqueus	Hn18c cf. <i>costatum</i>	Top	33.96	-	33.96	-	9.66
21	Liasicus	Laqueus	Hn18c cf. <i>costatum</i>	Base	33.46	-	33.46	-	9.53
22	Liasicus	Laqueus	Hn18b cf. <i>gallbergensis</i>	Top	33.08	34.74	33.08	-	9.25
23	Liasicus	Laqueus	Hn18b cf. <i>gallbergensis</i>	Base	33.00	34.21	33.00	-	9.18
24	Liasicus	Laqueus	Hn 18a <i>laqueus</i>	Top	33.00	33.81	33.00	-	9.03
25	Liasicus	Laqueus	Hn 18a <i>laqueus</i>	Base	32.88	33.53	32.88	-	8.97
26	Liasicus	Portlocki	Hn17c cf. <i>latimontanum</i>	Top	32.48	33.10	32.48	-	8.94
27	Liasicus	Portlocki	Hn17c cf. <i>latimontanum</i>	Base	32.28	32.92	32.28	-	-
28	Liasicus	Portlocki	Hn17b aff. <i>benecke</i>	Top	29.94	-	29.94	-	-
29	Liasicus	Portlocki	Hn17b aff. <i>benecke</i>	Base	29.86	-	29.86	-	-
30	Liasicus	Portlocki	Hn17a cf. <i>gottingense</i>	Top	29.14	-	29.14	-	-
31	Liasicus	Portlocki	Hn17a cf. <i>gottingense</i>	Base	28.94	-	28.94	-	8.84
32	Liasicus	Portlocki	Hn16b grp. <i>portlocki</i>	Top	28.46	-	28.46	-	8.80
33	Liasicus	Portlocki	Hn16b grp. <i>portlocki</i>	Base	28.16	-	28.16	-	8.70
34	Liasicus	Portlocki	Hn16a cf. <i>crassicosta</i>	Top	27.20	-	27.20	-	-
35	Liasicus	Portlocki	Hn16a cf. <i>crassicosta</i>	Base	25.92	-	25.92	-	-
36	Liasicus	Portlocki	Hn15 <i>hagenowi</i>	Top	25.62	-	25.62	-	8.21
37	Liasicus	Portlocki	Hn15 <i>hagenowi</i>	Base	25.12	-	25.12	-	8.16
38	Liasicus	Portlocki	Hn14d <i>harpotychum</i>	Top	19.16	-	19.16	-	-
39	Liasicus	Portlocki	Hn14d <i>harpotychum</i>	Base	19.11	-	19.11	-	-
40	Liasicus	Portlocki	Hn14c <i>Waehneroceras</i> sp. nov.	Top	17.68	-	17.68	-	-
41	Liasicus	Portlocki	Hn14c <i>Waehneroceras</i> sp. nov.	Base	17.44	-	17.44	-	-
42	Liasicus	Portlocki	Hn14b <i>iapetus</i>	Top	15.60	-	15.60	-	6.66
43	Liasicus	Portlocki	Hn14b <i>iapetus</i>	Base	13.92	-	13.92	-	6.61
44	Liasicus	Portlocki	Hn14a aff. <i>franconium</i>	Top	13.62	-	13.62	14.67	-
45	Liasicus	Portlocki	Hn14a aff. <i>franconium</i>	Base	13.54	-	13.54	14.58	6.58
46	Planorbis	Johnstoni	Hn13c 'post'- <i>intermedium</i>	Top	13.50	-	13.50	14.46	-
47	Planorbis	Johnstoni	Hn13c 'post'- <i>intermedium</i>	Base	13.42	-	13.42	14.19	-
48	Planorbis	Johnstoni	Hn13b grp. <i>intermedium</i>	Top	13.10	-	13.10	12.93	6.42
49	Planorbis	Johnstoni	Hn13b grp. <i>intermedium</i>	Base	12.82	-	12.82	12.84	-
50	Planorbis	Johnstoni	Hn13a aff. <i>torus</i>	Top	-	-	-	12.51	-
51	Planorbis	Johnstoni	Hn13a aff. <i>torus</i>	Base	-	-	-	12.39	6.08
52	Planorbis	Johnstoni	Hn12 <i>johnstoni</i>	Top	12.48	-	12.48	12.12	5.90
53	Planorbis	Johnstoni	Hn12 <i>johnstoni</i>	Base	12.10	-	12.10	11.43	5.86
54	Planorbis	Johnstoni	Hn11d <i>Caloceras</i> sp. 5	Top	-	-	-	10.77	-
55	Planorbis	Johnstoni	Hn11d <i>Caloceras</i> sp. 5	Base	-	-	-	10.65	-
56	Planorbis	Johnstoni	Hn11c <i>Caloceras</i> sp. 4	Top	11.30	-	11.30	10.53	-
57	Planorbis	Johnstoni	Hn11c <i>Caloceras</i> sp. 4	Base	11.22	-	11.22	10.41	-
58	Planorbis	Johnstoni	Hn11b aff. <i>tortlie</i>	Top	10.94	-	10.94	10.17	5.20
59	Planorbis	Johnstoni	Hn11b aff. <i>tortlie</i>	Base	10.78	-	10.78	10.11	5.14
60	Planorbis	Johnstoni	Hn11a <i>Caloceras</i> sp. 2	Top	10.02	-	10.02	-	-
	Planorbis	Johnstoni	Hn11a <i>Caloceras</i> sp. 2	Base	9.98	-	9.98	-	5.06
	Planorbis	Johnstoni	Hn10 aff. <i>aries</i>	Top	9.82	-	9.82	9.87	-

1									
2									
3	Planorbis	Johnstoni	Hn10 aff. <i>aries</i>	Base	9.66	-	9.66	9.72	4.88
4	Planorbis	Planorbis	Hn9 <i>bristoviense</i>	Top	-	-	-	9.45	4.79
5	Planorbis	Planorbis	Hn9 <i>bristoviense</i>	Base	-	-	-	9.39	4.76
6	Planorbis	Planorbis	Hn8 <i>sampsoni</i>	Top	-	-	-	8.25	-
7	Planorbis	Planorbis	Hn8 <i>sampsoni</i>	Base	-	-	-	8.10	-
8	Planorbis	Planorbis	Hn7 <i>plicatulum</i>	Top	9.08	-	9.08	7.44	3.78
9	Planorbis	Planorbis	Hn7 <i>plicatulum</i>	Base	8.78	-	8.78	7.35	3.72
10	Planorbis	Planorbis	Hn6 <i>planorbis</i> $\beta$	Top	8.58	-	8.58	6.93	3.70
11	Planorbis	Planorbis	Hn6 <i>planorbis</i> $\beta$	Base	8.18	-	8.18	6.72	3.66
12	Planorbis	Planorbis	Hn5 <i>planorbis</i> $\alpha$	Top	8.18	-	8.18	6.72	3.66
13	Planorbis	Planorbis	Hn5 <i>planorbis</i> $\alpha$	Base	5.98	-	5.98	6.33	3.42
14	Planorbis	Planorbis	Hn4 <i>antecedens</i>	Top	5.58	-	5.58	6.15	3.02
15	Planorbis	Planorbis	Hn4 <i>antecedens</i>	Base	5.42	-	5.42	6.06	2.94
16	Planorbis	Planorbis	Hn3 <i>imitans</i>	Top	-	-	-	5.49	-
17	Planorbis	Planorbis	Hn3 <i>imitans</i>	Base	5.42	-	5.42	4.71	2.82
18	Tilmani		Hn2 <i>erugatum</i>	Top	5.38	-	5.38	4.65	-
19	Tilmani		Hn2 <i>erugatum</i>	Base	5.26	-	5.26	4.56	-
20	Tilmani		Hn1 (no ammonites)	Top	5.26	-	5.26	4.56	-
21	Tilmani		Hn1 (no ammonites)	Base	?1.50	-	?1.50	?1.86	?0.60

1719

---

1720 Height in metres of biohorizon boundaries above base of the Blue Lias Formation. The value

1721 in ***bold italics*** for the base Angulata Zone at Lyme Regis was estimated using the correlation

1722 with the St. Audries Bay section (see Fig. 8, Section 5.a.). Pos. = Position, St A. = St Audries

1723 Bay section, Somerset, Qu. H. = Quantock's Head section, Somerset, CWS = Composite

1724 West Somerset coastal sections using common splice level at 56.90 m (below this level the

1725 heights for Quantock's Head differ from the CWS heights), Lav. = St. Mary's Well Bay

1726 section near Lavernock, South Wales, L.R. = Pinhay Bay to Devonshire Head section, Lyme

1727 Regis, Dorset.

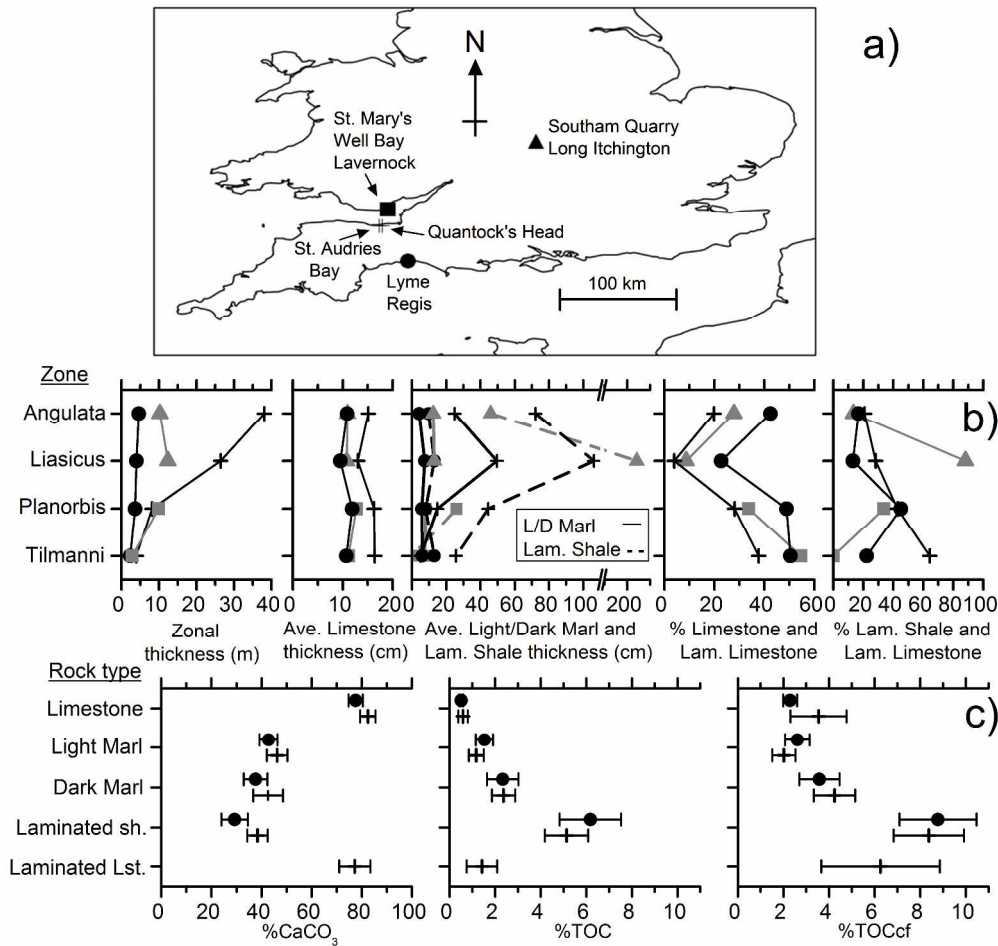


Figure 1. (a) Location of the sections illustrated in Figs 3–6. (b) Formation characteristics according to Hettangian ammonite zone and location. Data from logs shown in Fig 3–6. The symbols in Fig. 1a indicate the localities. The percentage of limestone refers to the thickness of limestone logged as limestone or laminated limestone beds, or if more than 50% of a particular level, limestone or laminated limestone nodules. Ave. = average, L/D = Light/Dark, Lam. = laminated. (c) Average rock-type composition at Lyme Regis and on the West Somerset coast (St Audries Bay and Quantock's Head sections) in terms of weight per cent calcium carbonate (%CaCO<sub>3</sub>), total organic carbon (TOC) and TOC re-expressed on a carbonate-free basis (TOCcf). Horizontal bars denote 95% confidence intervals around the mean. Data and analytical methods from Weedon (1987a): 90 samples from the Angulata and Bucklandi zones at Lyme Regis and 57 samples from the Tilmanni to Bucklandi zones on the West Somerset coast. These data are supplemented using a further 38 SAB samples (Hesselbo et al., 2008) from the Tilmanni and Planorbis zones at St Audries Bay. Numbers of samples analyzed by rock-type for Lyme Regis vs West Somerset coast respectively are: limestone and limestone nodules 31 vs 17; light marl 23 vs 17; dark marl 20 vs 19; laminated shale 16 vs 35; laminated limestone samples from west Somerset coast alone, 7. The average %TOCcf values and their uncertainties in the different rock types are consistent with the limestones formed by carbonate cementation of light marls and with the laminated limestones formed by carbonate cementation of laminated shales.

Fig. 1

874x827mm (150 x 150 DPI)



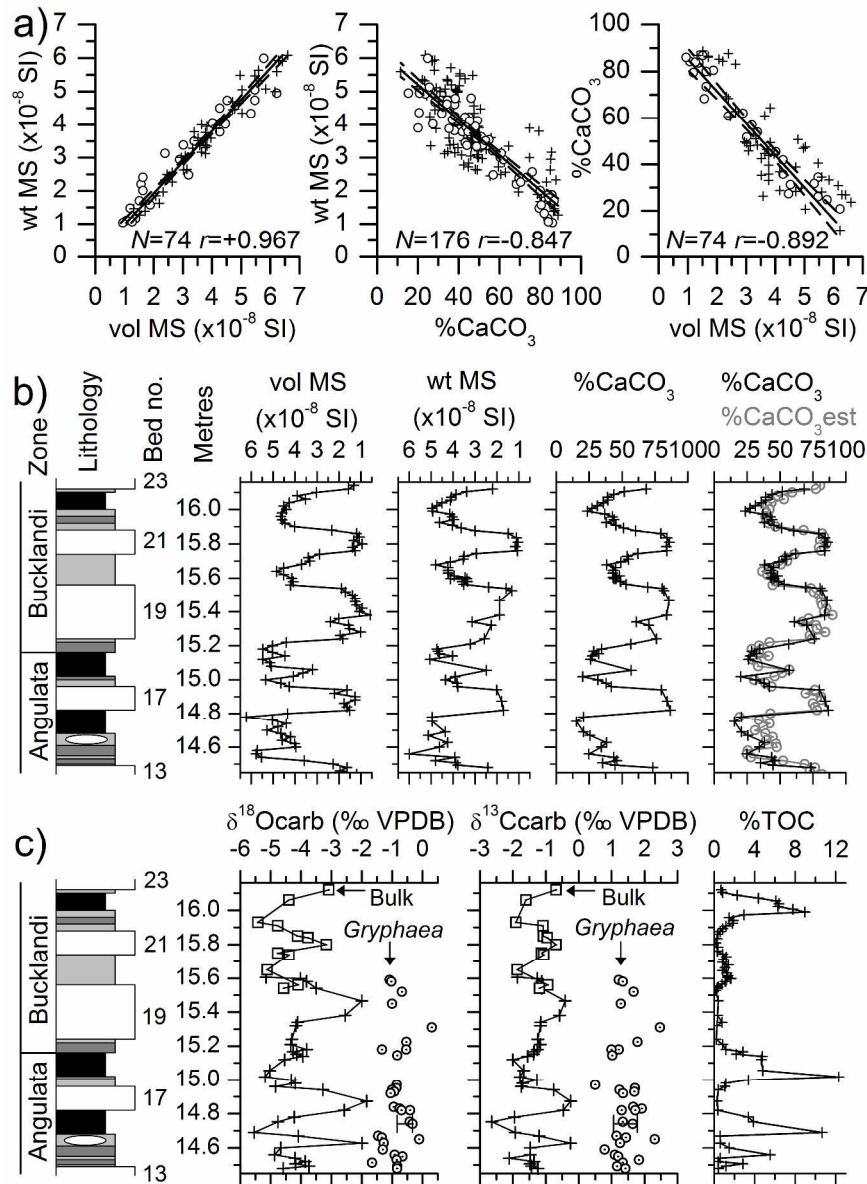


Figure 2. (a) Scatter plots of field measurements of vol MS, and laboratory measurements of wt MS and %CaCO<sub>3</sub>. *N* = number of samples, *r* = Pearson's *r* (degree of correlation). ○ = sample from Lyme Regis, + = sample from West Somerset coast. The stratigraphic locations of the samples are indicated in Figs 4 and 5. (b) Profiles of vol MS and %CaCO<sub>3</sub> measurements at Lyme Regis in beds 13 to 23 (bed numbers from Lang, 1924). + = measurement of vol MS, wt MS or %CaCO<sub>3</sub>, ○ = estimated %CaCO<sub>3</sub> based on regression between vol MS and %CaCO<sub>3</sub> (Fig. 2a) – see text Section 3.b. (c) Profiles of measurements of δ<sup>18</sup>O and δ<sup>13</sup>C and %TOC at Lyme Regis in beds 13 to 23. + = bulk sample δ<sup>18</sup>O and δ<sup>13</sup>C from Weedon (1987a), □ = bulk sample δ<sup>18</sup>O and δ<sup>13</sup>C from Paul, Allison, & Brett (2008), ○ = *Gryphaea* sp. sample δ<sup>18</sup>O and δ<sup>13</sup>C from Weedon (1987a). Key to rock-types in Fig. 3.

Fig. 2

800x1094mm (150 x 150 DPI)



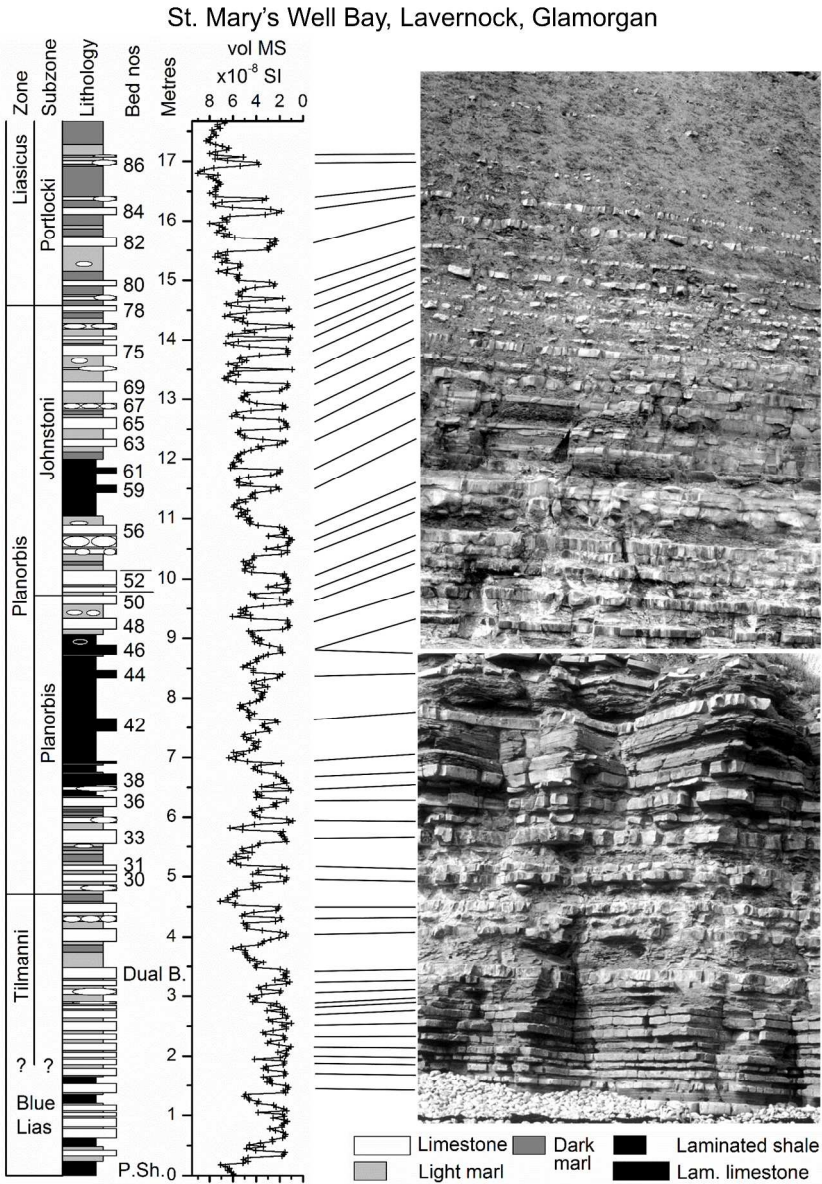


Figure 3. Lithostratigraphic log, vol MS measurements and ammonite biostratigraphy at St. Mary's Well Bay, Lavernock, Wales. Homogeneous limestone nodules are indicated by black ellipses. Laminated limestone nodules are indicated by white ellipses. At the levels where vol MS was measured within limestone nodules rather than light marl, the nodules are indicated on the right of the lithostratigraphic log. Bed numbers from Waters & Lawrence (1987).

Fig. 3  
232x334mm (600 x 600 DPI)

Lyme Regis (Pinhay Bay – Devonshire Head), Devon

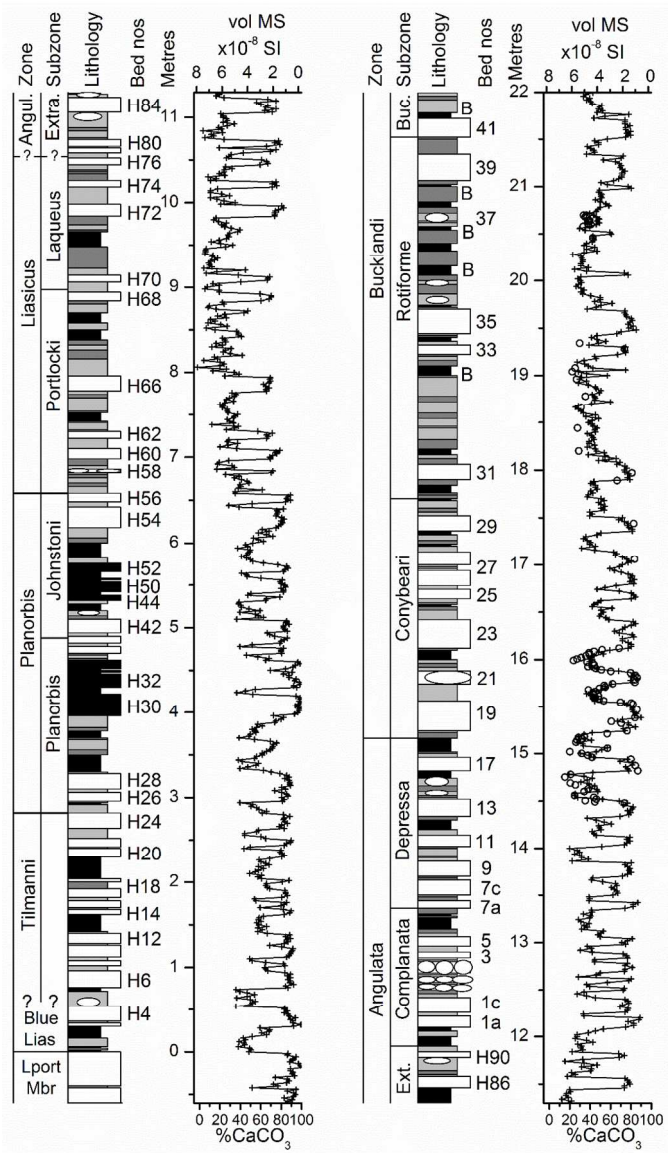


Figure 4. Lithostratigraphic log, vol MS and %CaCO<sub>3</sub> measurements and ammonite biostratigraphy to the west of Lyme Regis, Devon. The location of the base of the Angulata Zone is discussed in Section 5.a. For key to lithologies see Fig. 3. The concentration of samples at the level of bed 37 relates to the profile shown in Figs 2b and 2c. ○ = sample measured for %CaCO<sub>3</sub> plotted with reference to lower horizontal axis, B = level with abundant calcite beef, Lport Mbr = Langport Member, Angul. = Angulata, Buc. = Bucklandi, Extra. = Extranodosa, Ext. = Extranodosa. Bed numbers from Lang (1924). Lang (1924) and Hesselbo & Jenkyns (1995) provide the names of limestone beds on the Devon/Dorset coast.

Fig. 4

220x398mm (600 x 600 DPI)

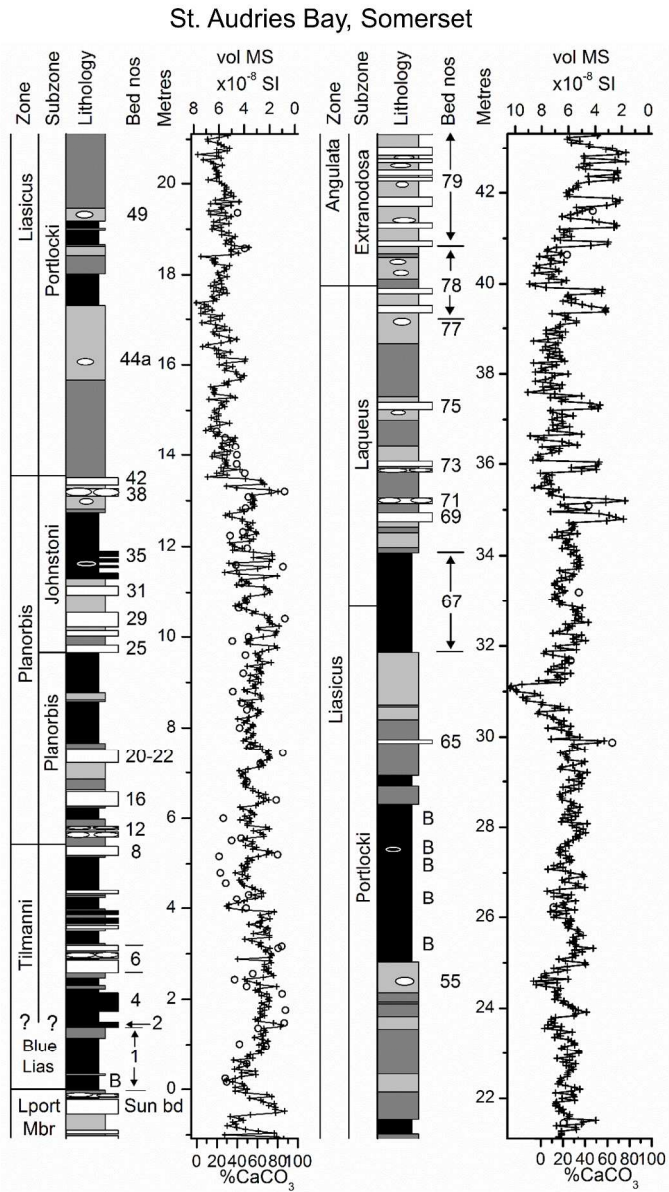


Figure 5a. Lithostratigraphic log, vol MS and %CaCO<sub>3</sub> measurements and ammonite biostratigraphy at St Audries Bay, Somerset. For key to lithologies see Fig. 3. Black circles indicate samples measured for %CaCO<sub>3</sub> plotted with reference to lower horizontal axis. ○ = sample measured for %CaCO<sub>3</sub> plotted with reference to upper horizontal axis, B = level with abundant calcite beef. Bed numbering from Whittaker and Green (1983).

Fig 5a  
226x401mm (600 x 600 DPI)

St. Audries Bay – Quantock’s Head, Somerset

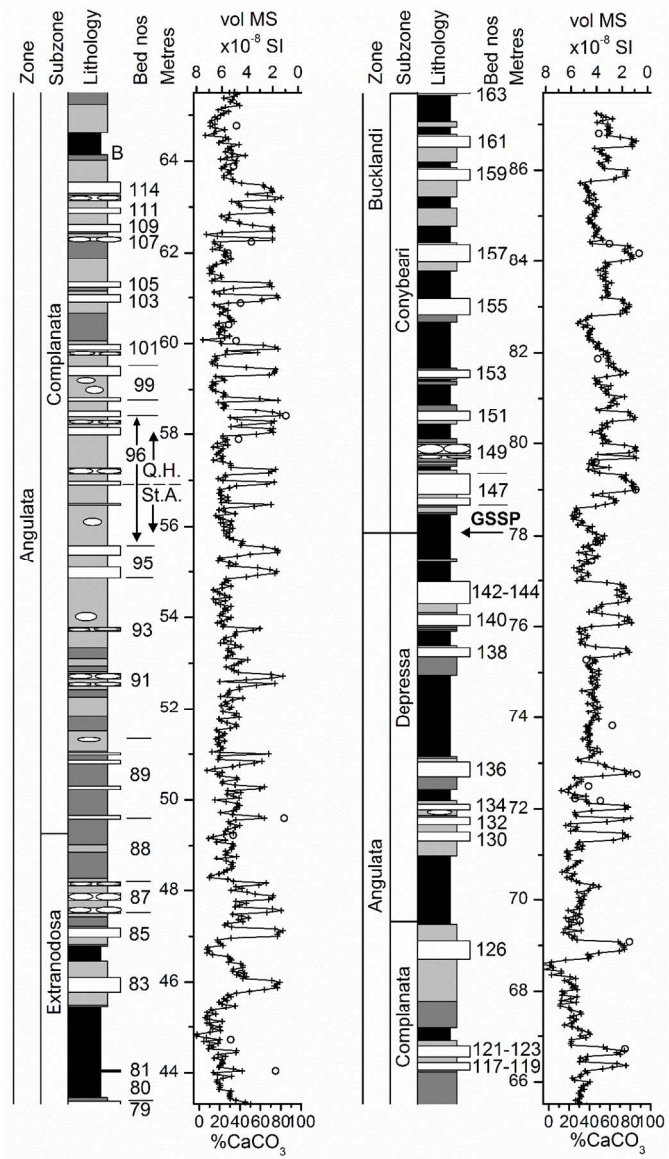


Figure 5b. As for 5a but a composite section from St Audries Bay and Quantock’s Head. The join (splice) of the St Audries Bay section (St A.) with the Quantocks Head section (Q. H.) is indicated within bed 96 (Section 3.a). GSSP = Global Stratigraphic Section and Point.

Fig. 5b

224x401mm (600 x 600 DPI)



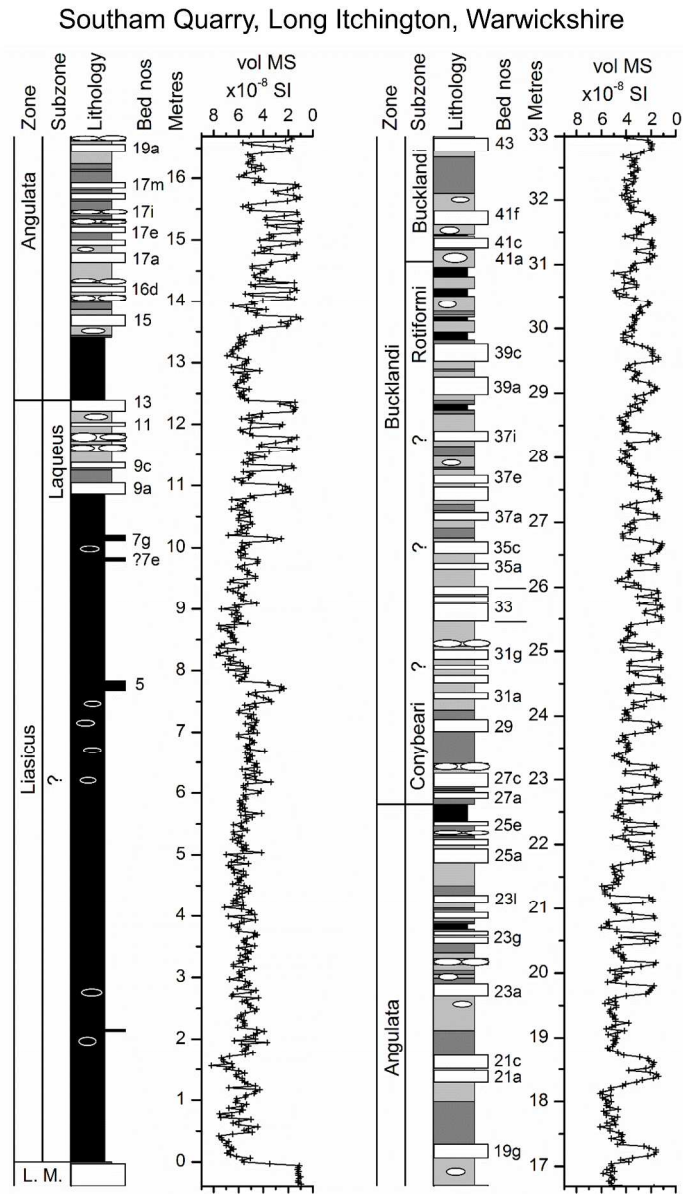


Figure 6. Lithostratigraphic log, vol MS measurements and ammonite biostratigraphy at Southam Quarry, near Southam and Long Itchington, Warwickshire. For key to lithologies see Fig. 3. L. M. = Langport Member. Bed numbers from Clements et al. (1975).

Fig. 6

220x383mm (600 x 600 DPI)

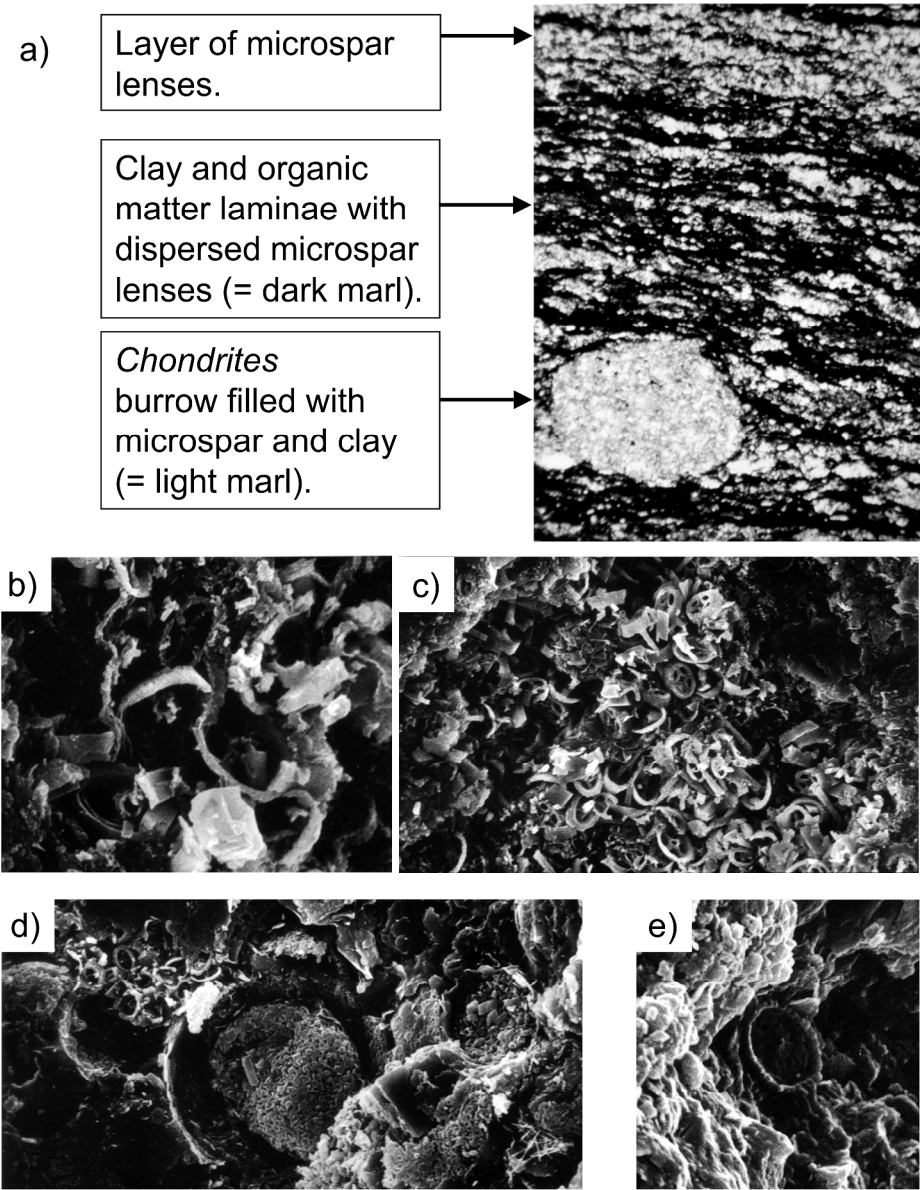


Figure 7. (a) Photomicrograph of dark marl thin-section (plane polarized light, width of view 3 mm). Sample BL120 and Fig. 2.2M of Weedon, (1987a) bed 32a, Rotiforme Subzone, Bucklandi Zone, Lyme Regis. (b) SEM photograph showing coccoliths *in situ* partly engulfed by euhedral microspar overgrowth (width of view 14  $\mu$ m). Dark marl sample BL120 and Fig. 2.4G of Weedon (1987a), bed 32a, Bucklandi Zone, Lyme Regis. (c) SEM photograph showing an aggregate of coccoliths surrounded by a matrix of organic matter and clay (width of view 56  $\mu$ m). Dark marl sample BL120 and Fig. 2.4F of Weedon (1987a), bed 32a, Bucklandi Zone, Lyme Regis. (d) SEM photograph showing an aggregate of coccoliths next to *Schizosphaerella punctulata* (centre) both surrounded by a matrix of organic matter, clay and calcite microspar (width of view 53  $\mu$ m). Laminated shale sample BL117, and Fig. 2.4H of Weedon (1987a), topmost laminated shale of bed 32, Bucklandi Zone, Lyme Regis. (e) SEM photograph showing a corroded coccolith in limestone (width of view  $\sim$ 8  $\mu$ m). Limestone sample BL103 and Fig. 2.4A of Weedon (1987a), bed 29, Conybeari Subzone, Bucklandi Zone, Lyme Regis.

Fig. 7

225x287mm (600 x 600 DPI)

Proof For Review



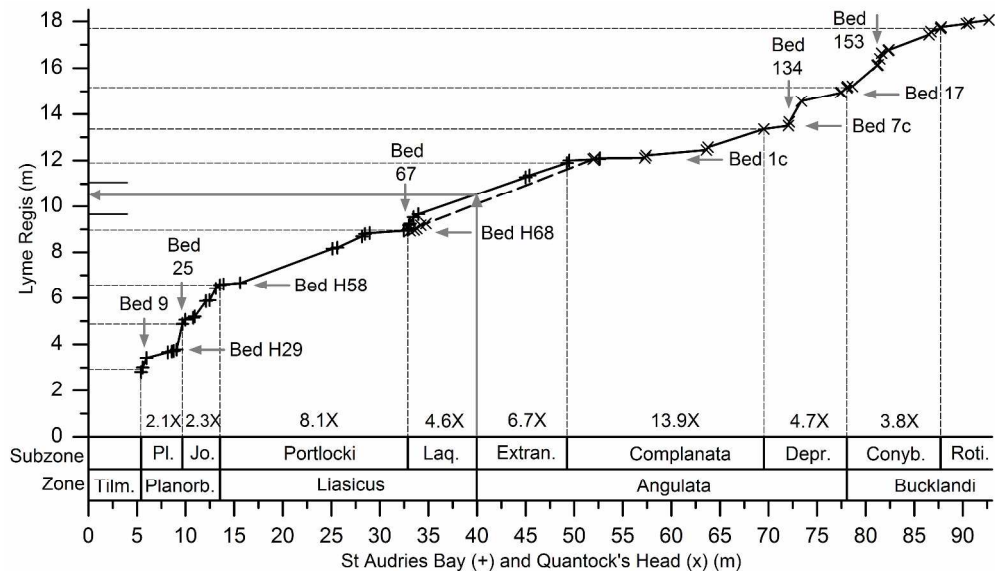


Figure 8. Shaw plot constructed using the joint locations of biohorizon bases and biohorizon tops at Lyme Regis and the West Somerset Coast (St Audries Bay and Quantock's Head sections) as listed in Table 1. The location of the base of the Angulata Zone at Lyme Regis has been estimated using the West Somerset data via the line of correlation data (long grey arrows, Section 5.a). The ratios of the thicknesses of subzones in the West Somerset composite section to subzones in the Lyme Regis section are indicated at the bottom of the plot. Vertical or horizontal arrows with bed numbers indicate the levels at which breaks in slope of the line of correlation imply relative condensation or intra-formational hiatuses. + = Lyme Regis section versus St Audries Bay section versus Lyme Regis section, x = Quantock's Head section versus Lyme Regis section. Tilm. = Tilmanni, Planorb. = Planorbis, Pl. = Planorbis, Jo. = Johnsoni, Laq. = Laqueus, Extran. = Extranodosa, Depr. = Depressa, Conyb. = Conybeari, Roti. = Rotiforme.

Fig. 8

969x555mm (150 x 150 DPI)

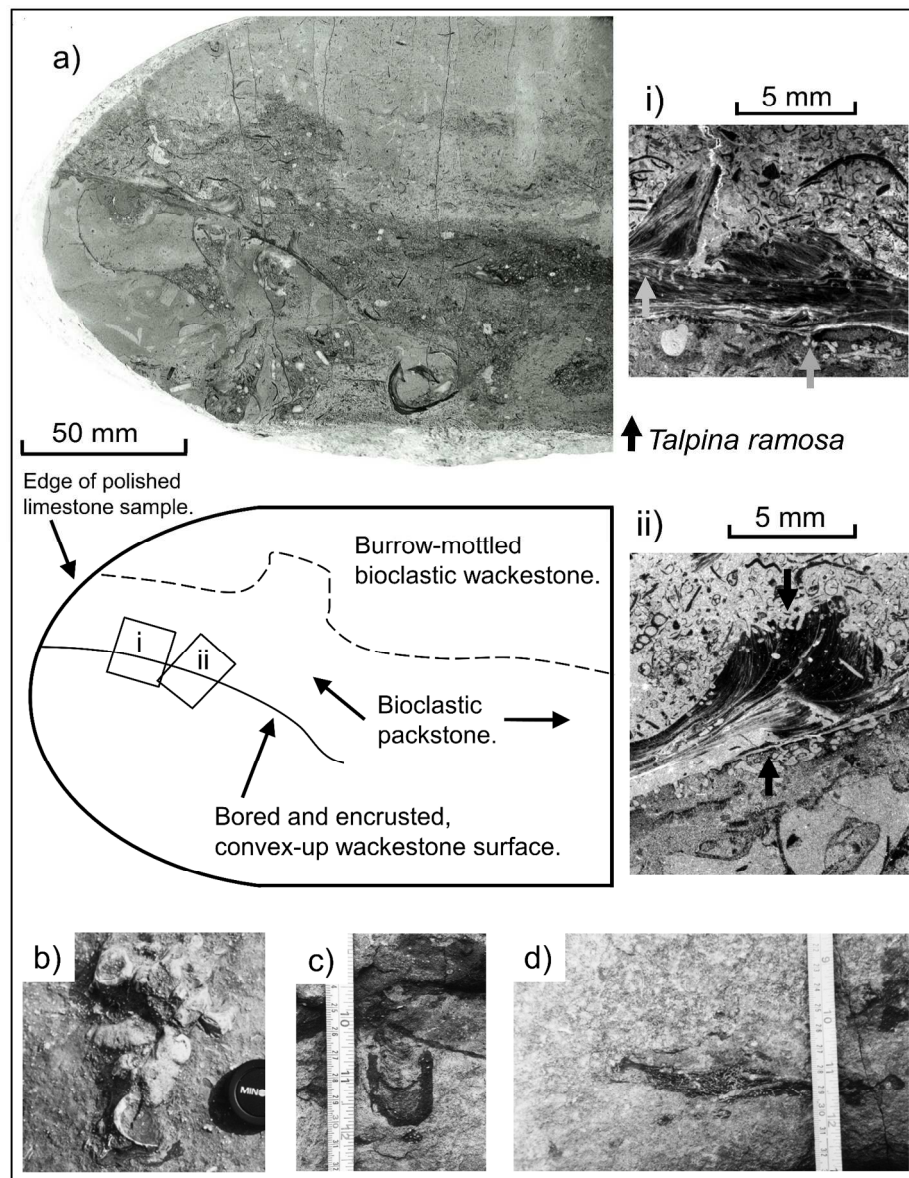


Figure 9. (a) Photograph of polished limestone section showing bored and encrusted limestone intraclast with a hardground-like surface (diagrammatic description below) collected *in situ* from within bed 25 (Top Copper) below Devonshire Head, Lyme Regis. i) Photographic negative image of acetate peel showing *Liostrea* encrusting the intraclast surface and overlain by bioclastic packstone. Two *Liostrea* individuals (left and right) encrust a third individual – demonstrating at least two generations of encrustation. Short arrows indicate the *Talpina ramosa* Von Hagenow borings into the intraclast surface and within the encrusting *Liostrea*. ii) As for i) but a different section of the intraclast surface (see diagram for location). (b) Limestone intraclasts on the surface of a fallen block of limestone, Monmouth Beach, Lyme Regis. The lens cap is 5 cm in diameter. (c) Protrusive *Diplocraterion* forming dark marl burrow-fill within limestone bed 19 (Specketty), Seven Rock Point, Lyme Regis. (d) Horizon of isolated dark marl burrow fills indicating the former presence of a bed of dark marl that has been removed locally by seafloor erosion, bed 19, Seven Rock Point, Lyme

Regis.  
Fig. 9

1  
2  
3  
4  
5  
6  
7  
8  
9  
10  
11  
12  
13  
14  
15  
16  
17  
18  
19  
20  
21  
22  
23  
24  
25  
26  
27  
28  
29  
30  
31  
32  
33  
34  
35  
36  
37  
38  
39  
40  
41  
42  
43  
44  
45  
46  
47  
48  
49  
50  
51  
52  
53  
54  
55  
56  
57  
58  
59  
60

173x222mm (600 x 600 DPI)

Proof For Review

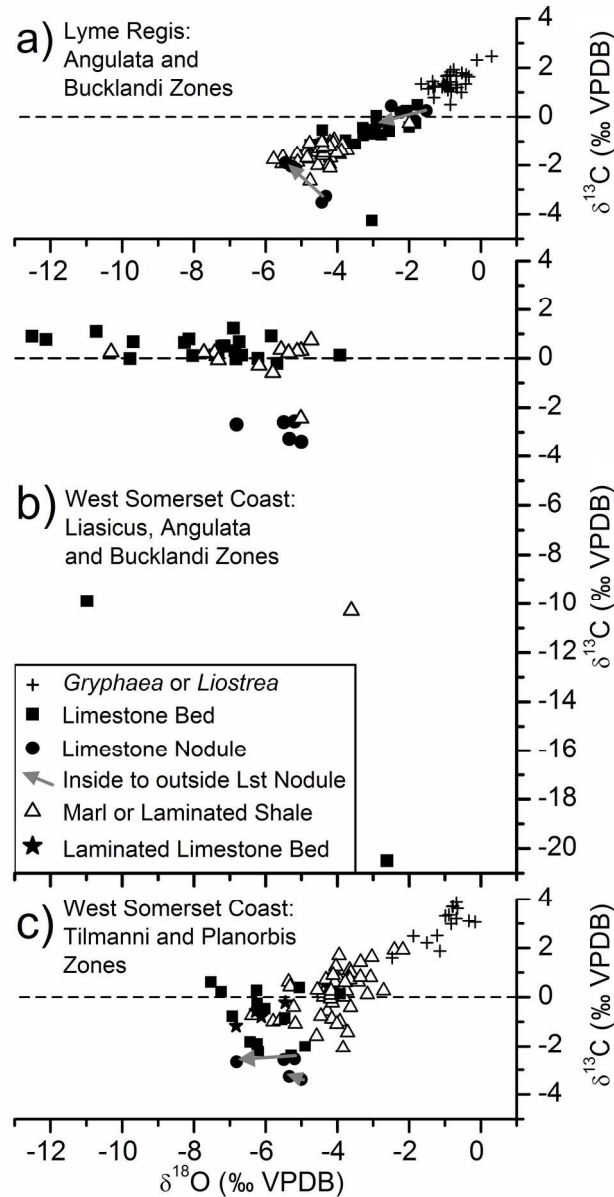


Figure 10. (a) Compilation of oxygen- and carbon-isotope measurements for Lyme Regis from the Angulata and Bucklandi Zones. Note several data points from limestone beds (black squares) near  $\delta^{18}\text{O} = -4.5$  and  $\delta^{13}\text{C} = -1.5$  ‰ VPDB are obscured by the data for marl or laminated shale (unfilled triangles). Sources of measurements for whole-rock: Campos and Hallam (1979); Gluyas (1984); Weedon (1987a); Arzani (2004; 2006); Paul, Allison & Brett (2008), for *Gryphaea* sp.: Weedon (1987a). (b) Compilation of oxygen- and carbon-isotope measurements for West Somerset Coast (Kilve) for the Bucklandi Zone. Sources of measurements for whole rock: Allison, Hesselbo & Brett (2008); Price, Vowles-Sheridan & Anderson (2008). Measurements plotted exclude atypical rock-types associated with the Bucklandi Zone mud mounds. (c) Compilation of oxygen- and carbon-isotope measurements for West Somerset Coast (St Audries and Doniford) for the Tilmanii and Planorbis Zones. Sources of measurements for whole rock: Arzani (2004; 2006); Clémence et al. (2010 as listed in Supplementary information of Paris et al., 2010); for *Liostrea* sp.: van Schootbrugge et al., (2007, their 'unaltered' samples only).

Fig. 10

1  
2  
3  
4  
5  
6  
7  
8  
9  
10  
11  
12  
13  
14  
15  
16  
17  
18  
19  
20  
21  
22  
23  
24  
25  
26  
27  
28  
29  
30  
31  
32  
33  
34  
35  
36  
37  
38  
39  
40  
41  
42  
43  
44  
45  
46  
47  
48  
49  
50  
51  
52  
53  
54  
55  
56  
57  
58  
59  
60

203x387mm (300 x 300 DPI)

Proof For Review